PhD degree in Molecular Medicine

Curriculum in: Molecular Oncology

European School of Molecular Medicine (SEMM)

University of Milan and University of Naples 'Federico II'

Settore disciplinare: Bio/11

Regulation of Notch signaling by the endo-lysosomal system in *Drosophila*: the role of ESCRT-0 and V-ATPase

Emiliana Tognon

IFOM – Milan

Matricola n. R09865

Supervisor: Dr. Thomas Vaccari

IFOM – Milan

Anno accademico: 2014/2015

In the loving memory of my mother who taught me to

always hang in there!

"You must endure long enough

to be victorious."

(Lailah Gifty Akita, Think Great: Be Great!)

1 TABLE OF CONTENTS

2 LIST OF ABBREVIATIONS

A/P	Anterior-Posterior
Ac	Achete
ADAM	A desintegrin and metallopepidase
ANK	Ankyrin
AP-3	Adaptor protein-3
APF	After Puparium Formation
Avl	Avalanche
Ax	Abruptex
bHLH	basic Helix-Loop-Helix
car	Carnation
CLEAR	Coordinated Lysosomal Expression and Regulation
CSL	CBF1, Su(H), Lag2
D/V	Dorsal-Ventral
Dl	Delta
Dll	Delta-like
dor	Deep orange
DSL	Deltal/Serrate/Lag-2
DUB	de -ubiquitynase
Dx	Deltex
E(spl)-C	Enhancer of split complex
EGF	Epidermal Growth Factor
EMT	Epithelial to mesenchymal transition
ER	Endoplasmic Reticulum
ESCRT	Endosomal sorting complex required for transport
FE	Follicle epithelium
FGF	Fibroblast growth factor
GPI	Glycophosphatidylinositol
HECT	Homologous to E6-AP carboxyl terminus
HES	Hairy enhancer of split
Hnt	Hindsight
HOPS	Homotypic fusion and vacuole protein sorting
Hrs	Hepatocyte growth factor (HGF)-regulated Tyrosine kinase substrate
Hrt	Hes-related
ILV	Internal luminal vesicle
JNK	Jun N-terminal kinase
Krz	Kurtz
Kuz	Kuzbanian
L(2)gl	Lethal (2) giant larvae
lgd	Lethal giant discs
Mam	Mastermind
Mcd	Michrochaete defective
MEF2	Myocyte enhancer factor 2

MENE	Mutant Eye No eclosion
MITF	Microphthalmia- associated Transcription Factor
MitfDN	Dominant negative form of the Mitf
mTORC1	mTOR Complex 1
MVE	Multivesicular endosome
NECD	Notch Extracellular Domain
Neur	Neuralized
NEXT	Notch Extracellular Truncation
NICD	Notch Intracellular Domain
NLS	Nuclear localization sequences
NRR	Negative regulatory region
PI3K	Phosphoinositide-3 kinase
PNC	Proneural cluster
Pnr	Pannier
PtdIns(3)P	phosphatidylinositol-3-phosphate
RAM	RBPjk association module
RAVE	Regulator of the ATPase of vacuolar and endosomal membranes
RING	Really Interesting New Gene
Sc	Scute
Ser	Serrate
Sgg/zw3	Shaggy/Zeste White 3 Kinase
SOP	Sensory Organ Precursor
Stam	Signal transducing adaptor molecule
Su(Dx)	Suppressor of Deltex
Su(H)	Suppressor of Hairless
TAD	Transactivation domain
TFEB	Transcription Factor EB
UEV	Ubiquitin E2 variant
UIM	Ubiquitin interaction motif
V-ATPase	Vacuolar-type H^+-ATPase
Vg	Vestigial
WD	Wing imaginal disc
Wg	Wingless
WT	Wild type

3 LIST OF FIGURES

4 LIST OF TABLES

5 ABSTRACT

During my Ph.D., I have been involved in two different projects:

1. The study of the role of ESCRT-0 in Notch signaling and tumor suppression.
2. The study of the regulation of V-ATPase in a subset of Notch-dependent developmental processes.

5.1 Abstract Project 1

Sorting and degradation of ubiquitylated cargoes depends on the endosomal sorting required for transport (ESCRT) machinery. The ESCRT machinery is composed of four multi-subunit ESCRT complexes (ESCRT-0, -I, -II, -III), which act in a sequential fashion to deliver endocytic cargoes into the internal luminal vesicles (ILVs) of the multivescicular endosome (MVE) for subsequent degradation. ESCRTs sort a number of transmembrane proteins including Notch and the JAK/STAT signaling receptor Domeless. In *Drosophila* epithelial tissue, mutation in ESCRT –I, -II, -III components results in misregulation of several signaling pathways, loss of epithelial polarity and unrestrained proliferation, suggesting that ESCRT genes act as tumor suppressors. Unexpectedly, *Drosophila Hrs,* one of the two components of the ESCRT-0 complex that acts upstream of the other ESCRT complexes have been found to be dispensable for tumor suppression. Thus, when I started my Ph.D. it was unclear whether ESCRT-0 had a tumor suppressive function. In my first project, I have found that mutation of *Stam,* a second ESCRT-0 component or of both *Hrs* and *Stam* result in accumulation of ubiquitinated proteins and of the signaling receptors Notch and Domeless. Nevertheless, mutant tissue displays normal tissue architecture, proliferation and

Notch signaling activation. Overall, our *in vivo* data indicate that the ESCRT-0 complex does not play a crucial role in tumor suppression.

5.2 Abstract Project 2

In mammals, the Transcription Factor EB (TFEB) family of basic Helix-Loop-Helix (bHLH) transcription factors regulates both lysosomal function and organ development. However, it is not clear whether and how these two processes are interconnected. In *Drosophila,* the Microphthalmia-associated Transcription Factor (Mitf) is the unique homolog of the TFEB family. In my second project I have found that Mitf acts similar to its mammalian counterparts as transcription factor shuttling from lysosomes to the nucleus to regulate V-ATPase expression and lysosomal biogenesis. Interestingly, I found that V-ATPase subunits display diverse expression patterns in the wing imaginal disc, suggesting complex regulation of V-ATPase during development. Remarkably, I could show that Mitf cooperates to regulate expression of a key component of the V-ATPase during differentiation of proneural clusters (PNCs), a process that specifies cells with neuronal identity. In addition, I have observed that the PNCs possess a distinctive endo-lysosomal compartment and Notch localization. Finally, I have determined that modulation of V-ATPase and Mitf in the disc alters endo-lysosomal function and PNC development. Overall my *in vivo* analysis indicates that lysosomal-associated functions regulated by V-ATPase/Mitf axis might play a role in tissue patterning during *Drosophila* development.

In addition to the work described above, I co-wrote a chapter on immunohistochemical tools and techniques to visualize Notch in *Drosophila*, in *Methods in Molecular Biology* Vol. 1187 (Tognon & Vaccari, 2014)

6 INTRODUCTION

6.1 Notch signaling

Notch signaling mediates cell fate decisions during development and tissue homeostasis in metazoans (Guruharsha, Kankel, & Artavanis-Tsakonas, 2012). The Notch pathway is remarkably pleiotropic and very context-specific; in certain contexts Notch promotes proliferation, whereas in others differentiation (Wilson & Radtke, 2006). As a consequence of the countless instances in which Notch operates, signaling alterations are observed in a wide array of diseases including cancers of the breast and lung (Pece et al., 2004; Westhoff et al., 2009).

6.1.1 Structure of Notch receptor and its ligands

Characterization of the Notch signaling pathway started at the beginning of the 20th century with the discovery of the *Notch* gene in *Drosophila* as a sex-linked mutation, which causes notches at the margins of the wing blades (Morgan, 1917). The *Notch* gene encodes for a single pass transmembrane protein, which is presented at the plasma membrane as a heterodimer composed of a large extracellular domain (Notch Extracellular Domain or NECD) non-covalently linked to a membrane tethered intracellular domain (Notch Extracellular Truncation-NEXT). NEXT can be in turn cleaved to generate a smaller intracellular fragment (Notch Intracellular Domain-NICD) as a consequence of signaling activation. The extracellular domain of Notch contains up to 36 Epidermal Growth Factor (EGF)-like repeats, some of which important for the interaction with its ligands (Rebay et al., 1991). Many EGF repeats bind to calcium ions, which play an important role in the stabilization of the receptor (Cordle et al., 2008). The EGF repeats are then followed by a unique negative regulatory region (NRR). The NRR modulates

interactions between the extracellular and the membrane-tethered-intracellular domains (Wharton, Johansen, Xu, & Artavanis-Tsakonas, 1985; Yochem, Weston, & Greenwald, 1988) and plays a critical role in preventing receptor activation in the absence of ligands. The NEXT fragment contains (i) a RAM (RBPjk association module) domain, which sits close to the membrane, (ii) seven ankyrin repeats (ANK domain), which are flanked by (iii) nuclear localization sequences (NLS), (iv) a loosely defined transactivation domain (TAD) and at the very C-terminus (v) a conserved proline/glutamic acid/serine/threonine-rich motifs (PEST) essential for sending Notch to proteasomal degradation (Gupta-Rossi et al., 2001)**(Fig. 1)**. In particular, the *C.elegans* and mammalian E3 ligases SEL-10/Fbw7 were shown to ubiquitinate the nuclear NICD in its PEST domain and promote proteasomal degradation in the nuclear compartment (Gupta-Rossi et al., 2001; Wu et al., 2001). In its intracellular region, Notch has a domain targeted by members of the HECT-type (homologous to E6-AP carboxyl terminus) E3 ubiquitin ligase: Nedd4 and *Drosophila* suppressor of Deltex [Su(Dx)]/mammalian Itch/AIP4 (Cornell et al., 1999; Qiu et al., 2000). Another region of Notch important for ubiquitination is the ankyrin repeats, which are modifies by Deltex (Dx), a RING (really interesting new gene) finger-type ubiquitin ligase (Diederich, Matsuno, Hing, & Artavanis-Tsakonas, 1994). To activate the pathway, the Notch protein interacts with ligands, which are also transmembrane proteins, therefore a cell-cell interaction is required to trigger the canonical pathway. The common feature of Notch ligands is the presence of two related structural motifs: an N-terminal DSL (Delta/Serrate/Lag-2) motif and several EGF-like repeats. The DSL region of the ligand mediates the interaction with Notch EGF-like repeats 11 and 12 (Rebay et al., 1991). In mammals, there are four *Notch* genes, which all exhibit the same overall structure, and five genes encoding ligands, three Delta-like ligands (Dll)

called Dll1, Dll2 and Dll4 and two Serrate-like ligands called Jagged1 and Jagged2. In addition, noncanonical ligands have been described, either secreted or membrane-tethered proteins (D'Souza, Meloty-Kapella, & Weinmaster, 2010).

Conversely, one of the advantages of studying Notch signaling in *Drosophila* depends on its high level of conservation in metazoans and its low redundancy compared to mammals. The *Drosophila* genome has one *Notch* gene encoding for the receptor and only two genes encoding the ligands Delta (Dl) and Serrate (Ser) (Lissemore & Starmer, 1999). The main structural difference between the Dl and Ser ligands is that Ser molecules contain in the extracellular region a greater number of EGF repeats and a cysteine-rich region that is absent in the Dl ligands **(Fig. 1).**

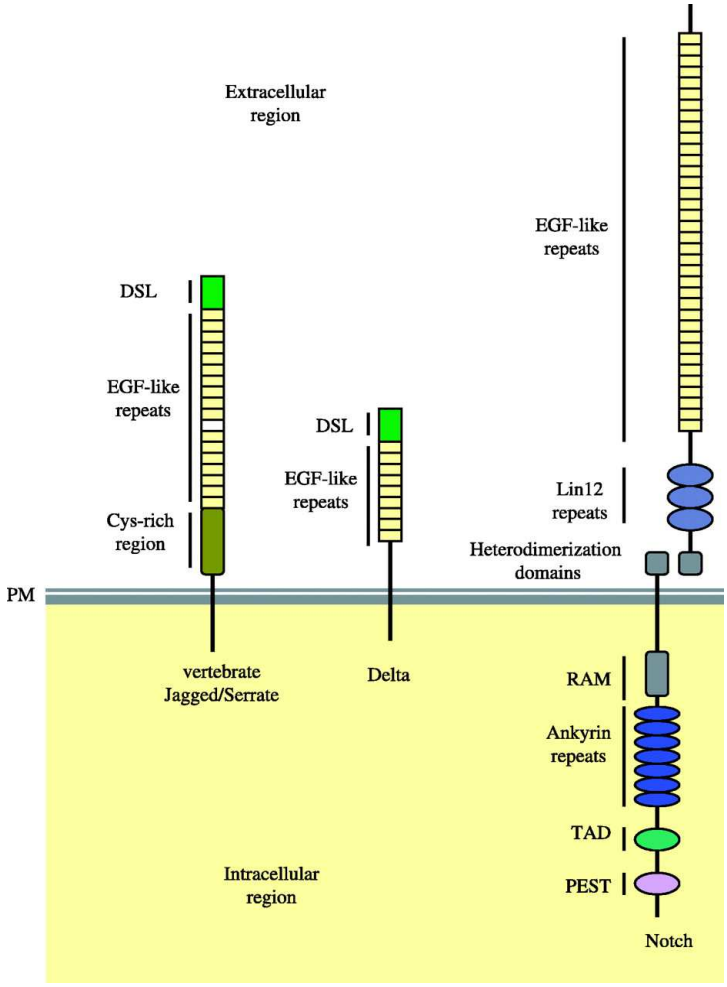

Figure 1 Structure of Notch receptor and DSL ligands.

All molecules are single-spanning transmembrane proteins. EGF: Epidermal Growth Factor-like repeats; RAM: RBPj-associated Molecule; TAD: Trans-activation domain; PEST: Proline (P), Glutamic Acid (E), Serine (S) et Threonine (T); DSL: Delta, Serrate, Lag-2; Cys: Cysteine. Adapted from (Fiúza & Arias, 2007).

6.1.2 Post-translational modification of Notch and its ligands

Notch and its ligands are glycoprotein, therefore subjected to two forms of O-glycosilation, O-fucose and O-glucose. Although these post-translational modifications seem in part dispensable for efficient signal transduction, it is likely that O-fucosilation can facilitate proper Notch folding in the endoplasmic reticulum (ER) and have a regulatory role on the ligand-binding properties of the receptors (Sakamoto, Ohara, Takagi, Takeda, & Katsube, 2002; A. Xu, 2005).

6.1.3 Canonical Notch signaling activation

It is very well established that Notch receptor activation is mediated by a sequence of proteolytic and endocytic events. The first Notch cleavage (S1) occurs in the *trans*-Golgi apparatus, where a furin-like convertase cleaves the Notch protein to form a non-covalently linked heterodimer that is mature to be exposed at the plasma membrane. The biological relevance of S1 cleavage for efficient Notch signaling is still controversial, but it seems dispensable for Notch activity in mammals (Gordon et al., 2009), and also in *Drosophila* whereby Notch does not appear to even undergo furin-processing (Kidd & Lieber, 2002). At the cell surface, Notch heterodimer can interact with one of its ligands expressed in a neighboring cell (signal-sending cell). The binding of the receptor to the ligand results in the shedding of the ectodomain and exposure of an extracellular metalloprotease site (S2) that can be cleaved by transmembrane proteases of the ADAM (a desintegrin and metallopepidase) family, which in *Drosophila* is primarily represented by kuzbanian (kuz) (Mumm et al., 2000; Nichols et al., 2007). In the signal-receiving cell, the remaining NEXT fragment is then a substrate for γ-secretase, a multicomponent member of a growing family of intramembrane cleaving

proteases (reviewed in (Selkoe & Wolfe, 2007)). NEXT fragment is then cleaved by γ-secretase at the S3 sites to generate the soluble fragment NICD, which can translocate in the nucleus and behave as a transcription factor **(Fig. 2).**

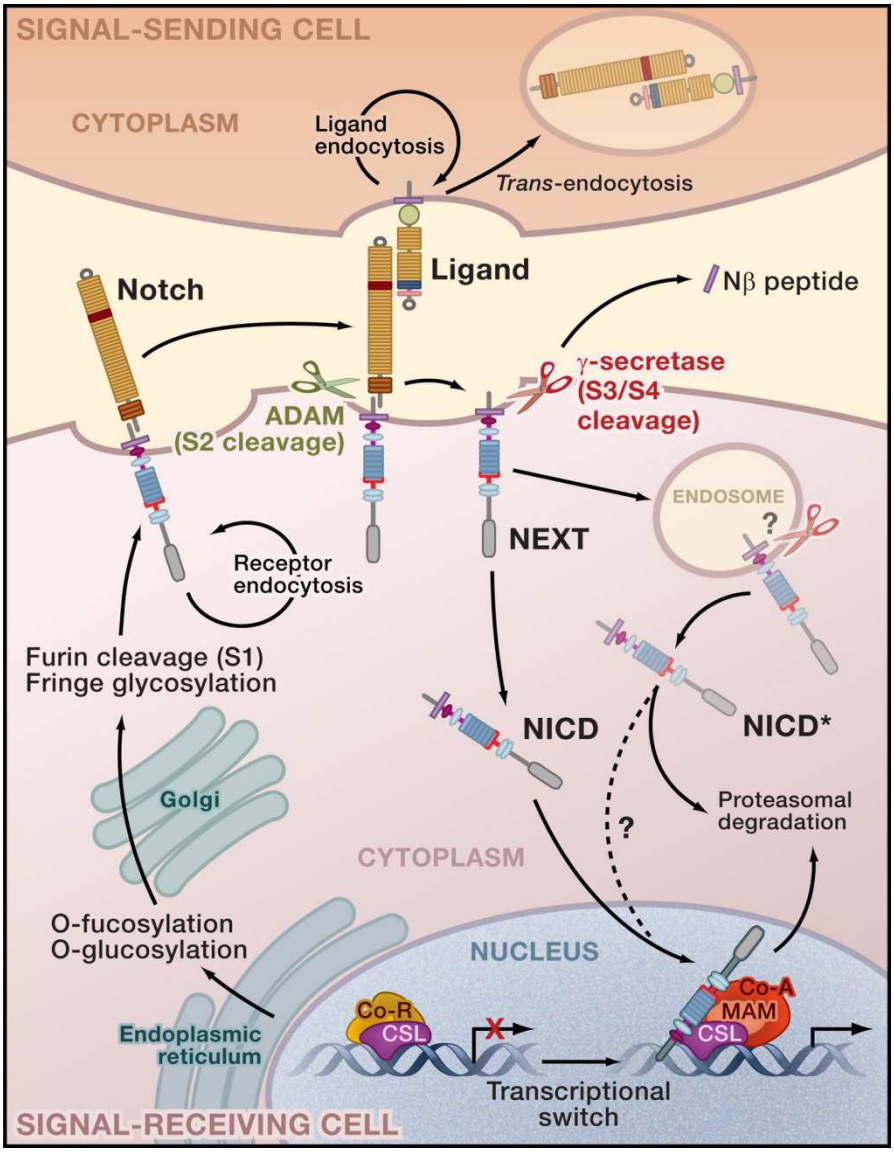

Figure 2 Schematic representation of canonical Notch signaling activation.

The binding of Notch to the ligand elicits a series of cleavage and endocytic steps. The first one is mediated by the protease ADAM. Then NEXT becomes substrate for the γ-secretase complex. Thus NICD is released and translocates into the nucleus where it dislodges co-R and forms a ternary complex with CSL and MAM leading to the recruitment of transcription factors and activation of target gene expression. Adapted from (Kopan & Ilagan, 2009)

Whether this S3 cleavage takes place at the plasma membrane or in endocytic compartments or in both places has long been debated (Kaether, Haass, & Steiner, 2006; Pasternak et al., 2003). In the nucleus, NICD interacts with a repressive transcriptional regulatory complex composed of CSL DNA binding proteins (RBPjk/CBF1 in vertebrates, Lag-2 in *Caenorhabditis* and suppressor of

hairless [Su(H)] in *Drosophila*) and co-repressors (co-R). In the nucleus, by displacing co-R, NICD binds to CSL and recruits one member of the Mastermind-like family (mam) that acts as a co-activator. The ternary complex then recruits transcription factors, thereby initiating a series of events to promote transcription of Notch target genes. The most classical target genes of Notch belong to the *HES* (*hairy enhancer of split*) and *Hrt* (*Hes-related*) families, which are members of the basic helix-loop-helix (bHLH) transcription factor family. The target of Notch signaling during lateral inhibition in *Drosophila* include the bHLH genes of *Enhancer of split complex [E(spl)-C]*(Bailey & Posakony, 1995; Fortini & Artavanis-Tsakonas, 1994; Jennings, Preiss, Delidakis, & Bray, 1994; Lecourtois & Schweisguth, 1995; Struhl & Adachi, 1998)while during the development of the wing NICD-CSL complex has different targets, for example it activates the expression of *vestigial* (Kim et al., 1996).

6.1.4 Inhibitory effects of ligands

In addition to an inter-cellular ligand-ligand interaction (*trans*-interaction) (Annette L Parks et al., 2006) an intra-cellular (*cis*-interaction) between ligands and Notch expressed by the same cell has been shown to repress ligand-dependent Notch signaling and to buffer cells against accidental activation of ligand-independent Notch signaling (del Álamo, Rouault, & Schweisguth, 2011; Micchelli, Rulifson, & Blair, 1997; Palmer, Jia, & Deng, 2015; Sakamoto et al., 2002). Ligands lacking only the intracellular domain or lacking both the intracellular domain and trans-membrane domains (secreted forms) lose their ability to *trans*-activate Notch but retain strong inhibitory interactions with the receptors suggesting that *cis*-inhibition requires sequences found in the extracellular domain of the ligands (Sun & Artavanis-Tsakonas, 1996, 1997). It has been reported that during *Drosophila* wing formation this mechanism contributes to restrict Notch signaling

activity to the dorsal/ventral (D/V) boundary, regulating correct wing margin formation (Micchelli et al., 1997). *Cis*-mediated inhibition has been reported also in *Drosophila* follicle cells where a miRNA promotes Notch activation by repressing expression of Dl, where in a cell autonomous context it acts as a repressor of Notch signaling (Poulton et al., 2011).

6.2 Three types of developmental Notch-dependent processes

Notch can have a permissive function in which it mediates decisions between two alternative fates such as in the processes of "lateral inhibition", or of "asymmetric cell fate decision". Notch signaling can also have a more instructive role, as in the case of the formation of boundaries between cells in *Drosophila* or during somitogenesis in vertebrates.

6.2.1 Lateral inhibition

Lateral inhibition is a central process to assign cell fate during tissue patterning. There are many examples where Notch functions in lateral inhibition. The best studied is the selection of the sensory organ precursor cells (SOP) among a cluster of cells (proneural cluster, PNC). This process can give rise to both macrochaete and microchaete bristles, which are sensory structures present in the thorax and in the wing of adult flies **(Fig.3).**

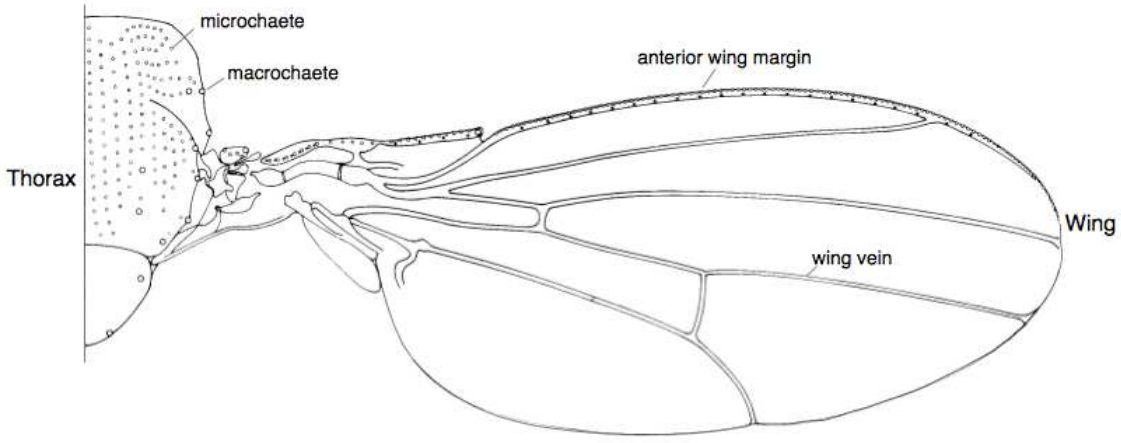

Figure 3 Positioning of macrochaete and microchaete in adult thorax and wing.

The small sensory bristles (microchaete) are arranged in rows. Within a row, the bristles are uniformly spaced and separated by epidermal cells. The microchaete precursors arise from stripes of Achaete (Ac) and Scute (sc) expression and are specified around 6-9 hours after puparium formation (APF) (Usui & Kimura, 1993). The large bristles arise from small groups of Ac-sc expressing cells that occupy stereotyped positions (Simpson, 1997). The formation of SOPs occurs in the *Drosophila* wing imaginal disc (WD), an epithelial sac that will give rise to the adult wing. This epithelial organ proliferates extensively during larval development achieving a final size of 50,000 cells **(Fig.4A).**

During development, the PNC have the same developmental potential, but only some cells within the group are singled out to finally adopt the potential. By amplification of small differences within the PNCs, SOPs start to express an increased levels of proneural proteins, which leads to inhibition of the neural potential and the activation of Notch signaling in the surrounding cells (Castro, Barolo, Bailey, & Posakony, 2005). Cells that trigger Notch signaling and activate genes of the *E(spl)-C* will maintain an epithelial fate and in turn repress *Ac* and *sc*, while those expressing more Dl will be locked in the proneural fate **(Fig.4B).** The PNC is recognizable by the expression of the bHLH transcriptional activators Ac-sc, which confer the ability to make SOPs (Skeath & Carroll, 1991). The SOPs are recognizable by the expression of other proteins, which are selectively retained in the proneural cells; these include Neuralized (Neur) and the transcription factor Hindsight (Hnt).

The differentiation cascade that forms SOPs is also in part dependent on Wnt/Wingless (wg) signaling activation and required the combinatorial activity of many bHLH transcription factors (Bray, 1997; Heitzler, Bourouis, Ruel, Carteret, & Simpson, 1996). Members of the bHLH family share a common structural motif

composed of a basic region followed by two α-helices joined by a flexible peptide loop (HLH domain). The basic domain makes site-specific contact with DNA at specific sequences, while the HLH domain is required for homo-or heterodimerization with other partners. Different members of the bHLH family act at different stages in the neuronal commitment. Some earlier factors regulate the expression of later differentiating factors. In contrast to bHLH proneural proteins, the bHLH family of the *E(spl)-C* act as transcriptional repressors (reviewed in (Philpott, 2010)).

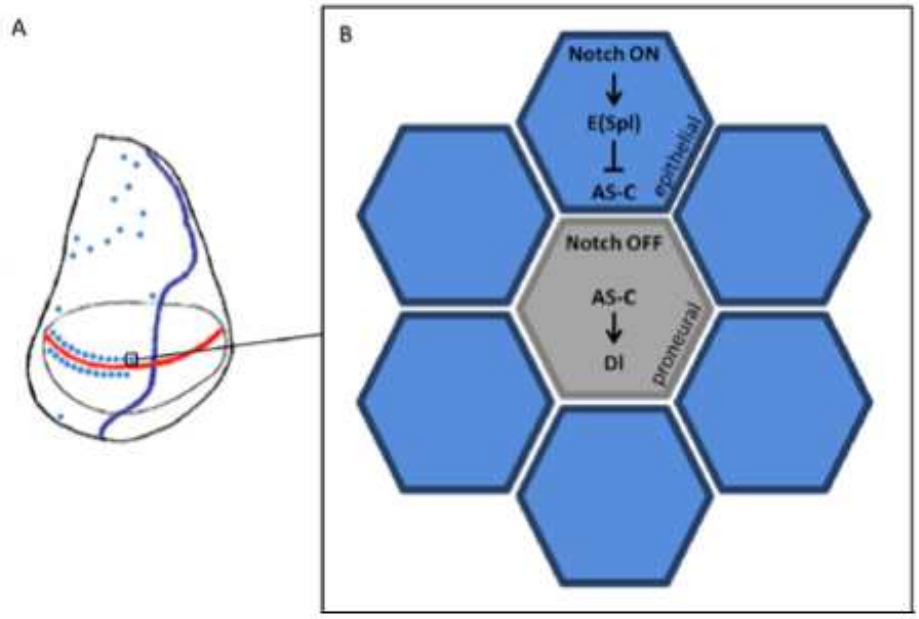

Figure 4 Positioning of SOPs in the wing imaginal disc.

A) Schematic representation of a *Drosophila* WD. The mechano-sensory bristles arise in the third instar WDs from clusters of Ac-sc (As-C)-expressing cells at specific sites (in blue). B) Schematic representation of the lateral inhibition process that occurs in the PNCs. Notch positive cells (blue) repress proneural genes (AS-C) and maintain an epithelial fate. The Dl (Dl;grey) cell instead upregulates proneural proteins and is locked in the proneural fate.

In the WD, Notch signaling also participates in the partitioning of vein and intervein cell fates (Huppert, Jacobsen, & Muskavitch, 1997). Mutations in genes that affect Notch signaling in these two processes result in either alteration of bristle numbers and/or aberrant wing vein morphogenesis (Goriely, Dumont, Dambly-Chaudière, & Ghysen, 1991; Lehmann, Jim�nez, Dietrich, & Campos-Ortega, 1983; Shellenbarger & Mohler, 1975). Hyperactivity of Notch signal in all

cells of the PNC results in the absence of SOPs (balding phenotype) and wing veins in the adult. Conversely, loss of Notch signaling results in dense patches of bristles in positions where only one bristle would normally be present due to supernumerary SOPs and thicker veins.

6.2.2 Lineage decisions

Notch signaling can participate in binary cell decisions, which result in unequal partitioning of regulators of Dl/Notch signaling and identification of two intrinsically different daughter cells. As a consequence, one of the daughter cell will present ligand molecules that cause Notch activation in its sibling. This process relies on cell polarization and polarity proteins (Schober, Schaefer, & Knoblich, 1999; Wodarz, Ramrath, Kuchinke, & Knust, 1999). Epithelial cells of the *Drosophila* WDs are polarized cells containing adherens and septate junctions in the apical region. In the dorsal thorax, the division of the SOP occurs in parallel to the anterior-posterior body axis.

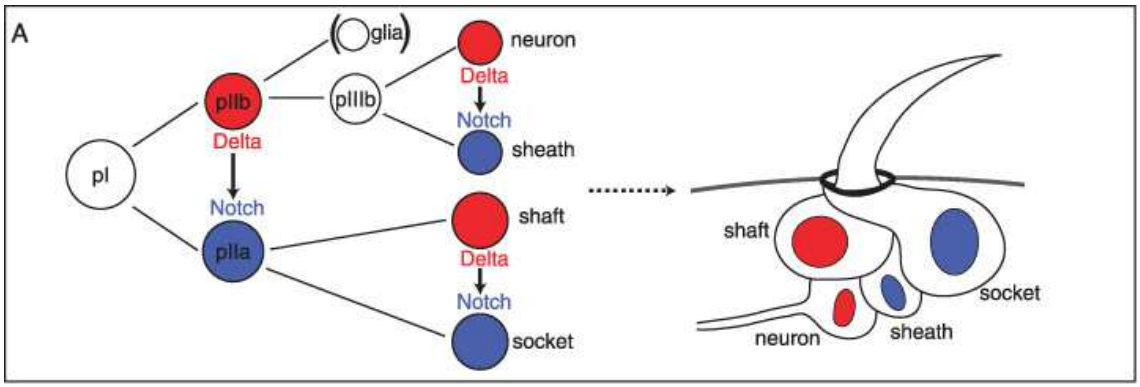

Figure 5 *Drosophila* sensory organ lineage.

Scheme of pupal lineage from the precursor cell pI to the specification of the adult sensory organ cells after several rounds of asymmetric cell divisions. Blue nuclei indicate cells responding to Notch signaling and red nuclei indicate cells sending Notch signals. On the right side schematic representation of how the four differentiated cells are organized to form the adult sensory organ. The shaft and socket form the external cells, whereas sheath and neuron are internal. Adapted from (Fürthauer & González-Gaitán, 2009)

After the SOP (pI) is chosen, this cell undergoes a series of asymmetric cell divisions where regulators of Notch signaling (e.g. Numb and Neuralized) are distributed asymmetrically between daughter cells, rendering the anterior cell

(pIIb) able to trigger Notch signaling in the posterior sibling cell (pIIa). Numb and Neuralized localize to the pIIb cell and are involved in enhancing the ability of Dl to signal. Numb in the signal-sending cell antagonizes Notch signaling (Tong et al., 2010). Asymmetric division of pIIb gives rise to a small glial cell that soon undergoes apoptosis (Gho, Bellaïche, & Schweisguth, 1999) and to a pIIIb precursor cell. The pIIIb cell then undergoes a second round of asymmetric cell division that gives rise to internal cells (sheath and neuron) whereas the pIIa becomes the progenitor of the external cells (socket and shaft) **(Fig.5)**. When Notch signaling is lost the pIIa transforms into a pIIb, leading to a loss of external cells and gain of internal cells (de Celis, Garcia-Bellido, & Bray, 1996). Conversely, when Notch signaling is ectopically activate there is a pIIb-to-pIIa transformation leading to gain of external cell at the expenses of internal cells (Guo, Jan, & Jan, 1996).

6.2.3 Boundaries formation

Compartment boundaries separate adjacent populations of cells and prevent them from mixing. Notch signaling is important for maintaining compartment boundaries, notably in the WD of *Drosophila* during development. At early stages of development, the WD is divided by two lineage boundaries: the anterior posterior (A/P) and the dorsal ventral (D/V) boundary (review in (Irvine & Vogt, 1997) **(Fig.6)**. The D/V compartment boundary of the WD acts as an organizing center important to keep the identity of the dorsal and ventral compartments distinct. The maintenance of the boundary depends on the differential expression of Notch ligands Ser and Dl in the dorsal and ventral cells, respectively. In this way Ser and Dl are expressed in a compartment-specific manner and Notch in the dorsal compartment only responds to Dl, while in ventral compartments it only responds to Ser (Micchelli & Blair, 1999). Thus, productive

ligand-receptor interaction can take place only at the cell surfaces facing the D/V boundary.

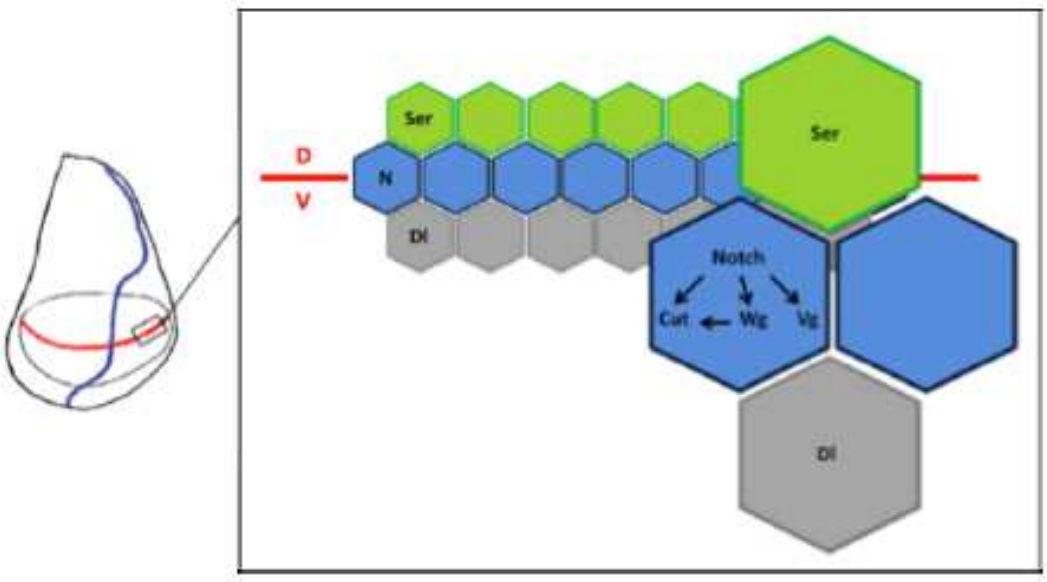

Figure 6 Notch signaling defines the D/V boundary.

On the left side, schematic representation of the wing imaginal disc divided by the two lineage boundaries: the D/V boundary (in red) and the A/P boundary (in blue). On the right panel, schematic representation of how Notch signaling maintains the D/V boundary. Ser (from dorsal green cells) and Dl (from ventral gray cells) activate Notch along the boundary and it, in turn, drives the expression of target genes including *wg*, *vg*, *cut*

Activation of Notch signaling in the D/V boundary leads to expression of Notch target genes such as *vestigial* (vg), *wingless* (wg) and *cut*. While wg is a soluble factor that diffuses, Vg and Cut are cell-autonomous transcription factors. Vg protein induces or maintains wg expression at the D/V boundary in the presence of high Notch signaling activity. Notch seems capable of inducing wg expression as well. Evidences indicate an elaborated feedback loop between Notch, wg and Cut in which Notch and wg cooperate to activate Cut expression and Cut and wg maintain each other expression (Neumann & Cohen, 1996) reviewed in (Brook, Diaz-Benjumea, & Cohen, 1996)).

6.3 The role of Notch signaling in cell-proliferation during development

In addition to controlling cell fate, Notch signaling has been also shown to support cell proliferation in a context-specific manner both in invertebrate and in vertebrates (Silvia Fre et al., 2005; Go, Eastman, & Artavanis-Tsakonas, 1998). Indeed, ectopic activation of Notch signaling in the WD results in substantial enlargement of the disc. Interestingly, Notch has both cell autonomous and non-cell-autonomous effect on mitotic activity (Go et al., 1998). Moreover the proliferative potential of certain tissues can be modulated by the synergistic action of Notch with other genes. Simultaneous activation of Notch and wg signaling results in synergistic effects inducing the formation of ectopic wing (Couso, Bishop, & Martinez Arias, 1994). The Notch/wg synergistic effect on cell proliferation is particularly interesting considering that abnormal activation of Notch or wg signaling in mammals has been associated with neoplasias (S. Fre et al., 2009; Ranganathan, Weaver, & Capobianco, 2011). In a genetic screen carried out in *Drosophila* for factors that synergize Notch-dependent proliferative events, the transcription factor Myocyte enhancer Factor 2 (Mef2) has been identified as a crucial partner of Notch in triggering massive proliferation and invasive metastatic growth through Jun N-terminal kinase (JNK) signal activation (Pallavi, Ho, Hicks, Miele, & Artavanis-Tsakonas, 2012).

6.4 The role of Notch signaling at mid-oogenesis in *Drosophila*

Notch signaling is also required for numerous important aspects of oogenesis in *Drosophila.* One of these occurs in the follicle epithelium (FE). The FE is a somatic monolayer of cells, which surrounds the cluster of 16 germ cells to form an egg chamber. Among the 16 germ cells, one differentiates as the oocyte

and the other 15 become nurse cells, which contribute maternal mRNAs and proteins and nutrients to the forming oocyte. Oogenesis occurs within the *Drosophila* ovary, which consists of 16-20 long tube-like structures called ovarioles. Each ovariole is formed by series of progressively older egg chambers. Egg chambers are staged depending on their morphological size from stage 1 (when the egg chamber is forming) to stage 14 (an egg chamber with a mature egg). The FE proliferates until stage 6 of oogenesis. At this point divisions cease and the FE nuclei undergo three rounds of endo-replication. Notch signaling activation is responsible for such proliferative to endo-replicative switch **(Fig.7A).** In fact, a Dl signal from the germ line has been proposed to activate Notch in the FE leading to the expression of the transcription factor Hnt and to downregulation of Cut **(Fig.7B).**

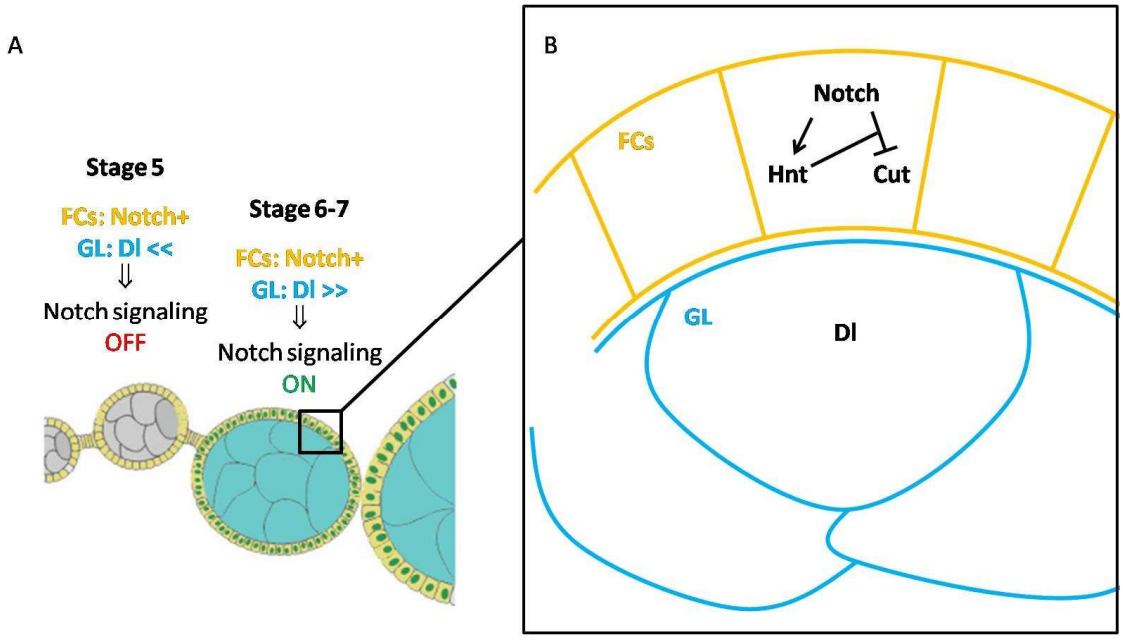

Figure 7 Notch signaling activation at mid-oogenesis.

A) At mid-oogenesis, follicle cells (FCs-yellow) switch from a proliferative to an endo-replicative stage due to Notch signaling activation. Low levels of Dl are expressed in the germ line cells (GL-blue). B) Notch signaling activation results in the upregulation of target genes including Hindsight (Hnt) and represses the transcription factor cut.

6.5 The importance of endocytosis in Notch signaling

Activation and deactivation of signaling can be tightly controlled by internalization, trafficking and degradation of receptors, ligands and transducers through the endocytic pathway (Sigismund et al., 2012). Consistent with this, endo-lysosomal components play a pleiotropic role in controlling signaling and tumor suppression. Notch signaling appears exquisitely regulated by endocytic trafficking. For the purpose of this Thesis, I will describe more in details two endocytic components extremely important for the trafficking of Notch and its activation.

6.6 The ESCRT machinery

6.6.1 ESCRT function

The Endosomal sorting complex required for transport (ESCRT) machinery controls endosomal sorting and multivesicular endosome (MVE) biogenesis, two key steps for the degradation of signaling molecules in the endo-lysosomal system **(Fig.8)**. The ESCRTs were originally identified in yeast for their crucial role in sorting ubiquitinated membrane proteins into the lumen of the vacuole, which functions as lysosome (Raymond, Howald-Stevenson, Vater, & Stevens, 1992). The main function of the ESCRT machinery is to deliver cargoes into intraluminal vesicles (ILVs) of newly formed MVE, and eventually send them toward degradation; In addition ESCRTs are also required for viral budding, for autophagy, for mRNA transport and for cytokinesis (reviewed in (Rusten, Vaccari, & Stenmark, 2011)). ESCRTs have been widely implicated in the regulation of many membrane-bound receptors (Camilla Raiborg & Stenmark, 2009). In *Drosophila,* loss of ESCRT function results in alteration of receptor signaling leading to excess of tissue

proliferation and to ectopic activation of several signaling pathways, including Notch. For this reason, ESCRT genes have been proposed to behave as tumor suppressor.

6.6.2 The composition of the ESCRT complexes

The ESCRT machinery is composed of four biochemically distinct protein complexes termed ESCRT-0, -I, -II, -III, according to their step-wise requirement to sort cargoes towards the lumen of MVEs. ESCRT-0, -I, -II possesses ubiquitin-interacting modules necessary for cargo sorting. In addition, ESCRT-I and –II cooperate to form invagination of the endosomal membrane. Conversely, ESCRT-III, the final complex in the pathway, has no ubiquitin-recognizing module but instead actively recruits de-ubiquitylating enzymes (DUBs) to remove ubiquitin from the cargoes before incorporation in ILVs. Moreover, the Vps32 subunits of the ESCRT-III complex form spiral-shaped oligomers that constrict the neck of the forming ILVs ultimately leading to severing the invaginating ILV neck. Finally, the ESCRT-III complex recruits the machinery that catalyzes the disassembly of the ESCRTs from the endosomal membrane at the end of the process of inward budding.

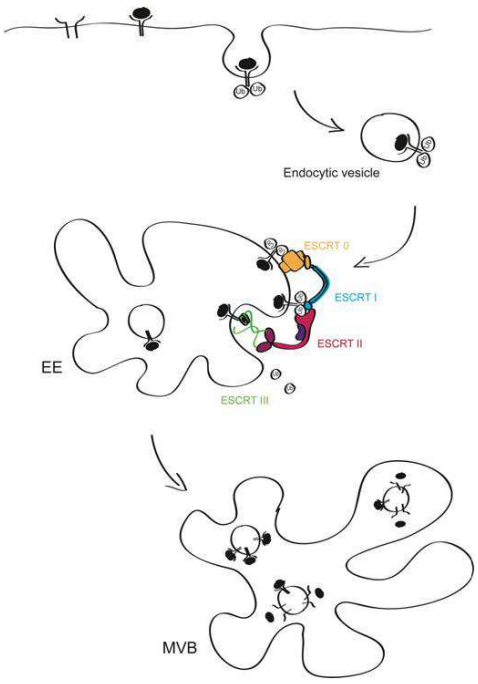

Figure 8 ESCRT machinery along the endocytic pathway

Early endosomes (EE) are predominantly tubule-vesicular structures, which constitute a major sorting platform in the cell, whereas late endosomes show the characteristics of typical MVE and are capable of fusing with lysosomes. The transition between these two stages occurs by progressive involution of the limiting membrane to form ILVs. The four ESCRTs are recruited to endosomes by the interaction with membranes, clathrin, lipids and ubiquitin and with each other.

The ESCRT-0 complex is formed by a heterodimer composed of Hrs (hepatocyte growth factor (HGF)-regulated Tyrosine kinase substrate) and Stam (signal transducing adaptor molecule). Hrs mediates the recruitment of ESCRT-0 to the endosomal membrane, through the interaction of the FYVE domain of Hrs with phosphatidylinositol-3-phosphate (PtdIns(3)P), present on endosomes. Eventually, clathrin is recruited to form a flat coat that sequesters ubiquitylated cargoes in microdomains on the endosomal membrane where ILV will occur (C Raiborg, Bremnes, et al., 2001). Hrs also possesses an ubiquitin interaction motif (UIM) to bind ubiquitin (Lloyd et al., 2002; Polo et al., 2002). Finally, ESCRT-0 recruits the ESCRT-I complex by direct interaction with the ESCRT-I component Tsg101. The ESCRT-I is made of Tsg101, vps28, vps37 and mvb12 (Chu, Sun, Saksena, & Emr, 2006; Morita, Sandrin, Alam, et al., 2007). The ESCRT-I is structurally organized in a core complex with flexible connected modules that

mediate interactions with other partners, including ESCRT-II components and ubiquitin through the ubiquitin E2 variant (UEV) domain of Tsg101.

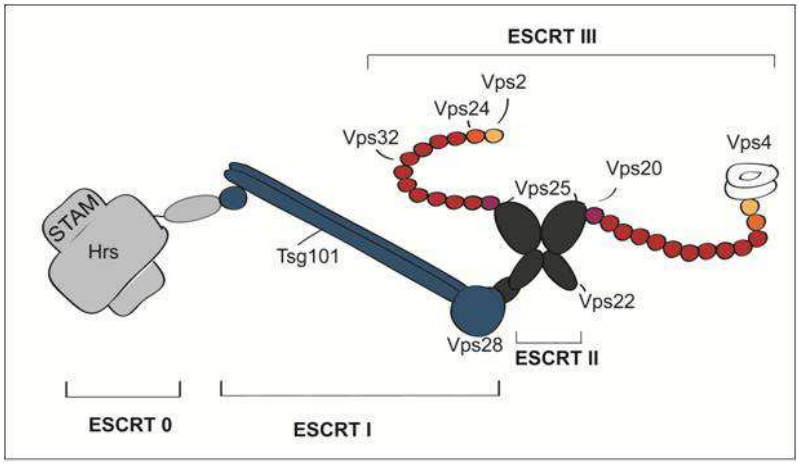

Figure 9 Schematic of the composition of ESCRT machinery in *Drosophila.*

ESCRT-II consists of a heterotetramer of two Vps25 molecules and one Vps22 and Vps36 (Im & Hurley, 2008; Teo, Perisic, González, & Williams, 2004), which act as a platform for assembly of ESCRT III. This complex consists of two polymeric filaments, each made of one Vps20, a polymer of Vps32 molecules, and one of each Vps24, and Vps2 (Teis, Saksena, & Emr, 2008). Vps2 and Vps24 cap the filament and provide connection to Vps4, an AAA ATPase that provides energy for disassembly and reuse of ESCRT III components (reviewed by (Williams & Urbé, 2007)) **(Fig.9).**

6.7 The V-ATPase

The Vacuolar-type H^+-ATPase (V-ATPase) is a proton pump that is conserved throughout the animal and plant kingdoms. It localizes at the plasma membrane and in a variety of intracellular compartments including lysosomes, endocytic and secretory vesicles (Stevens and Forgac, 1997). The V-ATPase has been mainly studied in yeast and its structure, function and regulation has been well characterized in the last 30 years. Yeasts lacking a functional V-ATPase are unable to grow at neutral pH and survive only at acid pH (5.5) (Nelson & Nelson, 1990; Yamashiro, Kane, Wolczyk, Preston, & Stevens, 1990). The structure of V-ATPases from animals, plants and fungi is quite similar and composed of two functional domains. V-ATPase shows a membrane-embedded V_0 sector and a peripheral catalytic V_1 sector (Stevens and Forgac, 1997). The integral membrane V_0 sector consists of at least six different subunits (a, c, c', c'', d, e), which assemble to form a 250-300 kDa highly hydrophobic proteolipid ring important for proton translocation. The cytoplasmic V_1 sector is formed by eight different subunits (A-H) and is a 570 kDa peripheral complex important for ATP hydrolysis (Forgac, 2007).

6.7.1 *Drosophila* V-ATPase

In *D. melanogaster* V-ATPase gene family has been identified during the late nineties by sequence similarities searches (Dow, 1999). The *Drosophila* V-ATPase is encoded by 33 genes **(Fig.10)**. Some subunits are represented by a single gene; this is the case of *vha55, vha44, vhaSFD, vhaAc45* and *vhaPRR*. Other subunits are encoded by multiple paralogs, and the expression of these genes varies considerably within the tissues (Allan, Du, Davies, & Dow, 2005). The presence of V-ATPase in *Drosophila* has been documented at apical membrane of highly

specialized epithelial cells such as those of salivary glands, Malpighian tubules and gut (Allan et al., 2005).

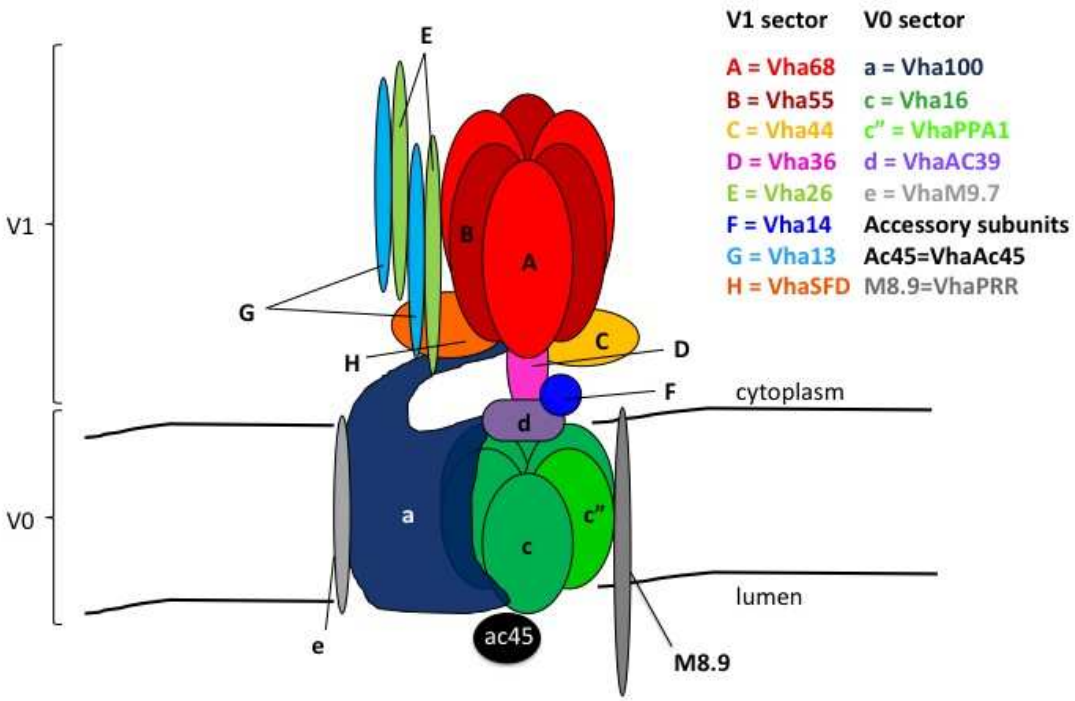

Figure 10 Schematic representation of *Drosophila* V-ATPase.

The genes that encode the V_1 sector of the *Drosophila* V-ATPase are the followings: *vha68-1*, *vha68-2*, *vha68-3* that codes for subunit A, *vha55* that codes for subunit B, *vhaSFD* for subunit SFD (H), *vha44* for subunit C, *vha36-1*, *vha36-2*, *vha36-3* for subunit D, *vha14-1*, *vha14-2* for subunit F, *vha13* for subunit G. The genes that encode for the V_0 sector instead are the followings: *vha100-1*, *vha100-2*, *vha100-3*, *vha100-4*, *vha100-5* for subunit a, *vha16-1*, *vha16-2*, *vha16-3*, *vha16-4*, *vha16-5* for subunit c, *vhaPPA1-1*, *vhaPPA1-2* for subunits PPA1 (c"), *vhaM9.7-1*, *vhaM9.7-2*, *vhaM9.7-3*, *vhaM9.7-4* for subunit M9.7 (e), *vhaAC39-1*, *vhaAC39-2* for subunit AC39 (d). The genes that encode for the accessory subunits are *vhaAC45* for AC45 subunit and *vhaM8.9* also known as *vhaPRR* for subunit M8.9.

Mutations in V-ATPase subunits show a Malpighian tubule phenotype due to defect in urinary acidification which prevents the precipitation of uric acid crystals (Allan et al., 2005). **Table 1** shows a comparative analysis of V-ATPase gene family for Human, *Drosophila* and Yeast.

Table 1 Comparative analysis of V-ATPase gene families.

Note that most subunits are shared by all V-ATPase. Only accessory subunits are not present in yeast.

Eukaryotic V-ATPase			
Subunits	***Drosophila***	**Human**	**Yeast**
V1			
A	*Vha68-1* *Vha68-2* *Vha68-3*	ATP6V1A - -	VMA1 - -
B	*Vha55* -‘	AT6V1B1 ATP6V1B2	VMA2 -
SFD (H)	*VhaSFD*	ATP6V1H	VMA13
C	*Vha44* -	ATP6V1C1 ATP6V1C2	VMA5 -
D	*Vha36-1* *Vha36-2* *Vha36-3*	ATP6V1D - -	VMA8 - -
E	*Vha26* -	ATP6V1E1 ATP6V1E2	VMA4 -
F	*Vha14-1* *Vha14-2*	ATP6V1F	VMA7 -
G	*Vha13*	ATP6V1G1 ATP6V1G2 ATP6V1G3	VMA10 - -
V0			
a	*Vha100-1* *Vha100-2* *Vha100-3* *Vha100-4* *Vha100-5*	ATP6V0A1 ATP6V0A2 ATP6V0A3 ATP6V0A4 -	VPH1 STV1 - - -
c	*Vha16-1* *Vha16-2* *Vha16-3* *Vha16-4* *Vha16-5*	ATP6V0C - - - -	VMA3 - - - -
c’	-	-	VMA11
PPA1 (c’’)	*VhaPPA1-1* *VhaPPA1-2*	ATP6V0B	VMA16
M9.7 (e)	*VhaM9.7-1* *VhaM9.7-2* *VhaM9.7-3* *VhaM9.7-4*	ATP6V0E - - -	VMA9 - - -
Ac39 (d)	*VhaAC39-1* *VhaAC39-2*	ATP6V0D1 ATP6V0D2	VMA6 -
Accessory subunits			
Ac45	*VhaAC45*	ATP6VAP1	-
M8.9	*VhaPRR*	ATP6VAP2	-

6.7.2 Mechanism of V-ATPase catalysis

V-ATPase operates with a rotary mechanism to drive protons across cell membranes. The translocation can occur only when the V_1 is assembled on V_0. ATP hydrolysis occurs at the interface of A and B subunits in the cytoplasmic V_1 sector, where they form the stator, a pseudo-hexameric arrangement with three catalytic sites for ATPs (Marshansky, Rubinstein, & Grüber, 2014; Muench, Trinick, & Harrison, 2011). Energy released from the ATP hydrolysis forces a proton to enter subunit a of the V_0 sector and protonate a universally conserved glutamic acid residue **(Fig.11)**.

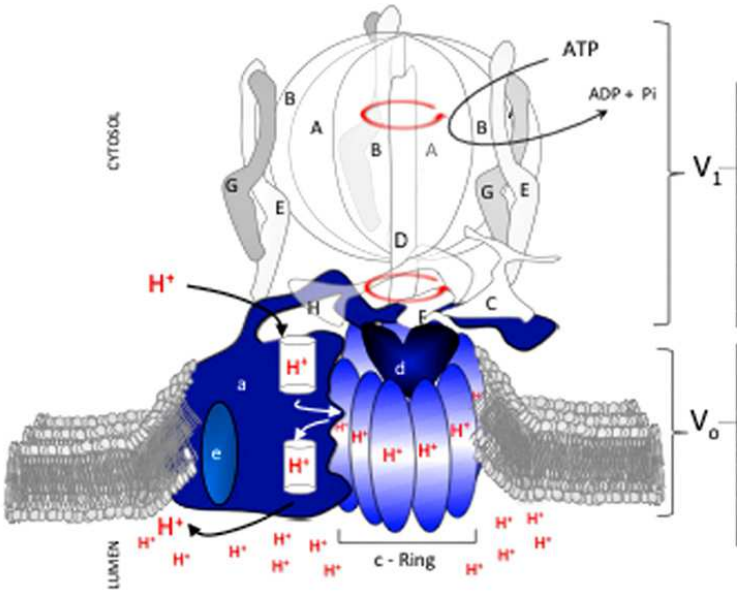

Figure 11 Mechanism of V-ATPase catalysis.

The V_1 sector is necessary for the hydrolysis of ATP at the cytosolic side of the membrane and V_0 to translocate protons against concentration gradients. Hydrolysis of 3 ATP in the stator (composed of subunits A and B) drives rotation of a shaft (subunits D, F, d) and is bound to a proteolipid ring that rotates and allow proton translocation. Adapted from (Hayek, Lee, & Parra, 2014)

Rotation of the central stalk formed by subunits F, D and d in turns drives rotation of the membrane-associated hexameric proteolipid ring composed of 5-6 subunits of c and one subunit of c'' (Y. Wang, Cipriano, & Forgac, 2007). Rotation of the proteolipid ring allows the proton to pass from two "half channels". One channel exchanges protons from one side of the membrane into the lipid bilayer,

and a second channel transfers the proton from the lipid bilayer to the other side of the membrane against a concentration gradient.

A core of three EG heterodimers serves to prevent rotation of the stator during ATP hydrolysis (Marshansky et al., 2014). Subunit C operates as a receptor for the dissociation signal. It is released from the pump when the V_0 and V_1 sectors need to be disassembled (Vitavska, Wieczorek, & Merzendorfer, 2003). Subunit H instead has been proposed to have an inhibitory effect on ATPase activity upon separation of the V_1 and V_0 sectors (Parra, Keenan, & Kane, 2000). Its absence in yeast results in the proper assembly of V-ATPase complex, which however do not possess any ATPase activity or the ability to translocate protons (Ho et al., 1993). In the integral V_0 domain, the membrane-embedded proteolipid ring is composed of several copies of the 16 kDa subunits c, which contain 4 transmembrane helices with two cytosolic loops exposed to the cytosol while the 23 kDa c'' subunit has five trasmembrane helices (Flannery, Graham, & Stevens, 2004; Y. Wang et al., 2007). The a subunit is the largest V_0 subunit of 100 kDa and possesses different isoforms (Manolson et al., 1994; Nishi & Forgac, 2000) that contain targeting information to direct V-ATPase complexes in different subcellular compartments (Manolson et al., 1994). For example, in budding yeast, the two isoforms of subunit a, Stv1 and Vph1are targeted to the late Golgi/endosome and to vacuoles, respectively (Manolson et al., 1994). Subunit d is present on the top of the proteolipid ring, it is peripherally associated to V_0 on the cytosolic side of the membrane and provides the connection between the central stalk and the ring. The e subunit is an extremely hydrophobic protein associated with the c subunit (Ludwig et al., 1998) that perhaps prevents proton leakage. In addition, two accessory subunits that are not present in yeast have been associated with the V_0 sector: Ac45 and M8-9 whose function might be dispensable for V-ATPase activity.

The accessory subunit Ac45 is a globular protein that resides in the luminal side of the V_0 sector (Rawson et al., 2015). Recent studies have shown that AC45 might be a regulatory subunit for proper V-ATPase recruitment at the plasma membrane and Ca^{2+}-dependent exocytosis (Jansen et al., 2012) . The subunit M8.9 has been recently identified as the (pro) renin receptor and it seems to have a dual role: (i) in the recruitment of Wnt receptor complex into the acidic microenviroment (Buechling et al., 2010; Cruciat et al., 2010; Hermle, Saltukoglu, Grünewald, Walz, & Simons, 2010) (ii) in the renin-angiotensin system that also regulates V-ATPase activity (Burcklé & Bader, 2006).

6.7.3 Regulation of V-ATPase function

Regulation of V-ATPase activity is accomplished through a number of mechanisms, including reversible dissociation of V_1V_0 complexes, control of their cellular localization, and changes in the coupling efficiency of ATP hydrolysis with proton transport. The V_1 sector can reversibly associate and dissociate from the V_0 sector depending on the cellular demand (review in (Forgac, 2007)). Subunits assembly into functional holoenzyme takes place in the ER and Golgi; alternatively, soluble V_1 and membrane-associated V_0 can be produced separately and later associated (Graham, Hill, & Stevens, 1998). Notably, neither disassembly nor reassembly of V-ATPase requires new protein synthesis. Dissociation and assembly appear to be independently controlled processes because dissociation but nor reassembly requires an intact microtubular network (T. Xu, 2001), whereas reassembly but not dissociation requires a protein complex called RAVE (regulator of the ATPase of vacuolar and endosomal membranes) (Seol, Shevchenko, & Deshaies, 2001). In yeast, dissociation of the complex occurs rapidly in response to glucose depletion. In insects assembly of the V-ATPase is under the control of Protein kinase A (PKA), although PKA independent

mechanism has also been demonstrated (Tiburcy, Beyenbach, & Wieczorek, 2013). In mammals, regulation of V-ATPase assembly appears to be dependent on Phosphoinositide-3 kinase (PI3K) in response to stimuli such as elevated glucose concentrations (Marjuki et al., 2011) and on mTOR complex 1 (mTORC1) activity (Y. Xu et al., 2012). Recently, it has been shown that the V-ATPase complex acts in nutrient sensing. Upon the current model, V-ATPase senses the amino acid levels in the lysosomes and is required for the switch between anabolic and catabolic processes of the cell (Zoncu et al., 2011) . Interestingly, V-ATPase assembly appears to be increased upon amino acid starvation and the amino acid-dependent change in assembly seem independent on mTORC1 or PI3K signaling, suggesting that V-ATPase assembly involve distinct signaling pathways and quite complex distinct mechanisms (Stransky & Forgac, 2015).

6.7.4 Main function of V-ATPase: acidification

The main function of the V-ATPase is to acidify intracellular compartments and the extracellular milieu by pumping protons across membranes. Acidification is required for a number of key cellular processes including lysosomal-mediated degradation, receptor-mediated endocytosis, proton-coupled transport of ions and small molecules, ligand-receptor dissociation and for the movement of carrier vesicles from early to late endosomes (reviewed in (Forgac, 2007; Stevens and Forgac, 1997). Physiologically, in renal intercalated cells, in osteoclasts and epididymal clear cells, V-ATPase is located at the plasma membrane where it exerts its role in urine acidification (Brown, Smith, & Breton, 1997), bone resorption (Chatterjee et al., 1992) and sperm maturation (Shum, Da Silva, Brown, & Breton, 2009) respectively. Accordingly, perturbation of V-ATPase function is associated with multiple diseases including lysosomal storage disorders, neurodegeneration, myopathy, bone diseases and even cancers. Increased

expression or activity of V-ATPase is displayed by almost all cancers, where it is thought to contribute to extracellular matrix degradation and tumor spreading (Martinez-Zaguilan, Lynch, Martinez, & Gillies, 1993). The V-ATPase activity is critical for pH homeostasis and organelle acidification, as well as generation of the membrane potential that drives cellular metabolism. In early *Xenopus* embryo, both cytoplasmic pH and membrane voltage are required for establishing the left-right axis (Dany S Adams et al., 2006). Moreover, ion flux *per se* is necessary for *Xenopus* tail regeneration and correct neuronal patterning in the new tissue (D. S. Adams, Masi, & Levin, 2007).

6.7.5 Unconventional V-ATPase functions

Beside its role in acidification, It has been suggested that V-ATPase might have different function beyond that of proton pump (Finbow et al., 1994; Hiesinger et al., 2005; Peters et al., 2001; Zoncu et al., 2011). Interestingly, evidence in *Drosophila* and *Manduca* have also shown that the c subunit of the V_0, also called ductin, can assemble in a ring-shaped structure which forms the connexon channel of gap junctions and mediates exchange of soluble factors (Finbow et al., 1994). The c subunits can therefore assemble to form a channel complex for the V_0 sector of the V-ATPase or as part of the connexon channel for gap junctions, depending on the dual orientation that the c subunit can assume (Dunlop, Jones, & Finbow, 1995).

In addition, it has been postulated that the V_0 sector of the V-ATPase in *S. cerevisiae* participates in membrane fusion events, independent of proton translocation (Peters et al., 2001). In *Drosophila* the neuronal specific isoform of a-subunit (Vha100-1) has been proposed to act in fusion of synaptic vesicles, a process necessary for neurotransmitter release (Hiesinger et al., 2005; Williamson, Wang, Haberman, & Hiesinger, 2010). In worms, the V_0 is required for apical

protein secretion and in *zebrafish* it appears to mediate fusion between phagosomes and lysosomes during phagocytosis (Peri & Nüsslein-Volhard, 2008). Finally in mammals V-ATPase regulates insulin secretion in pancreatic beta-cells independent of the pH of the secretory granules (Sun-Wada et al., 2006). However the role of V_0 sector in membrane fusion is considered controversial and it remains difficult to rule out indirect effects on acidification (Coonrod et al., 2013).

6.7.6 Transcriptional regulation of V-ATPase expression: the role of TFEB/Mitf transcription factors family

Recently, studies in vertebrate systems have indicated that V-ATPase expression is regulated by the Transcription Factor EB (TFEB), a member of the TFEB/Microphtalmia associated transcription factor (Mitf) bHLH leucine-zipper family (Palmieri et al., 2011; Sardiello et al., 2009). TFEB proteins preferentially form homodimers or heterodimers with family members and bind to E-box related DNA sequences (CANNTG) in the promoter region of target genes. These sequences have been named Coordinated Lysosomal Expression and Regulation (CLEAR) sites and consist of a palindromic 10-base pair GTCACGTGAC motif present either as a single sequence or in multiple copies, which appear highly enriched in the promoter regions of not only V-ATPase subunit genes but of several lysosomal and autophagy genes (Palmieri et al., 2011). In vertebrates, TFEB functions as a regulator of lysosomal biogenesis and autophagy in an axis with V-ATPase and mTOR that senses the nutritional status of the cell (Settembre et al., 2011; Zoncu et al., 2011). Interestingly, TFEB was also shown to be essential for placental vascularization (Steingrímsson, Tessarollo, Reid, Jenkins, & Copeland, 1998) while MITF, another member of the family, has been shown to have a role in eye development and development of specialized cell types, including osteoclasts, melanocytes and mast cells (Hemesath et al., 1994)(reviewed in (José A Martina, Diab, Li, & Puertollano, 2014)). Therefore, the transcription factor TFEB/MITF

family might control organ development by regulating signaling in the endo-lysosomal system. A single ortholog of vertebrate TFEB/MITF transcription factors is encoded by the *Drosophila* genome (Jón Hallsteinn Hallsson, Haflidadóttir, Schepsky, Arnheiter, & Steingrímsson, 2007). Over-expression of *Drosophila* Mitf in eye imaginal discs has been shown to perturb eye development (Jón H Hallsson et al., 2004). This phenotype resembles the one of its vertebrate MITF counterpart suggesting that the function of the TFEB/MITF family in tissue patterning is evolutionarily conserved (Jón H Hallsson et al., 2004). Despite this, it is unknown whether *Drosophila* Mitf controls transcription of homologs of TFEB target genes, including V-ATPase subunits or endo-lysosomal biogenesis and autophagy, and finally how it functions in regulation of tissue patterning.

6.8 Roles of endocytic trafficking components in ligand-dependent and ligand-independent Notch activation

As previously discussed, Notch signaling is highly sensitive to dis-regulation of the endo-lysosomal system. *Drosophila* mutations that block Notch trafficking at different endocytic steps have different effects on Notch signaling activity. In general, mutations that block endocytic transport from the cell surface to the endosome appear to inhibit Notch signaling, whereas mutations that block endosomal sorting lead to excess of signaling (reviewed in (Baron, 2012; Hori, Sen, Kirchhausen, & Artavanis-Tsakonas, 2012)). The molecular basis of such effects is discusses below.

6.8.1 Current models for ligand endocytosis in activation of Notch signaling

The first evidence that endocytosis was required for Notch signaling came from the observation that transient removal of the vesicular trafficking regulator dynamin in developing flies phenocopies loss of Notch signaling, highlighting for

the first time the importance of endocytosis for both ligand and receptor to activate signaling (A L Parks, Klueg, Stout, & Muskavitch, 2000; Seugnet, Simpson, & Haenlin, 1997). Dynamin and other specialized components involved in endocytic internalization, including the epsin liquid facets, the E3 ubiquitin ligase Neuralized and Mind Bomb are required for ligand internalization and signaling ability of the signal-sending cells (Itoh et al., 2003; Overstreet, 2004; W. Wang & Struhl, 2004). Notch ligands are ubiquitinated by Neuralized and Mind Bomb and endocytosed in a process that requires liquid facets in the signal-sending cell (W. Wang & Struhl, 2004, 2005). Two popular models for the role of ligand endocytosis in Notch signaling have been proposed: (i) prior to Notch binding, endocytosis is required for ligand processing and recycling of a competent ligand back to the cell surface **(Fig.12a)**(W. Wang & Struhl, 2004) (reviewed in (Le Borgne, Bardin, & Schweisguth, 2005; M. B. Wilkin & Baron, 2005)) and (ii) endocytosis by the ligand cell produces mechanical force to pull on Notch and induce structural changes leaving the S2 cleavage site unprotected allowing proteolysis and NICD release **(Fig. 12b)** (Meloty-Kapella, Shergill, Kuon, Botvinick, & Weinmaster, 2012; Nichols et al., 2007; A L Parks et al., 2000; Windler & Bilder, 2010).

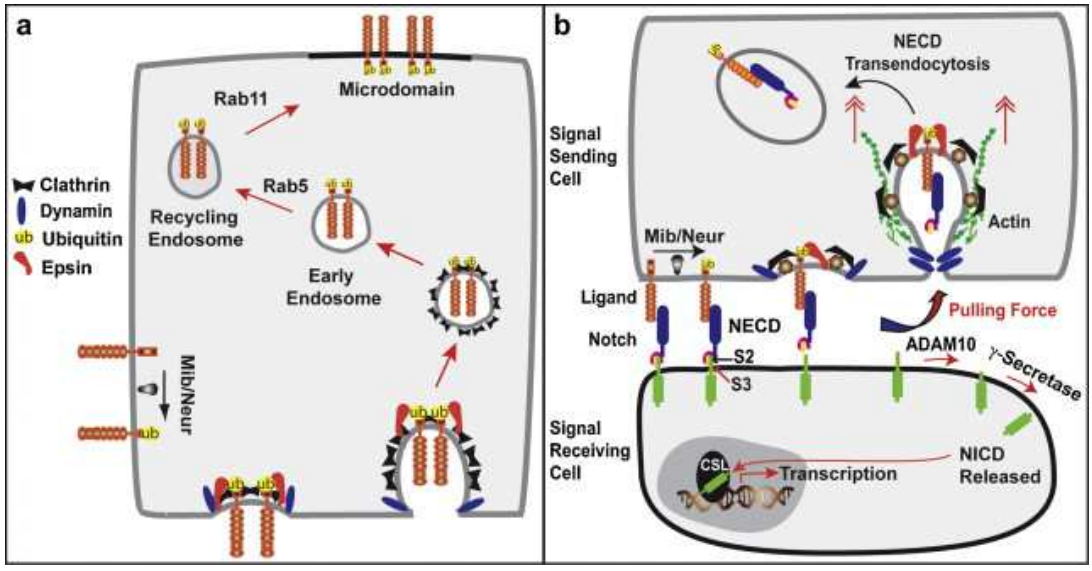

Figure 12 Proposed models for ligand-induced endocytosis in Notch signaling.

A) Schematic representation of the "recycling model" where ligands need to be endocytosed and reach microdomains to activate Notch pathway. B) Schematic representation of the "pulling force" model, where the endocytosis of the ligand is needed to generate the force sufficient for Notch ectodomain shedding. Adapted from (Musse, Meloty-Kapella, & Weinmaster, 2012)

6.8.2 Canonical ligand-dependent Notch activation

A number of studies have highlighted the requirement of endocytosis also of Notch receptor itself in productive signaling. In particular, in *Drosophila* mutants for proteins such as dynamin, the GTPase Rab5 and the endocytic syntaxin avalanche(Avl), which are required for cargo internalization and fusion with early endosomes, Notch accumulates at or below the plasma membrane and Notch signaling activation is significantly reduced in imaginal discs and in the FE at mid-oogenesis, a model of ligand-dependent signaling (Lu & Bilder, 2005; Vaccari, Lu, Kanwar, Fortini, & Bilder, 2008). In addition, previous work in our lab using the same *Drosophila* tissues has demonstrated the importance of V-ATPase activity for ligand-dependent Notch signaling activation (Vaccari, Duchi, Cortese, Tacchetti, & Bilder, 2010). *Drosophila* V-ATPase mutants show impaired acidification of the endo-lysosomal compartment and are unable to degrade cargoes, thus suggesting that V-ATPase-dependent acidification not only promotes the degradation of Notch in the lysosome but also its activation. Concomitantly, another study in *Drosophila* have reached the same conclusion by showing that mutants for Rabconnectin-3 alpha and beta, proteins implicated in the regulation of V-ATPase display impairment in Notch signaling activation (Yan, Denef, & Schüpbach, 2009).

6.8.3 Ligand-independent Notch activation

ESCRT complexes are instead required for attenuation of Notch signaling. In fact, mutations in *Drosophila* components ESCRT-I, ESCRT-II and ESCRT-III complexes all display accumulation of Notch receptor in early endosomes and ectopic ligand-independent Notch signaling activation (Herz et al., 2006; Menut et al., 2007; Moberg, Schelble, Burdick, & Hariharan, 2005; Thompson et al., 2005;

Vaccari & Bilder, 2005; Vaccari et al., 2009, 2008). Mechanisms underlying Notch signaling by ESCRTs might be complex, as distinct members of the ESCRT complexes exhibit non-overlapping phenotypes (Herz, Woodfield, Chen, Bolduc, & Bergmann, 2009). Moreover, *Drosophila* Hrs, which codes for one of the two obligate ESCRT-0 component has been shown to be dispensable for Notch signaling activation and tumor suppression (Vaccari et al., 2008). In addition, in a Hrs mutant, Notch fails to be degraded but it is otherwise normally activated (Lloyd et al., 2002; Vaccari et al., 2008). Another tumor suppressor gene involved in Notch trafficking has been identified in the *lethal giant discs (lgd)* gene that codes for a conserved C2 protein that binds to phospholipids and phosphorylated proteins present on endosomes. When *lgd* function is compromised strong ligand-independent Notch activation and hyperplastic overgrowth of *Drosophila* imaginal discs are observed. In addition, endosomes are enlarged and accumulate ubiquitinylated transmembrane proteins including Notch. Later studies have shown that Lgd interacts with the ESCRT-III component Shrub the *Drosophila* homologue of Vps32, and this interaction, which takes place in the cytosol is required for the function of Shrub, indicating that Lgd might modulate the function of the ESCRT-III complex (Troost, Jaeckel, Ohlenhard, & Klein, 2012). Consistent with this, Hrs, Shrub and other ESCRT components are needed for the ectopic Notch signaling seen in *lgd* mutants (Childress, Acar, Tao, & Halder, 2006; Gallagher & Knoblich, 2006; Jaekel & Klein, 2006; Troost et al., 2012).

The observations that different defects in vesicular trafficking affect Notch signaling confirm that endocytosis is required for Notch signaling and raise also the possibility that Notch trafficking is an important mechanism for Notch signaling modulation. It is apparent that in the case of *lgd* mutant tissue, Notch must be transported to late endosome/lysosomes for activation to occur and

required the fusion of endosome with lysosomes, while in ESCRT mutant cells Notch seems to accumulate in an earlier endosomal compartment, which is Hrs-positive (Schneider, Troost, Grawe, Martinez-Arias, & Klein, 2013; Troost et al., 2012; Vaccari & Bilder, 2005). This evidence suggests that activation of Notch may occur in different endosomal compartments with different mechanisms.

Fig. 13 shows the role of endocytic components in ligand-dependent and ligand-independent Notch signaling

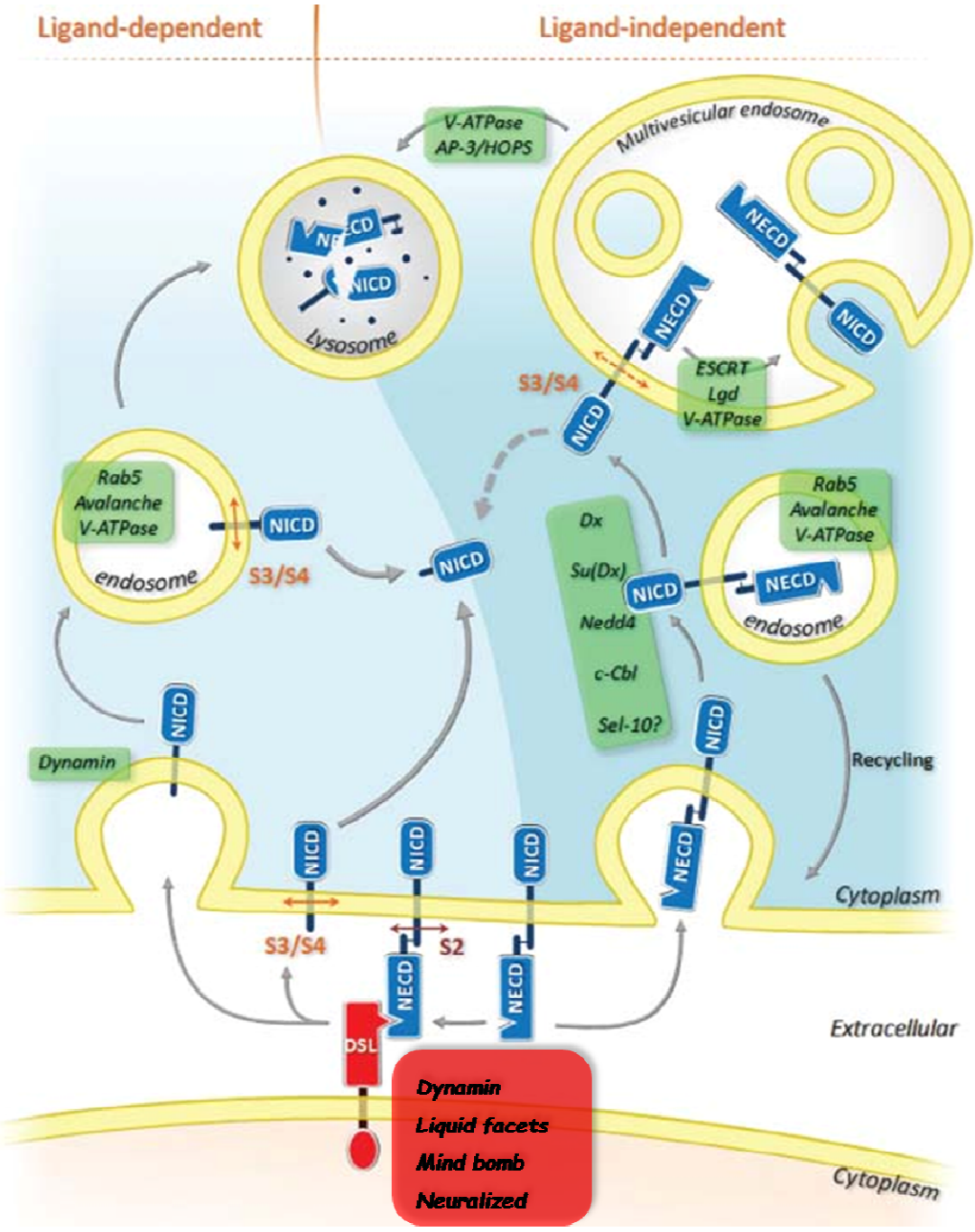

Figure 13 Endocytic regulation of Notch signaling.

Endocytic factors that promote signaling are Dynamin, liquid facets, neuralized, Mind bomb, Rab5,Avalanche V-ATPase Deltex and AP-3, HOPs, while those involved in signaling downregulation are Kurtz, ESCRTs, ITCH/[Su(Dx)], Lgd, cbl and Sel10. Adapted from (Le Bras, Loyer, & Le Borgne, 2011)

6.8.4 Notch ubiquitination

The ability of the Notch receptor to traffic via different endocytic routes depends on its ubiquitination. E3 ubiquitin ligases have been shown to ubiquitinate Notch, to regulate its trafficking and sorting and ultimately its signaling activity. In particular, overexpression of the RING finger E3 ubiquitin ligase Deltex (Dx) in *Drosophila* mimics the phenotypes associated with *Notch* gain-of-function mutations, and loss of Dx function results in wing-margin phenotypes that are reminiscent of loss of *Notch* function, indicating a positive role in Notch signaling (Hori et al., 2004; Matsuno, Diederich, Go, Blaumueller, & Artavanis-Tsakonas, 1995; A. Mukherjee et al., 2005). However, complete elimination of Dx function affects only a narrow subset of Notch-dependent patterning processes in *Drosophila* suggesting that Dx contributes to the robustness of signaling in some context but is dispensable for most of Notch decisions. Genetic studies uncovered a number of components required for Dx-induced Notch signaling. Mukherjee et. al showed that Dx, in combination with Kurtz (Krz), the single *Drosophila* homologue of mammalian non-visual β-arrestins, functions as a negative regulator of Notch promoting polyubiquitination of the receptor (A. Mukherjee et al., 2005). The strong downregulation of Notch signaling produced by the combined effect of Dx and Krz is suppressed by chloroquine, a reagent known to inhibit lysosomal degradation by raising intracellular pH, confirming that Dx and Krz regulate the sorting and degradation of Notch protein via an endosomal/lysosomal pathway. The Dx and Krz co-expression phenotype is also suppressed by reducing the activity of the ESCRT III component Shrub (Hori, Sen, Kirchhausen, & Artavanis-Tsakonas, 2011). Mutation or RNAi knock-down of Shrub results in a strong-upregulation of the Dx-induced

Notch signal in a ligand-independent manner. In contrast, co-expression of Dx with Shrub results in Notch signal-downregulation. In both circumstances Notch accumulates on the Rab7-positive, late endosomes. Other members required for Dx-induced Notch activation have been identified in components of the HOPS (homotypic fusion and vacuole protein sorting) and AP-3 (Adaptor protein-3) complexes, genes that are known for their role in biogenesis of lysosomal-related pigment granules, lysosomes and autophagy (M. Wilkin et al., 2008). Mutations in genes encoding members of these complexes result in loss of Notch signaling activity. Interestingly, the differences between up and down-regulation of Notch is correlated with its ubiquitination status.

Interaction of Dx with Krz promotes poly-ubiquitination of Notch associated with its down-regulation. Conversely, Dx promotes Notch mono-ubiquitination, which helps to evade ESCRT-mediated sorting and ultimately lysosomal degradation (M. Wilkin et al., 2008). In such condition, the cytoplasmic domain of Notch would be exposed to the cytoplasm while its extracellular domain to the intra-luminal environment. Therefore, NECD is subjected to proteolytic degradation by a yet unknown mechanism that however seems independent of Kuz-mediated S2 cleavage (Schneider et al., 2013; Shimizu et al., 2014). The resulting membrane tethered, truncated product would be then a substrate for intra-membrane proteolysis by γ-secretase, which is required for Dx and lgd-induced Notch activation and is present and more active in the limiting lysosomal membrane (Pasternak et al., 2003).

Other E3 ubiquitin ligases involved in Notch signaling include members of the HECT E3 ligases, such as Su(Dx)/Itch/AIP4 and Nedd4, which are implicated in the sorting and lysosomal degradation of unactivated Notch. Gain-of-function of *Su(Dx)* and *Nedd4* cause a *Notch* loss-of-function phenotype in the *Drosophila* wing

margin, indicating that these E3 ligases exert a negative regulation on Notch signaling in a subset of Notch decisions (Fostier, Evans, Artavanis-Tsakonas, & Baron, 1998; Sakata et al., 2004; M. B. Wilkin et al., 2004). Su(Dx) blocks Dx-induced Notch activation by diverting endocytosed Notch from the late endosome limiting membrane into the MVEs, thus sequestering it from activation. Su(Dx) has been considered a negative regulator of Notch signaling, however, the phenotype of Su(Dx) null mutations were also shown to be temperature sensitive (Cornell et al., 1999; Fostier et al., 1998; Mazaleyrat et al., 2003). A recent study revealed that Su(Dx) can also promote Notch signaling at low temperatures (Shimizu et al., 2014). Interestingly, it has been shown that Su(Dx) promotes Notch endocytosis through a glycophosphatidylinositol (GPI)-positive, sterol-dependent endosomal route in a temperature-dependent manner. Conversely, Dx promotes Notch internalization through a GPI-negative sterol-independent route toward late endosomes/lysosomes and this route is insensitive to temperature (Shimizu et al., 2014). Interestingly, at low temperatures, both Dx- or Su(Dx)- dependent routes leads to Notch activation. Conversely, at moderate temperatures, Su(Dx) induces Notch degradation, and both Dx and Su(Dx) are in competition for Notch to enter their routes (Shimizu et al., 2014).

6.9 The role of ligands in ligand-independent Notch activation

Ligands have been vey recently shown to protect the cell from ligand-independent Notch signaling activation *in cis*. Surprisingly, upon removal of both *cis*- and *trans*- ligands, Notch appears to become activated cell autonomously in both the ovarian follicle cells and WDs in *Drosophila,* suggesting that *cis*-inhibition efficiently blocks ligand-independent Notch activity (Palmer et al., 2015). Moreover, it has been shown that increasing *cis*-ligand expression levels can reduce ligand-independent Notch signaling activation that occurs in mutants for

lgd, *shrub*, and *dx* (Mukherjee et al., 2011; Palmer et al., 2015). Finally, ligand-independent activation of the receptor has been recently shown to be essential for the normal development of *Drosophila* blood cells (Mukherjee et al., 2011). However, there has been little evidence that such mechanism is required in mammalian development.

6.10 CSL-independent Notch signaling activation

Several papers suggested that Notch could signal independently of CSL. In these cases, NICD have been proposed to interact directly with transcription factors other than members of the CSL family, such as Mef2 and LEF1 (Ross & Kadesch, 2001; Wilson-Rawls, Molkentin, Black, & Olson, 1999). In addition, it has been shown that Notch receptor can interact with proteins within the cytoplasm that function without changes in gene expression. This is the case of several *Notch* alleles that alter adult *Drosophila* SOP development. In particular, in one class of Notch alleles represented by certain Abruptex (Ax) mutations (Ax^{59d}, Ax^{M1}) and *Michrochaete defective (Mcd)* mutations, the establishment of the PNC does not occur. In fact, the alleles prevent Ac-sc expression resulting in loss of the adult sensory bristle phenotype. The phenotype has been shown to be independent of CSL/Su(H) and it is suppressed by removing the function of the Wnt regulator *Shaggy/Zeste White 3 Kinase (Sgg/zw3)* or of Dx (Brennan et al., 1999; Ramain et al., 2001), supporting a possible interaction of Notch receptor with component of the wg pathway. Consistent with this, it was demonstrated that a membrane-bound form of Notch physically interacts with β-catenin and modulates Wnt signaling by negatively regulating β -catenin activity in flies (Hayward et al., 2005).

7 AIM OF THE WORK

During my Ph.D, I have been involved in two different projects;

7.1 Project 1: The role of ESCRT-0 in Notch signaling and tumor suppression

It has been previously shown that *Drosophila* epithelial imaginal discs lacking components of the ESCRT-I, -II, or -III complexes overproliferate, fail to polarize apico-basally, lack terminal differentiation and display increased Notch signaling and JNK-and Hippo-dependent apoptosis (Herz et al., 2006, 2009; Menut et al., 2007; Moberg et al., 2005; Thompson et al., 2005; Vaccari & Bilder, 2005; Vaccari et al., 2009). In contrast, the role of ESCRT-0 in such processes had not been studied. A *Stam* mutant and a double mutants for *Hrs* and *Stam*, encoding for two components of the ESCRT-0 complex had just been characterized in *Drosophila* tracheal cells when I started to work on the project. They were shown to possess reduced FGF (fibroblast growth factor) receptor signaling and to fail to undergo correct morphogenesis (Chanut-Delalande et al., 2010). However, it was not clear whether they display loss of tumor suppression or altered Notch trafficking and signaling. Thus, in this project I investigated whether mutations in *Stam* or both *Hrs* and *Stam* led to loss of tumor suppression phenotype in *Drosophila* epithelial tissues, and whether ESCRT-0 complex is required for endosome maturation and for Notch signaling activation or downregulation.

7.2 Project 2: Regulation of V-ATPase expression in a subset of Notch-dependent developmental processes

In the second part of my Ph.D, I have been involved in studying the role and the regulation of V-ATPase in Notch-dependent developmental processes in *Drosophila* developing tissues. Recently, it has been found that the V-ATPase is controlled by the lysosomal transcription factor TFEB and is required to regulate mTOR as well as Wnt and Notch signaling (Cruciat et al., 2010; Palmieri et al., 2011; Vaccari et al., 2010; Zoncu et al., 2011) . In particular, we recently reported a key role of V-ATPase in the activation of Notch in endosomes (Vaccari et al., 2010). However, whether and how the TFEB/V-ATPase axis controls N signaling is not known. In this study, I investigated whether Mitf, the unique *Drosophila* homolog of TFEB, regulates V-ATPase expression, lysosomal biogenesis and Notch signaling activation in *Drosophila*.

8 MATERIALS AND METHODS

8.1 Fly cultivation

Flies were maintained on standard yeast/cornmeal/agar media. All crosses were performed at 25°C unless otherwised stated.

8.2 Genetics

8.2.1 Genetics of Project 1

Drosophila lines used in the first projects are: FRT40AHrs^{D28} referred in the text as *Hrs* (Lloyd et al., 2002); and FRT40A$Stam^{2L289}$ referred in the text as *Stam* (Chanut-Delalande et al., 2010) and the triple mutant *Hrs Staml(2)gl*. (Bloomington *Drosophila* Stock Center (BDSC) #3914, #41804 and #41806, respectively). Genetically, the mutations Hrs and *Stam* behave as null alleles. Due to early stop codon Hrs^{D28}expresses only the amino terminal first quarter of the protein, lacking most functional domains (Lloyd et al., 2002). Similarly, $Stam^{2L2896}$ harbors a nonsense mutation leading to an early stop codon at amino acid 6 (Chanut-Delalande et al., 2010).

Genotypes of the experiments presented in the figures for project 1 are listed in more detail in **Table 2**.

8.2.1.1 Generation of Hrs,Stam recombinants

The *Hrs*, *Stam* recombinants were generated via standard genetic procedures. *Hrs* females were crossed with *Stam* males to generate recombinogenic F_1 females. These were then crossed to a balancer stock and the F_2 male progeny was stocked and crossed back to *Hrs* and *Stam* mutants and relative deficiencies (*Hrs* deficiency: BDSC #9543; *Stam* deficiency BDSC #7821). Males that failed complementation with both loci but complemented $l(2)gl^4$or a *l(2)gl*

deficiency (BDSC #3634) were kept as independent recombinant fly lines (**see** complementation test in **Table 4**.

Table 2 Genotypes Project 1

Fig Panel	Label, if any	Genotype
Fig. 15		
A	WT mosaics	*P(mini-w, ubi-GFP) FRT40A/FRT40A; GR1-GAL4 UAS-FLP/+;*
B	Hrs mosaics	*P(mini-w, ubi-GFP) FRT40A/FRT40A $Hrs^{D28;}$ GR1-GAL4 UAS-FLP/+;/+*
C	Stam mosaics	*P(mini-w, ubi-GFP) FRT40A/FRT40A $Stam^{2L2896;}$ GR1-GAL4 UAS-FLP/+;/+*
D	Hrs, stam mosaics	*P(mini-w, ubi-GFP) FRT40A/FRT40A Hrs^{D28} $Stam^{2L2896;}$ GR1-GAL4 UAS-FLP/+;/+*
E	WT mosaics	*eyFLP/+; FRT40A/FRT40A P(mini ubi GFP)*
F	Hrs mosaics	*eyFLP/+; FRT40A Hrs^{D28}/FRT40A P(mini ubi GFP)*
G	Stam mosaics	*eyFLP/+; FRT40A $Stam^{2L2896}$/FRT40A P(mini ubi GFP)*
H	Hrs, stam mosaics	*eyFLP/+; FRT40A Hrs^{D28} $Stam^{2L2896}$/FRT40A P(mini ubi GFP)*
I	WT	*eyFLP/+; FRT40A /FRT40A P(mini w, cl)*
L	Hrs	*eyFLP/+; FRT40A Hrs^{D28} /FRT40A P(mini w, cl)*
M	Stam	*eyFLP/+; FRT40A $Stam^{2L2896}$/FRT40A P(mini w, cl)*
N	Hrs Stam	*eyFLP/+; FRT40A Hrs^{D28} $Stam^{2L2896}$/FRT40A P(mini w, cl)*
Fig. 16		
A	WT	*eyFLP/+; FRT40A /FRT40A P(mini w, cl)*
B	Hrs	*eyFLP/+; FRT40A Hrs^{D28} /FRT40A P(mini w, cl)*
C	Stam	*eyFLP/+; FRT40A $Stam^{2L2896}$/FRT40A P(mini w, cl)*
D	Hrs Stam	*eyFLP/+; FRT40A Hrs^{D28} $Stam^{2L2896}$/FRT40A P(mini w, cl)*
Fig. 17		
A	WT mosaics	*eyFLP/+; FRT40A/FRT40A P(mini ubi GFP)*
B	Hrs mosaics	*eyFLP/+; FRT40A Hrs^{D28}/FRT40A P(mini ubi GFP)*
C	Stam mosaics	*eyFLP/+; FRT40A $Stam^{2L2896}$/FRT40A P(mini ubi GFP)*
D	Hrs, stam mosaics	*eyFLP/+; FRT40A Hrs^{D28} $Stam^{2L2896}$/FRT40A P(mini ubi GFP)*

Fig. 18		
A-C	Vps25	*eyFLP/+ FRT42D vps25^{A3}/FRT42D P(mini-w, cl)*
	Stam	*eyFLP/+; FRT40A Stam^{2L2896}/FRT40A P(mini w, cl)*
	hrs	*eyFLP/+; FRT40A Hrs^{D28} /FRT40A P(mini w, cl)*
	hrs, stam, lgl	*eyFLP/+; FRT40A Hrs^{D28} Stam^{2L2896}lgl/FRT40A P(mini w, cl)*
	WT	*eyFLP/+; FRT40A /FRT40A P(mini w, cl)*
Fig. 19		
A	WT	*eyFLP/+; FRT40A/FRT40A P(mini ubi GFP)*
B	Hrs	*eyFLP/+; FRT40A Hrs^{D28}/FRT40A P(mini ubi GFP)*
C	Stam	*eyFLP/+; FRT40A Stam^{2L2896}/FRT40A P(mini ubi GFP)*
D	Hrs Stam	*eyFLP/+; FRT40A Hrs^{D28} Stam^{2L2896}/FRT40A P(mini ubi GFP)*
E	Hrs	*P(mini-w, ubi-GFP) FRT40A/FRT40A HrsD28; GR1-GAL4 UAS-FLP/+;/+*
F	Stam	*P(mini-w, ubi-GFP) FRT40A/FRT40A Stam^{2L2896}; GR1-GAL4 UAS-FLP/+;/+*
G	Hrs	*P(mini-w, ubi-GFP) FRT40A/FRT40A HrsD28; GR1-GAL4 UAS-FLP/+;/+*
H	Stam	*P(mini-w, ubi-GFP) FRT40A/FRT40A Stam^{2L2896}; GR1-GAL4 UAS-FLP/+;/+*
Fig. 20		
A	WT	*eyFLP/+; FRT40A/FRT40A P(mini ubi GFP)*
B	Hrs Stam	*eyFLP/+; FRT40A Hrs^{D28} Stam^{2L2896}/FRT40A P(mini ubi GFP)*
C	Hrs Stam	*eyFLP/+; FRT40A Hrs^{D28} Stam^{2L2896}/FRT40A P(mini ubi GFP)*
D	Hrs Stam	*eyFLP/+; FRT40A Hrs^{D28} Stam^{2L2896}/FRT40A P(mini ubi GFP)*
Fig. 21		
A	WT	*eyFLP/+; FRT40A /FRT40A P(mini w, cl)*
B	Vps25	*eyFLP/+ FRT42D vps25^{A3}/FRT42D P(mini-w, cl)*
C	hrs, stam, lgl	*eyFLP/+; FRT40A Hrs^{D28} Stam^{2L2896}lgl/FRT40A P(mini w, cl)*
Fig. 22		
A	Hrs mosaics	*eyFLP/+; FRT40A Hrs^{D28}/FRT40A P(mini ubi GFP)*
B	Stam mosaics	*eyFLP/+; FRT40A Stam^{2L2896}/FRT40A P(mini ubi GFP)*
C	Hrs, stam mosaics	*eyFLP/+; FRT40A Hrs^{D28} Stam^{2L2896}/FRT40A P(mini ubi GFP)*

Fig. 23		
A	WT	*P(mini-w, ubi-GFP) FRT40A/FRT40A; GR1-GAL4 UAS-FLP/+;*
B	Stam	*P(mini-w, ubi-GFP) FRT40A/FRT40A $Stam^{2L2896;}$ GR1-GAL4 UAS-FLP/+;/+*
C	Hrs Stam	*P(mini-w, ubi-GFP) FRT40A/FRT40A Hr Hrs^{D28} $Stam^{2L2896;}$ GR1-GAL4 UAS-FLP/+;/+*
D	WT	*P(mini-w, ubi-GFP) FRT40A/FRT40A; GR1-GAL4 UAS-FLP/+;*
E	Stam	*P(mini-w, ubi-GFP) FRT40A/FRT40A $Stam^{2L2896;}$ GR1-GAL4 UAS-FLP/+;/+*
F	Hrs Stam	*P(mini-w, ubi-GFP) FRT40A/FRT40A Hrs^{D28} $Stam^{2L2896;}$ GR1-GAL4 UAS-FLP/+;/+*

8.2.2 Genetics of Project 2

8.2.2.1 GFP-trapped lines

The GFP trap lines: *GFP::Vha16-1* (G00007,); *GFP::VhaAC45* (ZCL0366), *GFP::Vha13*(CA07644); *YFP::Vha55* (CPTI100063); *GFP::VhaSFD* (G00259) were obtained from large-scale random transposon insertion project where a mobilizing transposable element containing an exon encoding GFP/YFP protein flanked by strong splice acceptor and donor sequences was randomly inserted in the *Drosophila* genome (Buszczak et al., 2007; Lowe et al., 2014; Morin, Daneman, Zavortink, & Chia, 2001). *YFP::Lamp1* insertion line CPTI001775 is from Kyoto/DGRC (Takáts et al., 2013). *GFP::CG8668* (117-2) was a gift of J. Zallen. The G/YFP cassette, which is inserted within the gene of interest behaves as an extra exon and undergoes splicing and translation to generate a chimeric protein. Therefore, the expression of the YFP/GFP is under the endogenous transcriptional and translational control of the gene of interest and it can be used to study the expression pattern of the gene of interest and sometimes its subcellular localization. **Fig.14** show schematic representations of the insertion points of the different *Drosophila* lines used in this study.

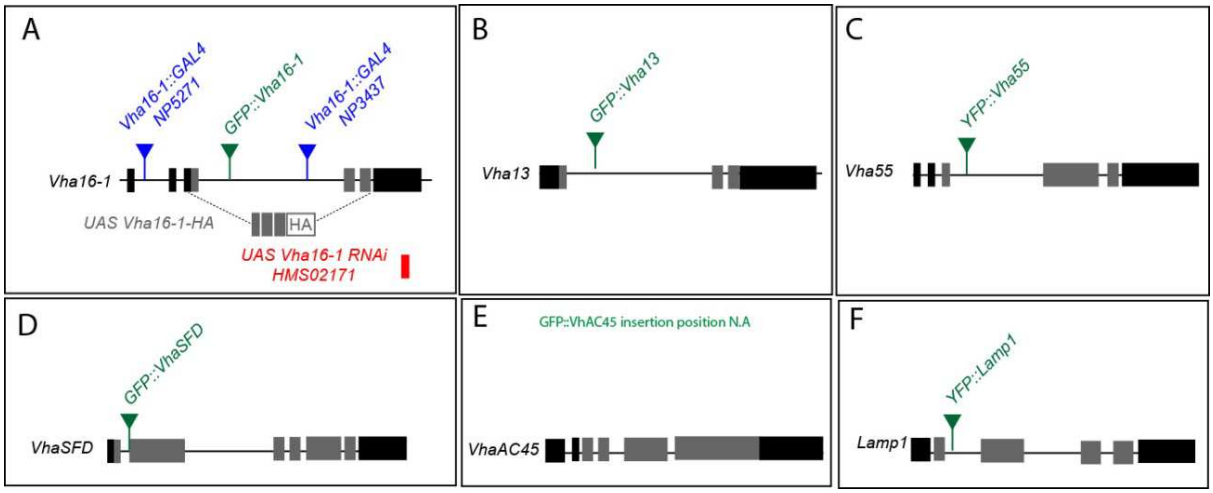

Figure 14 Schematic representation of the loci of the genes, which are potential target of TFEB.

A-F) Coding exons are in grey and non coding exons are in black. The GFP/YFP insertion points are shown in green, according to FlyBase. For Vha16-1 gene, two other Vha16-1::Gal4 lines were used. Gal4 insertion points are indicated in blue. A schematic of the UASVha16-HA is shown in grey while the region of the 3'UTR targeted by the Vha16-1RNAi line used in this study is shown in red.

8.2.2.2 Other Drosophila lines used for Project 2

Lines obtained from the Bloomington *Drosophila* Stock Center (BDSC) are: UAS Vha16-1 RNAi (#40923); Neur-LacZ (#4369); UASmCD8GFP(#5137); UASmCD8RFP; PannierGAL4 (#3039); Ms1096-Gal4 (#8860); Neur-Gal4 A101(#6393); Df(2R)BSC326 (#24351); Df(2R)ED1791 (#9063); Df(3R)ED6025 (#8964); P{lacW}Vha55j2E9 (#12128); P{EPgy2}VhaSFD EY04644 (#15758). The Vha16-1-Gal4 lines NP5271 and NP3437 are from Kyoto. UAS VhaPPA1-1 RNAi (#v47188) is from Vienna *Drosophila* Resouce Center (VDRC). UAS NICD and UAS NEXT were a gift of M. Fortini. E(spl)mβ lacZ and E(spl)m4 LacZ were gifts from E. Lai. UAS MITF and Uas MITFDN was a gift from F. Pignoni (Jón H Hallsson et al., 2004). The MitfDN carries a point mutation in the basic domain of the protein, preventing its binding with the DNA but not its homodimerization with other transcription factor molecules. Neur-GFP and NiGFP4mCherry5 (Couturier, Trylinski, Mazouni, Darnet, & Schweisguth, 2014)were a gift from Francois Schweisguth, ActGal4>GFPhLamp1 was a gift from Helmut Kramer. UAS E(spl)m8, and m4 were a gift of C. Delidakis. Misexpression in either larval or adult tissues

was achieved using the Gal4/UAS system (Duffy, 2000). Genotypes of the experiments presented in the figures for project 2 are listed in **Table 3**

Table 3 Genotypes Project 2

Fig Panel	Label, if any	Genotype
Fig. 24		
	control	w[1118]
	control	w[1118]
	ms1096>Mitf	Ms1096 GAL4/+;;Uas-Mitf/+
Fig. 25		
A	control	Ms1096 GAL4/+;
	ms1096>Mitf	Ms1096 GAL4/+;;Uas-Mitf/+
	ms1096>Mitf DN	Ms1096 GAL4/+;Uas-Mitf EA /+
B	control	Ms1096 GAL4/+;
	ms1096>Mitf	Ms1096 GAL4/+;;Uas-Mitf/+
Fig. 26		
A	ms1096>cd8GFP	Ms1096 GAL4/+;Uas-cd8GFP/+
B	control	Ms1096 GAL4/+;
	ms1096>Mitf	Ms1096 GAL4/+;;Uas-Mitf/+
	ms1096>Mitf DN	Ms1096 GAL4/+;Uas-Mitf EA /+
Fig. 27		
	ms1096>	Ms1096 GAL4/+;
	ms1096>Mitf	Ms1096 GAL4/+;;Uas-Mitf /+
	ms1096>Mitf DN	Ms1096 GAL4/+;Uas-Mitf EA /+
Fig. 28		
A and B	ms1096>YFP::Lamp1	Ms1096 GAL4/+; PBac{681.P.FSVS-1}Lamp1[CPTI001775]/+;
	ms1096>Mitf YFP::Lamp1	Ms1096 GAL4/+; PBac{681.P.FSVS-1}Lamp1[CPTI001775]/+; Uas-Mitf/+
Fig. 29		
A and B	control	Ms1096 GAL4/+;

	ms1096>Mitf	Ms1096 GAL4/+;;Uas-Mitf/+
	ms1096>Mitf DN	Ms1096 GAL4/+;Uas-Mitf EA /+
	ms1096>Nicd	Ms1096 GAL4/+;Uas-Nicd /+
Fig. 30		
A and B	ms1096>	Ms1096 GAL4/+;
	ms1096>Mitf	Ms1096 GAL4/+;;Uas-Mitf /+
Fig. 31		
	control	Ms1096 GAL4/+;
	ms1096>Mitf	Ms1096 GAL4/+;;Uas-Mitf/+
	ms1096>Mitf DN	Ms1096 GAL4/+;Uas-Mitf EA /+
Fig. 32		
	control	Ms1096 GAL4/+;
	ms1096>Mitf	Ms1096 GAL4/+;;Uas-Mitf/+
	ms1096>Mitf DN	Ms1096 GAL4/+;Uas-Mitf EA /+
Fig. 33		
A	ms1096>Mitf;YFP::Vha55	Ms1096 Gal4/+; ;Vha55[CPTI100063]/UAS-Mitf
	ms1096>Mitf;GFP::VhaSFD	Ms1096 Gal4/+; VhaSFD[G00259}/+; UAS-Mitf/+
	ms1096>Mitf;GFP::Vha13	Ms1096 Gal4/+; ;Vha13[CA07644]/UAS-Mitf
	ms1096>Mif;GFP::Vha16-1	Ms1096 Gal4/+; Vha16[G0007}/+; UAS-Mitf/+
	ms1096>; MitfGFP::VhaAC45	Ms1096 Gal4/+; VhaAC45[ZCL0366}/+; UAS-Mitf/+
	ms1096>Mitf; YFP::Lamp1	Ms1096 Gal4/+; Lamp1 [CPTI001775]/+; UAS-Mitf/+
B	YFP::Vha55	w[1118]; PBac{544.SVS-1}Vha55[CPTI100063]/TM3
	GFP::VhaSFD	w1118; P{PTT-GA}VhaSFDG00259/CyO
	GFP::Vha13	y1 w*; P{PTT-GA}Vha13CA07644/TM3, Ser1 Sb1
	GFP::Vha16-1	w1118; Vha16-1 G0007/CyO
	GFP::VhaAC45	y1 w1118; P{PTT-GB}VhaAC45ZCL0366/CyO
	YFP::Lamp1	w1118; PBac{681.P.FSVS-1}Lamp1CPTI001775/CyO
Fig. 34		

	E(spl)mβ lacZ ;GFP::Vha16-1	E(spl)mβ-HLH-lacZ 0.9/+ ;GFP::Vha16-1/+
Fig. 35		
A	ms1096>	Ms1096 GAL4/+;
	ms1096>Nicd	Ms1096 GAL4/+;Uas-Nicd /+
B	ms1096>	Ms1096 GAL4/+;
	ms1096>Nicd	Ms1096 GAL4/+;Uas-Nicd /+
Fig. 36		
A and B	GFP::Vha16-1	w1118; Vha16-1 G0007/CyO
	ms1096>NICD;GFP::Vha16-1	Ms1096 GAL4/+,Vha16-1 G0007/UAS-NICD;
C and D	GFP::Vha13	GFP::Vha13/Tm3
	ms1096>NICD;GFP::Vha13	Ms1096 GAL4/+;UAS-NICD/+;GFP::Vha13/+
E	ms1096>NICD;YFP::Vha55	Ms1096 Gal4/+;Uas-NICD/+ ;Vha55[CPTI100063]/+
	ms1096>NICD;GFP::VhaSFD	Ms1096 Gal4/+; VhaSFD[G00259}/UAS-NICD;
	ms1096>; NEXT; GFP::VhaAC45	Ms1096 Gal4/+; VhaAC45[ZCL0366}/+; UAS-NEXT/+
F	GFP::CG8668	;CG8668 117-2 (II)
	ms1096>NICD;GFP::CG8668	Ms1096 Gal4/+;Uas-NICD/CG8668 117-2 (II)
Fig. 37		
A	GFP::Vha16-1;Neur101-LacZ	Vha16-1 G0007/+;Neur101-LacZ/+
B	GFP::Vha16-1;E(spl)m4-LacZ	Vha16-1 G0007/;E(spl)m4-BFM-LacZ
Fig. 38		
A	control	w[1118]
	control	w[1118]
Fig. 39		
	GFP::Vha16-1	w1118; Vha16-1 G0007/CyO
Fig.40		
A	Vha16-1::GAL4 NP5271> CD8GFP	w*; P{GawB}Vha16-1NP5271/UAS-cd8GFP
B	Vha16-1::GAL4 NP3437> CD8GFP	w*; P{GawB}Vha16-1NP3437/UAS-cd8GFP
Fig. 41		

A	ms1096>GFP::Vha16-1	Ms1096 Gal4/+; Vha16[G0007}/+;
B	ms1096>E(spl)m4;GFP::Vha16-1	Ms1096 Gal4/+; Vha16[G0007}/+; Uasm4/+
C	ms1096>E(spl)m8;GFP::Vha16-1	Ms1096 Gal4/+; Vha16[G0007}/UAS-m8
Fig. 42		
A	ms1096>	Ms1096 GAL4/+;
	ms1096>Nicd	Ms1096 GAL4/+;Uas-Nicd /+
B	ms1096>	Ms1096 GAL4/+;
	ms1096>Nicd	Ms1096 GAL4/+;Uas-Nicd /+
Fig. 43		
	ms1096>GFP::Vha16-1	Ms1096 Gal4/+; Vha16[G0007}/+;
	ms1096>Mif DN;GFP::Vha16-1	Ms1096 Gal4/+; Vha16[G0007}/ UAS-Mitf EA;
Fig. 44		
A-F	ms1096>	Ms1096 GAL4/+;
	ms1096>Mitf	Ms1096 GAL4/+;;Uas-Mitf/+
	ms1096>Mitf DN	Ms1096 GAL4/+;Uas-Mitf EA /+
G-N	ms1096> neur-GFP	Ms1096 GAL4/+;;Neuralized-GFP/+
	ms1096>Mitf neur-GFP	Ms1096 GAL4/+;;Neuralized-GFP/Uas-Mitf
	ms1096>Mitf DN	Ms1096 GAL4/+;Uas-Mitf EA /Neuralized
Fig. 45		
	ms1096>	Ms1096 GAL4/+;
	ms1096>Mitf	Ms1096 GAL4/+;;Uas-Mitf/+
	ms1096>Mitf DN	Ms1096 GAL4/+;Uas-Mitf EA /+
Fig. 46		
A	GFP::Vha16-1;neur101>RFP	Vha16-1 G0007/Uas-cd8RFP;neuralized GAL4/+
B	ms1096>	Ms1096 GAL4/+;
	ms1096>Vha16-1 Rnai HMS02171;	ms1096 GAL4/+; Vha16-1 Rnai HMS02171/+
C	ms1096>Vha16-1 Rnai HMS02171; GFP::Vha16-1	Ms1096 GAL4/+; Vha16-1 Rnai HMS02171/Vha16::GFP [G007];

D and E	pnr>	;; Pannier GAL4/+
	pnr>Vha16-1-HA	Pannier GAL4/UAS Vha16-1-HA
	pnr>Vha16-1 Rnai HMS02171	Vha16-1 Rnai HMS02171/+; Pannier GAL4/+
	pnr>Vha16-1 Rnai HMS02171; Vha16-1-HA	Vha16-1 Rnai HMS02171/+; Pannier GAL4/UAS Vha16-1-HA
F	pnr>	;; Pannier GAL4/+
	pnr>VhaPPA1-1 Rnai GD16478	VhaPPA1-1 Rnai GD16478/+; Pannier GAL4/+
Fig. 47		
A	YFP::Lamp1	w1118; PBac{681.P.FSVS-1}Lamp1CPTI001775/CyO
B	neur-GFP	Neuralized-GFP/TM3
C	act>GFP-hLAMP1	Actin GAL4, UAS GFP-Lamp1/Cyo
D	wild type	w[1118]
E	NiGFP4Cherry5	See (Couturier et al., 2014)

8.3 Complementation test

8.3.1 Complementation test in Project 1

In the first project, complementation test has been used to make sure that both the *Hrs*^{D28} and *Stam*^{2L2896} single mutants did not contain lesions in the lethal(2) giant larvae (*l(2)gl)* gene. Indeed, *l(2)gl* gene, which behaves as tumor suppressor in *Drosophila* is frequently lost due to the fact that it resides very close to the subtelomeric region of the second chromosome (Agrawal, Kango, Mishra, & Sinha, 1995; Roegiers et al., 2009). To test this, we crossed the *Hrs*^{D28} and *Stam*^{2L2896} single mutants with the null allele *l(2)gl*^{4}. Moreover, we also used the complementation test to assess that the *Hrs* and *Stam* double mutant line we generated carried both mutations and was devoid of the *l(2)gl* lesion **(Table 4)**.

Both the *Hrs*^{D28} and *Stam*^{2L2896} fly lines carry a recessive lethal mutation, and therefore the mutations can be maintained only in heterozygosis over a balancer chromosome. The balancer is a rearranged chromosome that prevents genetic recombination between homologs during meiosis and carries a phenotypic marker that can be used to sort flies. These lines were balanced over CyO, a balancer that showed a curled-up wing. Thus the progeny from the cross was scored for the wing phenotype. “Complementation” reveals that the mutations are in two different genes and it is revealed by the presence of straight wings in the progeny, while “non complementation” means that the mutations occur in the same gene and it is revealed by the absence of progeny with straight wings.

Table 4 Test of complementation Project 1

cross row by colum	Stam	Hrs	Hrs stam	lgl
Stam	F	C	-	C
Hrs	C	F	-	C
Hrs stam	F	F	F	C
Hrs stam lgl	F	F	F	F

F: failed complementation C: complementation

Genotypes:

Stam: : *FRT40A Stam^{2L2896}/Cy0*

Hrs: : *FRT40A Hrs^{D28}/Cy0*

Lgl; *FRT40A lgl/ Cy0*

Hrs stam: *FRT40A Hrs^{D28} Stam^{2L2896}/Cy0*

Hrs stam lgl: : *FRT40A Hrs^{D28} Stam^{2L2896}lgl/Cy0*

8.3.2 Complementation test in Project 2

In the second project, GFP-trapped lines were crossed with lines carrying a deletion of the locus of interest or a P-element insertion that likely disrupts the gene function and assay for the ability to complement. This assay was useful to investigate whether the GFP insertion would disrupt the gene function.

This analysis revealed that most knock-in lines in V-ATPase genes behave as loss-of-function mutants, presumably because of effects of the GFP insertion on the functionality of the tagged proteins **(Table 5)**. However, all lines are viable and fertile in heterozygosis and we do not observe dominant effects. Thus, these exon traps can be used in heterozygosis to study regulation of expression *in vivo*.

Table 5 Test of complementation Project 2.

GFP-trapped lines were crossed for each other or with deletion lines or P-element insertions as indicated.

cross row by colum	YFP::Vha55	vha55 p_EL	GFP::VhaSFD	vhaSFD p_EL	GFP::Vha13	Vha13 deletion	GFP::Vha16-1	Vha16-1 deletion	GFP::VhaAC45	VhaAC45 deletion
YFP::Vha55	F	F	-	-	-	-	-	-	-	-
GFP::VhaSFD	-	-	C	F	-	-	-	-	-	-
GFP::Vha13	-	-	-	-	F	F	-	-	-	-
GFP::Vha16-1	-	-	-	-	-	-	F	F	-	-
GFP::VhaAC45	-	-	-	-	-	-	-	-	F	F

Genotypes	
YFP::Vha55	FlyProt CPTI Vha55[CPTI100063]/Tm3
Vha55 p_El	y1 w*; P{lacW}Vha55j2E9/TM3, Sb1
GFP::VhaSFD	FlyTrap VhaSFD[G00259]/CyO
VhaSFD p_El	P{EPgy2}VhaSFDEY04644/CyO
GFP::Vha13	FlyTrap Vha13[CA07644]/Tm3
Vha13 deletion	w1118; Df(3R)ED6025 , P{3'.RS5+3.3'}ED6025/TM6C, cu1 Sb1
GFP::Vha16-1	FlyTrap Vha16[G0007]/CyO;
Vha16-1 deletion	w1118; Df(2R)BSC326/CyO
GFP::VhaAC45	FlyTrap VhaAC45[ZCL0366]/CyO;
VhaAC45 deletion	w1118; Df(2R)ED1791 , P{3'.RS5+3.3'}ED1791 /SM6a

C= Complementation
F= Failure to complement

8.4 Live thorax imaging of intact pupae.

Collect the pupae at the appropriate stage. Gently adhere the pupae to a double-side tape with the ventral side up. Cut the edge of the operculum (the circular batch on the anterior dorsal tip of the pupal case) and remove the whole pupal case. Be careful of not pinching the fly. Once the fly is free from the pupal case, use a brush to move the fly into a slide object dorsal side up. Make a square frame of Whatman paper with a small open in the middle and soak it into water. Place the paper around the pupae. Use a syringe filled with silicone vacuum grease to create a layer of grease around the paper frame. Place a small drop of water (1 µl) on the center of the coverslip and seal the pupa with the coverslip. For a detailed video description see (Zitserman Diana, 2011)

8.5 Adult wing, thorax and eye preparation

Adult flies were scored 2-3 days after enclosure, and only females were taken into account. More than 10 females from crosses were collected in isopropanol and kept at room temperature until preparation. Wings were dissected in isopropanol and mounted on microscopy slides using a mixture of Canadian balm (xylem-free) with methyl salicylate 1:1. Preps were dried at room temperature and analyzed and imaged with a Nikon SMZ1500 microscope using the NCIS Elements 5.0 software. Images displayed in figures are representative examples out of at least 10 images per samples. To image thoraces, legs and wings from the adult flies were removed with forceps, and the body of the fly was placed on a soft agar plate dorsal side up and directly imaged with a Nikon SMZ1500 microscope. Stacks of approximately 10 sections with step size of 0.59 µm were taken. Each image represents the max projection of each z-stack. To image the adult eye, the adult

head of a fly was placed on soft agar plate on a side and the eye was imaged with the Nikon SMZ1500 microscope.

8.6 Misexpression using the GAL4/UAS system

This technique is used to control when and where specific genes are expressed (Duffy, 2000). This technique is based on the transactivator GAL4, which is a yeast protein that binds to upstream activating sequences (UAS) to drive the expression of any gene of interest. Any gene of interest can be mis-expressed in different cells and tissues simply crossing the line carrying a UAS-gene of interest with any Gal4-activator lines. In addition a UAS sequence can be introduced upstream to a RNAi sequence for the gene of interest. In this case the GAL4/UAS system would lead to the downregulation of the mRNA of the gene of interest rather than its overexpression.

8.7 Generation of clones with FLP/FRT system

This method is used to create homozygous mutations in a patch of cells that express the FLP enzyme. This is particularly useful for mutant alleles that are homozygous lethal. The mutation for the gene of interest is distal to an FRT site. When FRT interacts with the FLP enzyme, recombination will occur between the identical FRT sites, which are in close proximity. This results in mosaic tissue containing cells homozygous for the mutation in the gene of interest. Predominantly mutant eye and WDs (referred to in the text as mutant discs) were generated with the eyeFLP cell lethal system as described (Newsome, Asling, & Dickson, 2000). Mutant eye disc clones were generated with the eyeFLP mosaic system as described previously (Tapon, Ito, Dickson, Treisman, & Hariharan, 2001). Mutant follicle epithelial cell clones were generated by using the heat shock-mosaic system (Lee & Luo, 2001) and the GR1 system (Goentoro, Yakoby,

Goodhouse, Schüpbach, & Shvartsman, 2006). For most of the mosaic experiments, female flies were heat-shocked at 37°C for 1 h two times a day for 2 days and then incubated at 25°C for 4 days before dissection.

8.8 Generation of transgenic UAS *Drosophila* lines

For the generation of the UAS Vha16-1-HA fly strain, we amplify the cDNA for Vha16-1 from the plasmid (pFLC-I #RH30178) using the following primers represented in **Table 6**:

Table 6 Oligonucleotides used for the generation of UASVha16HA fly line.

Orientation	Sequence	Lenght	Features
Forward	5' GATCGAATTC**ATG**TCTTCTGAAGTGAGCAG 3'	30	EcoRi site ATG start codon
Reverse	5'GATCTCTAGA**TTA**GGCGTAGTCAGGCACGTCG TAAGGATATTTCGTGTACAGGTAAATGGC 3'	61	XbaI Site HA tag TTA Stop codon

An HA tag was inserted at the C-term of the protein. The amplicon of Vha16-1-HA was inserted into the pUAST expression vector and injected into the ZH-86fb landing site (Basler lab). Transgenesis was performed by Genetic Services inc.

8.9 Genomic Dna extraction

Files were homogenized with a pestle in lysis buffer (100 mM Tris-HCl pH 7.5, 100 mM EDTA, 100 mM NaCl, 0.5% SDS) and Proteinase K (sigma P2308). After incubation for 30 minutes at 70°C, a solution composed of 1 part 5M KAc and 2.5 parts 6M LiCL was added to the mix. Isopropanol and 70% ethanol were then added to allow DNA precipitation. DNA was resuspended in autoclaved water and 1 µl of genomic DNA was used as a template for PCR reactions.

8.10 Antibody production

A polypeptide for Mitf protein that lacks the basic helix-loop-helix leucine zipper domains to prevent cross-reactions with other bHLH-Zip proteins was selected as immunogen. The fragment of the whole Mitf cDNA was amplified by PCR using the Taq Polymerase (Promega M3175) , as template the genomic DNA extracted from flies carrying the construct UAS-MITF (Jón H Hallsson et al., 2004) and the following primers presented in **Table 7**.

Table 7 Primers used for the generation of Mitf antibody

Orientation	Sequence	Lenght	Features
Forward	5'GATCGGATCC**ATG**ACGGAATCTGGAATCG 3'	29	BamHI Site ATG start codon
Reverse	5'GATCGTCGAC**TTA**CGAATGATGGTAGCTCAGA GAC 3'	34	SalI Site TTA Stop codon

The PCR product was inserted into the prokaryotic expression vector pGEX, containing the GST sequence (pGEX-GST), using BamHI and SALI sites. Expression was carried out in the E. coli rosetta (Millipore 70956) adding IPTG 0.5 mM overnight at 18°C. Purification was performed by the IFOM antibody-service facility according to standard protocols. Purified peptides were consigned to Eurogentech for rabbit immunizations. The polypeptide sent for immunization has the following predicted sequence **(Table 8)**:

Table 8 Mitf fragment sequence used for rabbit immunization

Met T E S G I D L G F D M E F D L N I N L L N D N D N M D F L P N V T E N M E F Y E L K S SS R C I R H N E I
P T F K T A T P T S R T Q L K L Q L Q R E Q Q Q Q M M I Q QQ T L D T A M D P K M H L L F G S G Q G L M E
S E F I D S G S T S A C G S G S SS L E Q M S Q L V Q M D N L I D S SS G A K L K V P L Q S I G V D V P P Q V L
Q V S T V L E N P T R Y H V I Q K Q K N Q V R Q Y L S E S F K P S M W G S H T S E I K L A N N S A S T G N L Q
N S S L Q K G I C D P L E R T N R F G C D S A V S A K R I M P S D D A M P I S P F G G S F V R C D D I N P I E P
T V L R P N S H G A G E P E N A H R T A Q L G L S K A N S S L S S T R S SS G I V N S I R I S S T S SS L Q S T S A
P I S P S V S S V A T S V S E L P S F D S D

Sera affinity purification was performed by the IFOM antibody-service facility, using AminoLink® Kit (Biotechnology).

8.11 Immunohistochemistry

8.11.1 Dissection of larval imaginal discs

The imaginal discs are located on the anterior portion of the larva, near the mouth hooks**.** To dissect them, tear the larva in half and discard the posterior. Invert the anterior like a sleeve by pushing in delicately on the mouth hooks. The wing and haltere discs are attached to tracheolae that branch off the two main tracheal tubes running below the cuticle along the body wall. The eye-antennal discs are located between the surface of the optical lobe of the larval brain and the mouth parts. Imaginal discs are kept attached to carcasses to facilitate handling. To prepare carcasses for fixation, clean them of the gut, fat tissue, and salivary glands. Transfer carcasses to a 1.5 mL tube filled with 1× PBS. Dissect 10–12 larvae per genotype within no more than 20 min and proceed to fixation. For a detailed video description of dissection of imaginal discs see (Purves & Brachmann, 2007).

8.11.2 Dissection of adult ovaries

Before ovarian dissection, feed mated flies in well-yeasted tubes to engorge ovaries for 24-48 hrs. At the appropriate moment, anesthetize the flies. Using a pair of forceps hold a female fly by the upper part of the abdomen and pull the tip of the abdomen out with the other forceps. Internal organs including the gut, the two ovaries and the oviducts will be exposed. Detach the pair of ovaries from other organs and collect them in a 1.5 mL tube then proceed with fixation.

8.11.3 Immunohystochemistry

Carcasses or ovaries were fixed using 4% PFA for 20-30 min at room temperature. After removal of the fixative, allow permeabilization using 0,1%

TRITON X-100 diluted in PBS 1X (PBT solution). Rinse the tissues for 5–10 min and repeat this step 3 times to remove all traces of fixative. Tissues were then incubated with the blocking solution, composed of 4%BSA diluted in PBT. Tissues are blocked for at least 30 min at room temperature. Pretreatment with 1× PBS, 1 % Triton X-100 for 30 min or 1 h may be needed to ameliorate the permeabilization of the membrane (in case of ovaries for example) and to increase the penetration of some antibodies. However, due to extraction of soluble proteins this treatment may reduce detection of some antigens. After removal of the blocking solution, add the desired primary antibody diluted in blocking solution. For a list of primary antibody used in this study refer to the following **Table 9**.

Table 9 List of antibodies used in this study.

Name of the Ab	Source	Dilution and species	Epitope	Example of use
a. Notch receptor				
Notch ECD	DSHB C458-2H	1:100 mouse	Notch extracellular domain	(Vaccari & Bilder, 2005)
Notch ICD	DSHB C17.9C6	1:100 mouse	Notch intracellular domain	(Vaccari & Bilder, 2005)
b. Notch target genes				
Anti-Cut (Cut)	DSHB 2B10 supernatant	1:100 Mouse monoclonal	Cut protein	(Le Borgne et al., 2005)
Anti-Wingless (Wg)	DSHB 4D4-c concentrate	1:100 Mouse monoclonal	Wingless protein	(Jafar-Nejad, Tien, Acar, & Bellen, 2006)
Anti-Hindsight (Hnt)	DSHB 1G9-s supernatant	1:25 Mouse monoclonal	Hindsight protein	(Vaccari et al., 2008)
c. Cell fate determinants associated to Notch signaling				

Anti-Achete	DSHB anti-achaete	1:100 mouse	Achaete protein	(Skeath, Panganiban, Selegue, & Carroll, 1992)
d. Others				
Anti-Domeless (Dome)	A gift from Stephane Noselli	1:50 rabbit	Domeless receptor	(Devergne, Ghiglione, & Noselli, 2007)
Anti-Avalanche/syntaxin (Avl)	Lu and Bilder 2005	1:100 rabbit	Early endosome	(Vaccari & Bilder, 2005)
Anti-Mitf	Generated in this study	1:200 Rabbit	Mitf protein	Tognon et. al 2015 in press.
Anti-GFP	Abcam ab13970	1:1000 Chicken	GFP protein	(Wernet, Klovstad, & Clandinin, 2014)
Anti-Ref(2)P	Gift from Tor Erik Rusten	1:100 Rabbit	ref(2)P protein, homolog of p62	(Takáts et al., 2013).
Anti-Atg8a	kind gift of G. Juhasz	1:300 rat	Atg8a protein	(Takáts et al., 2013).
Anti cleaved Caspase-3	Cell signaling 9661	1:200 Rabbit	Caspase-3 protein	(Takáts et al., 2013).
Anti- β–Gal	DSHB 401a-c	1:25 mouse	β–Galactosidase	(Djiane et al., 2013)
Anti-unbiquitinylated protein (FK2)	BML-PW8819 Enzo life sciences	1:1000	Mono-polyubiquitinylate conjugates	(Vaccari & Bilder, 2005)

Incubate primary antibody overnight on the nutator at 4°C. Primary antibody can be reused if needed. Rinse the samples 3 times for 5-10 min in PBT. Then add the fluorophore-conjugated secondary antibody diluted in PBT for 2 hrs at room temperature on the nutator in the dark. At this step, together with the secondary

antibody it is possible to add fluorophore-conjugated phalloidin, such as phalloidin- TRITC (Sigma P1951), to mark F-actin and visualize the overall morphology of cells. Alexa 488- or Alexa 647- (Life technologies A-21202 (mouse), A-21206 (rabbit), A-21203 (rat), A-31571 (mouse)) and Cy3-conjugated secondary antibodies (Jackson immunoresearch Laboratories 715-165-150 (mouse), 711-165-154 (rabbit), 712-165-150 (rat)) were used. Wash tissues 3 times for 10 min each with PBT. To perform a nuclear counter stain, samples can be incubated for 10 min with PBT solution containing 1× DAPI (4′,6-diamidino-2-phenylindole) in the dark. Wash tissues once in PBT for 10 min before proceeding with mounting.

8.11.4 Mounting

To mount imaginal discs, transfer carcasses to the slide, blot excess of liquid with paper tissue and add a couple of drops (approximately 20 μl) of mounting medium: 1.5 % DABCO (1,4-diazabicyclo[2.2.2] octane) on the tissue using a pasteur pipette. Gently remove the imaginal discs from the carcasses. WDs appear as pear-shaped organs flapping on either side of the carcass attached to the tracheolae. To remove eye-antennal imaginal discs instead, gently rip the nerves connecting the ventral ganglion with the carcass wall by sliding the forceps tips between them. Grab the base of mouth hooks with one forceps and pull the mouthparts away from the rest of the body with the other forceps. Eye-antennal imaginal discs and brain will be removed from the carcass as a single mass, together with the mouth hooks. To separate the brain from the eye-antennal discs, use one forceps to carefully pinch the nerve connecting each optic lobe to its discs. Transfer discs to the slide by holding them by the attached mouth hooks. Detach the eye-antennal discs from the mouth hooks by pinching the narrow connection between the antennal disc and the mouth hooks. Discard the mouth hooks. To mount ovaries, allow them to settle to the bottom of the tube, then dissociate

ovaries into ovarioles and individual egg chambers by pipetting up and down several times, using 200 µl pipet tip. Gently transfer the egg chambers by delicate resuspension to the slide using a glass pipet. Remove the excess of PBS and add a couple of drop of mounting medium. Make sure that the tissue is flat and unwanted tissue parts are removed from the slide, before covering with a coverslip. In particular, parts thicker than the tissue to be analyzed should be removed to avoid excess spacing between slide and coverslip, which creates movement/vibration of the sample during imaging. Conversely, when z dimensions need to be preserved (i.e., for z-confocal sectioning), a Dakopen or other hydrophobic barrier marker can be used to ensure appropriate spacing between slide and coverslip. Seal the edges with nail polish. Store the slide at 4 °C in the dark. Allow 12–24 h before imaging to ensure hardening of the resin. Analyze the sample at a fluorescent microscope. Whole-mount preparations are perfectly suited for confocal microscopy.

8.11.5 Confocal Imaging

All images shown are confocal sections taken with TCS microscope (Leica, Heidelberg, Germany) using 20x/NA 0.5, 40x/NA 1.25 or 63x/NA 1.4 oil-immersion lenses. Digital images were processed and assembled using ImageJ, Photoshop and Illustrator with minimal manipulations. All images are single confocal sections unless otherwise stated.

8.12 Trasmission Electron Microscopy

Eye discs wild type or mutant for *Hrs*, *Stam*, *l(2)gl* or *Vps25* were fixed in 2.5% glutaraldeyde diluted in 0.1M sodium cacodylate buffer for 3 hours at room temperature. Eye discs were post-fixed in 1% osmium tetroxide (Electron Microscopy Science, Hatfield, PA, USA) for 2 hours at room temperature and subsequently in 1% uranyl acetate (Electron Microscopy Science) for 1 hour.

Samples were dehydrated through a graded ethanol series and next in propylene oxide before embedding in epoxy resin (Poly-Bed, Polyscience, Warrington, PA, USA) overnight at 42°C and then 2 days at 60°C. Searching for the eye disc epithelium was performed on semi-thin sections (500 nm) stained with toluidine blue. Ultrathin sections of 50 nm were then cut and stained with 5% uranyl acetate and lead citrate. Representative TEM micrographs of each sample were taken with Tecnai 12-G2 microscope (FEI company, Eindhoven, The Netherlands) and processed with Adobe Illustrator CS5. Quantifications were performed with ImageJ on a set of approximately 20 micrographs per sample.

8.13 Lysotracker assay

The Lysotracker assay was performed by adding lysotracker (Red-DND-99 Life technologies L-7528) directly to M3 medium [(Shields and Sang M3 insect medium (Sigma #S3652)] of *ex vivo* WDs after dissection. WDs were incubated for 5 min in medium containing 1 µM lysotracker. They were then rinsed twice with PBS1X and mounted immediately in antifade-Glycerol 1:1 solution for confocal examination.

8.14 Quantitative Real Time PCR

8.14.1 Rna extraction

Total RNA was isolated from third instar larvae WDs. Approximately 40 discs per sample were dissected and collected within 30 min in M3 medium (Shields and Sang M3 insect medium (Sigma S3652)) and total RNA was extracted using TRIZOL Reagent (invitrogen 15596-026) and RNAase Mini kit (Quiagen 74104). Tissues were spin down; medium was removed and directly frozen at -80 °C after addition of 300 µl Trizol. Samples were thawed on ice and homogenized with a pestle pretreated with RNAse free buffer and ethanol. After 5

min incubation at room temperature, 60µl of chloroform were added, the mix was vortexed and after 2 min at room temperature centrifuged at 12 000 g for 15 min at 4°C. All centrifugations up to 2 ml were performed using the Eppendorf Centrifuge 5415 D. The aqueous white upper phase was transferred into a new tube and mixed with the equal amount of 70% ethanol to promote selective binding of RNA to the RNeasy membrane. The mix was transferred to an RNeasy Mini Spin column. RNA was bound to the silica matrix by centrifugation for 15 s at 8000 g and washed with 350 µl of RW1 buffer (QIAGEN RNaesy Mini kit) for 15 s at 8000 g. Then proceed with on-column DNAse digestion using QIAGEN RNAse free DNAse set. Add in a RNA-free tube 10 µl of DNAse I stock solution and 70 µl of RDD buffer and mix gently. Add the DNase I incubation mix (80 µl) direcly on the column. Dnase digestion will take place directly on the column in 10-15 min at room temperature. Then proceed by adding 350 µl Buffer RW1, centrifugate for 15s at 8000g and then wash the column twice with the RPE buffer and centrifugate for 15s at 8000g. Centrifugate the column again to let it dry, and place it additionally 10 min open under the hood to let the complete evaporation of ethanol. Proceed with RNA eluition, by adding 15 µl of RNAse-free water on the columns, after 1 min incubation at room temperature centrifugate at max speed for 1min. The recovered RNA-concentration was measured using Nano-drop and RNA was stored at -80°C until usage.

8.14.2 cDNA synthesis

The extracted RNA has to be transcribed in cDNA before running the real time PCR. To this end, the invitrogenTM SuperScript® VILOTM cDNA Synthesis Kit was used following the manufacturer's instructions. cDNA was generated starting from 1µg of RNA. Samples were incubated for 10 min at 25°C, 60 min at 42°C and 5

min at 85°C and stored at -20°C. A no template reaction was used as negative control.

8.14.3 Quantitative Real Time PCR

Synthesized cDNA samples were kindly analyzed by the Real Time PCR Service facility from *Cogentech* provided at the IFOM-IEO campus.
5 ng of cDNA was amplified (in triplicate). RT-PCR was carried out on the ABI/Prism 7900 HT Sequence Detector System (Applied Biosystems, Carlsbad, CA, USA), using a pre-PCR step of 10 min at 95°C, followed by 40 cycles of 15s at 95°C and 60s at 60°C.

The following primers (5′-3′) were designed from Universal Probe Library Roche (UPL)**(Table 10)**:

Table 10 List of primers used for qPCR analysis generated using the UPL library.

Gene	Primers	Sequence	UPL library
Vha16-1	Vha16-1_Fow	5'cacaacaacaacagatagacaaacg 3'	66
	Vha16-1_Rev	5'gaagctgctgctgatgttgat 3'	
Vha55	Vha55_Fow	5'atcgctgtcgcgtttgat 3'	121
	Vha55_Rev	5'agagtggtccttacgggtcat 3'	
VhaSFD	VhaSFD_Fow	5'aggtgctgaagcagctatcc 3'	1
	VhaSFD_Rev	5'ctctacgtcggcggtaatgt 3'	
Vha13	Vha13_Fow	5' aggagttcgaggccaagc 3'	158
	Vha13_Rev	5'ccaggatgaacgggtcct 3'	
VhaAc45	VhaAc45_Fow	5'ccctgtttgtgaccttcgag 3'	109
	VhaAc45_Rev	5'cactcgaactgcttgctgat 3'	
Lamp1	Lamp1_Fow	5' gctttcctttatgcaaattcatc 3'	27
	Lamp1_Rev	5'gctgaaccgtttgattttcc 3'	

Ref(2)P	Ref(2)P _Fow	5’ agacagagcccctgaatcct 3’	77
	Ref(2)P _Rev	5’ggcgtctttcctgctctgt 3’	
Atg8a	Atg8a _Fow	5’ catgggctccctgtacca 3’	101
	Atg8a _Rev	5’ctcatcggagtaggcaatgt 3’	
Vps25	Vps25 _Fow	5’ ccttcccacccttctttaca 3’	161
	Vps25 _Rev	5’ tgcctgaggtatttgagaaagag 3’	
Stam	Stam Fow	5’ ggaatctttgggcagtcgt 3’	49
	Stam _Rev	5’ ccagttgtcgttggtattagtttc 3’	
Notch	Notch _Fow	5’ ccgttcgcggaactgata3’	4
	Notch _Rev	5’ cattctggcaaccgacact3’	
Hrs	Hrs _Fow	5’ tcaaccagaaagatgtcactcc 3’	143
	Hrs _Rev	5’ ccaggagggaatagcagga 3’	
RPL32	Rpl32 _Fow	5’cggatcgatatgctaagctgt 3’	117
	Rpl32 _Rev	5’ cgacgcactctgttgtcg 3’	

To assay MITF expression, the following Applied Biosystem (Applied Biosystems, Carlsbad, CA, USA) probes listed in **Table 11** were used:

Table 11 Primers for qPCR using the applied biosystem platform.

Gene	Taqman gene expression assay
Mitf	Dm02749950_m1
RPL32	Dm02151827_g1.

Amplicon expression in each sample was normalized to its RpL32-RA mRNA content. Note that ms1096-Gal4 is expressed in approximately 50% of the disc tissue.

8.15 In situ experiments

8.15.1 Probe synthesis

Single strand sense and antisense RNA probes for Vha16-1 and Mitf were generated using the following primers listed in **Table 12**:

Table 12 Primers used to create the probe for in situ hybridization

Probe for	Orientation	Sequence	Features
Vha16-1	Forward	5'TAATACGACTCACTATAGGGAGAGTGTCA AGCCAATGAGCAAC 3'	T7 promoter sequence
	Reverse	5'AATTAACCCTCACTAAAGGGAGAAGTTGG TTTCCGCAGTTGAC 3'	T3 promoter sequence
Mitf	Forward	5'TAATACGACTCACTATAGGGAGAGTGCTG CAGGTCAGTACAGTG 3'	T7 promoter sequence
	Reverse	5'AATTAACCCTCACTAAAGGGAGAGGCGAA ATAGGAGCTGAGG 3'	T3 promoter sequence

As templates we used a plasmid carrying the Vha16-1 cDNA (pFLC-I RH30178) or the genomic DNA from flies carrying the pUASTMitfWT construct. PCR product has been used as a template for in vitro transcription with the T3/T7 polymerase (promega P207B/P208C) according to manufacturer's instructions.

8.15.2 In situ hybridization

In situ experiments were performed in WDs. One probe lacking the most conserved bHLH-Zip domain was used against Mitf mRNAs. This probe has been designed to prevent cross-reactions with other mRNAs coding bHLH-Zip proteins. One probe used for Vha16-1 was design in the 4th exon, 600 bp long. The probes were labeled with digoxigenin-UTP (Roche 11209256910) and expression patterns revealed using a Digoxigenin antibody conjugated to alkaline phosphatase (Roche 11093274910). Alkaline phosphatase activity was revealed using the NBT/BCIP substrates (Roche 11383213001/11383221001) according to manufacturer's instructions.

8.16 Wester blotting

8.16.1 Protein extraction

WDs (50 discs per sample) were dissected in M3 medium, then lysate in RIPA buffer freshly supplemented with protease inhibitors (Calbiochem 539134). Lysate were cleared from membranes by centrifugation. Quantification of the protein extract was performed using BCA assay kit.

8.16.2 Western blot

Samples from WDs were denatured by adding β-mercaptoethanol containing loading dye and by heating for 5 min at 98 °C. They were then resolved on 8-12% polyacrylamide gels and transfer onto nitrocellulose membranes according to standard methods. Membranes were blocked with 5% milk and subsequently stained with primary antibodies also diluted in 5% milk. Primary antibody used in this study was rabbit anti-Mitf diluted at 1:1000; Normalization of cell extracts was performed with mouse anti-tubulin (1:10000 Sigma T6074). Goat anti-rabbit, Goat anti-mouse 1:8000 HRP conjugated with secondary antibodies (GE Healthcare NA934 and NXA931) were used. Signal was detected using Pierce ECL Western Blotting Substrate (Thermo Scientific 34080-34095), and imaged using a Chemidoc molecular imager (Biorad, Hercules CA USA).

8.17 Quantifications

To quantify colocalization of YFP::Lamp1 with Mitf, WDs were immunostained using anti-GFP and anti-Mitf antibodies. Secondary antibodies using anti-chicken Alexa Fluor 488 and anti-rabbit Alexa fluor 633 were used to avoid bleed-through. Images were recorded as optical z-sections. 3 sets of z-stack of 20 sections each with step size of 0.24 µm were analyzed using imageJ for each

sample. Clear and distinct YFP-lamp1 positive compartments were selected blindly with no other channel visible using a Region of Interest (ROI) with a surface area of 4 μm^2. Each YFP-Lamp1 compartment was subsequently manually assessed for colocalization with Mitf. 240 ROIs were analyzed for each sample in total and score for “overlap”, “no overlap” or “proximity” colocalization of the two signals. As negative controls we also performed the quantification on the pictures in which the two signals were randomly rotated of 90°. Statistical analyses were performed using Chi-square test, with Bonferroni correction for multiple comparison analyses.

For quantification of Lysotraker analysis, optical sections corresponding to 6 fields of 3 independent WDs for each sample were analyzed. Particles with a discrete dimension size that ranged from 5 to infinity pixels were then considered. For each particle the following measurements were performed: number of puncta, area of puncta, integrated density density of puncta (sum of the pixel intensities divided by the number of pixels). Statistical analyses were performed using Kruskal-Wallis test, with Dunn’s multiple comparison test.

To count bristles, adult torax microchaete of female’s nota were considered. Area of each notum was calculated and density of bristle calculated by dividing number of bristles by the area. Data were then subjected to Statistical analysis based on Kruskal Wallis Test with Dunn’s multiple comparison relative to control. All analyses were performed with imageJ and statistically analyzed and graphed with GraphPad Prism.

9 RESULTS

9.1 Results Project 1

9.1.1 ESCRT-0 components are not required for tumor suppression in *Drosophila*

To compare the phenotype of the *Stam* or of the *Hrs, Stam* double mutant with that of *Hrs* or of ESCRT-I, -II, -III mutants, using the FLP/FRT system we generated clones of cells mutant for *Stam* (Mutant cells are GFP-negative; see Material and Methods) or for a double mutation in *Hrs* and *Stam* in the follicular epithelium (FE) of the *Drosophila* ovary (Chanut-Delalande et al., 2010), taking advantage of the fact that *Hrs* and *Stam* map to the same chromosome arm. As it is the case of FE cells mutant for *Hrs*, *Stam* mutant FE cells display normal epithelial morphology **(Fig. 15 A-C)**. Similarly, we observed no detectable phenotype when we generated mosaic eye imaginal discs **(Fig. 15E-G)** or eye imaginal discs consisting predominantly of mutant cells **(Fig.15I-M)** for either *Hrs* or *Stam*. Interestingly, mosaic FE or eye discs consisting predominantly of cells mutant for both *Hrs* and *Stam* also do not display loss of tissue architecture **(Fig. 15 D-H-N)**. This data indicate that simultaneous loss of both ESCRT-0 components do not lead to loss of tissue architecture, a striking difference to what was observed in ESCRT-I, -II, -III mutants (Herz et al., 2009; Vaccari & Bilder, 2005; Vaccari et al., 2009).

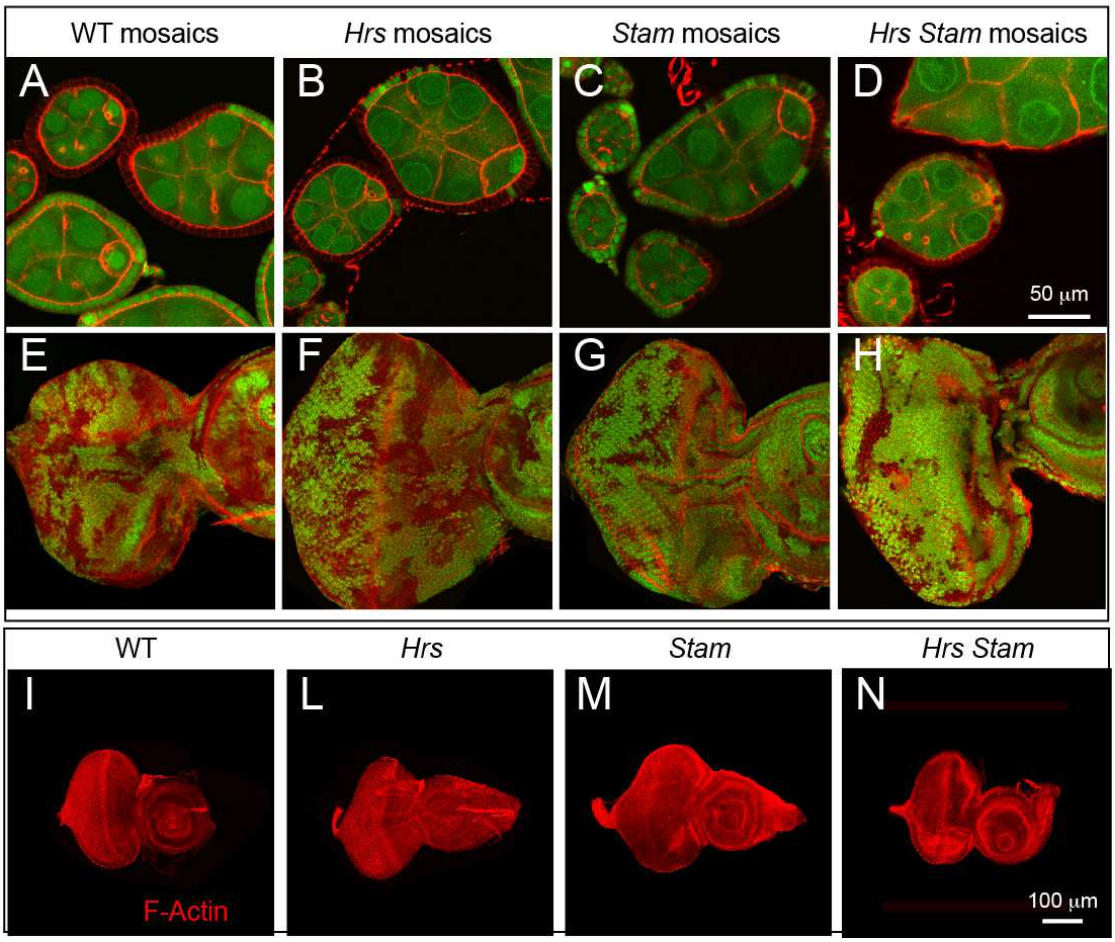

Figure 15 *Stam* mutation or *Hrs*,*Stam* double mutations do not lead to loss of epithelial polarity and tissue architecture.

(A-H) Epithelial morphology of mosaic FE cells (A-D) and eye discs (E-H) revealed by phalloidin staining to detect F-actin. FE cells of 5-7 stage egg chambers or eye imaginal discs homozygous for the mutation (GFP-negative) show normal epithelial architecture compared to control (WT) (GFP-positive). (I-N) WT and predominantly mutant eye-antennal discs stained with phalloidin revealed that *Hrs* or *Stam* or the double *Hrs, Stam* mutations do not affect the overall morphology of the eye imaginal disc.

Consistent with such surprising difference, we found that eye discs consisting predominantly of cells mutant for *Hrs* or *Stam* or both *Hrs* and *Stam* progress to form adult eyes. These are smaller than wild-type (WT) and have a rough appearance but contain mutant photoreceptors **(Fig.16A-D)**. In sheer contrast to these, a number of ESCRT-I, -II, -III mutations, such as those mapping to *Tsg101*, *vps28*, *vps25*, *vps20*, when homozygous in eye discs, display a Mutant Eye No Eclosion (MENE) phenotype that have been associated with loss of tumor suppression in *Drosophila* (Menut et al., 2007).

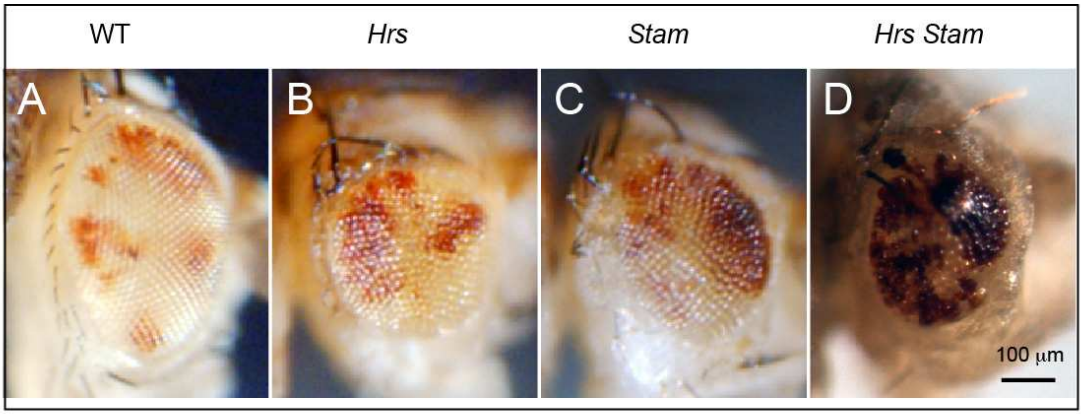

Figure 16 *Hrs* or *Stam* or *Hrs, Stam* double mutants develop adult eye.

(A-D) Adult eyes deriving from mosaic discs of the indicated genotype. WT (A) or mutant cells (B-D) are marked by the absence of red pigment. Although smaller in size, mutant eye display normal photoreceptors.

The scarcity of mutant adult photoreceptors might be due to cell death, as we occasionally see apoptotic cells in clones of *Hrs* or *Stam* or both *Hrs* and *Stam* double mutants **(Fig.17 A-D)**.

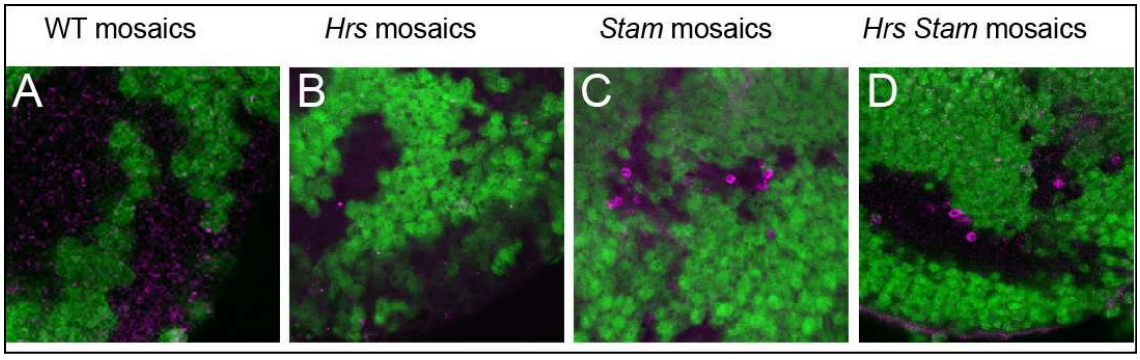

Figure 17 *Hrs* or *Stam* or both *Hrs* and *Stam* mutant cells display apoptotic cells

Higher magnification of mosaic clones in the eye imaginal disc of the indicated genotype. Homozygous cells are marked by the absence of GFP. Apoptotic cells are stained with anti-Caspase 3 antibody (magenta). Mutant cells for *Hrs, Stam* or both *Hrs* and *Stam* display a small amount of apoptotic cells compared to control.

Overall, these data suggest that the activity of *Hrs* and *Stam* is not tumor suppressive in two different *Drosophila* epithelial tissues. To make sure that neither *Hrs* or *Stam* mutations might have a residual functional activity, we performed a quantitative RT-PCR to assess the transcript level of Hrs and Stam. Genetically, the mutations behave as null alleles. Due to early stop codon Hrs^{D28} expresses only the amino terminal first quarter of the protein, lacking most functional domains (Lloyd et al., 2002). Similarly, $Stam^{2L2896}$ harbors a nonsense

mutation leading to an early stop codon at amino acid 6 (Chanut-Delalande et al., 2010).

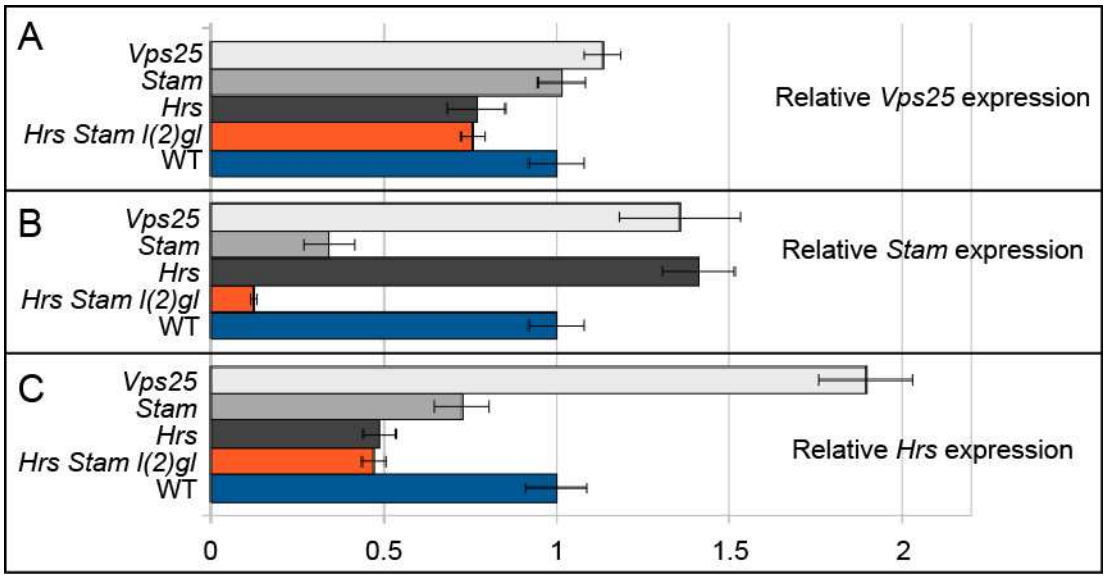

Figure 18 Mutant *Hrs* and *Stam* residual transcripts are subjected to non-sense mediated decay.

Quantitiative RT-PCR experiment on mRNA extracts from eye imaginal discs from single *Hrs* or *Stam* or triple *Hrs, Stam l(2)gl* mutant tissues compared to control indicates reduction of *Hrs* or *Stam* mRNA expression in corresponding mutant extracts.

The qPCR analysis reveals that only 50% of *Hrs* transcript is present in mutant tissues for *Hrs* or for *Hrs*, *Stam l(2)gl* while only 20-30% of the *Stam* transcript is present in mutant tissues for *Stam* or *Hrs*, *Stam l(2)gl* **(Fig. 18 A-C)**, indicating that mutant *Hrs* and *Stam* transcripts are subjected to non-sense mediated decay, as predicted by the nature of the mutations. These data strengthen the conclusion that the mutations are null and thus that ESCRT-0 does not act as a tumour suppressor.

9.1.2 Impaired ESCRT-0 activity leads to accumulation of ubiquitin, Notch and Dome

We next asked whether ESCRT-0 mutants are able to sort ubiquitylated cargoes. To this end, we immunostained mosaic eye disc and FE cells containing clones of cells mutant for *Hrs* or *Stam* or both *Hrs* and *Stam* with an antibody specific to ubiquitin chains. In contrast to WT cells, but similarly to previous reports of *Hrs* and ESCRT-I, -II, -III mutants (Jékely and Rørth, 2003; Lloyd et al.,

2002; Vaccari et al., 2008), *Hrs, Stam* and *Hrs* and *Stam* mutant cells accumulates ubiquitin **(Fig.19 A-F).**

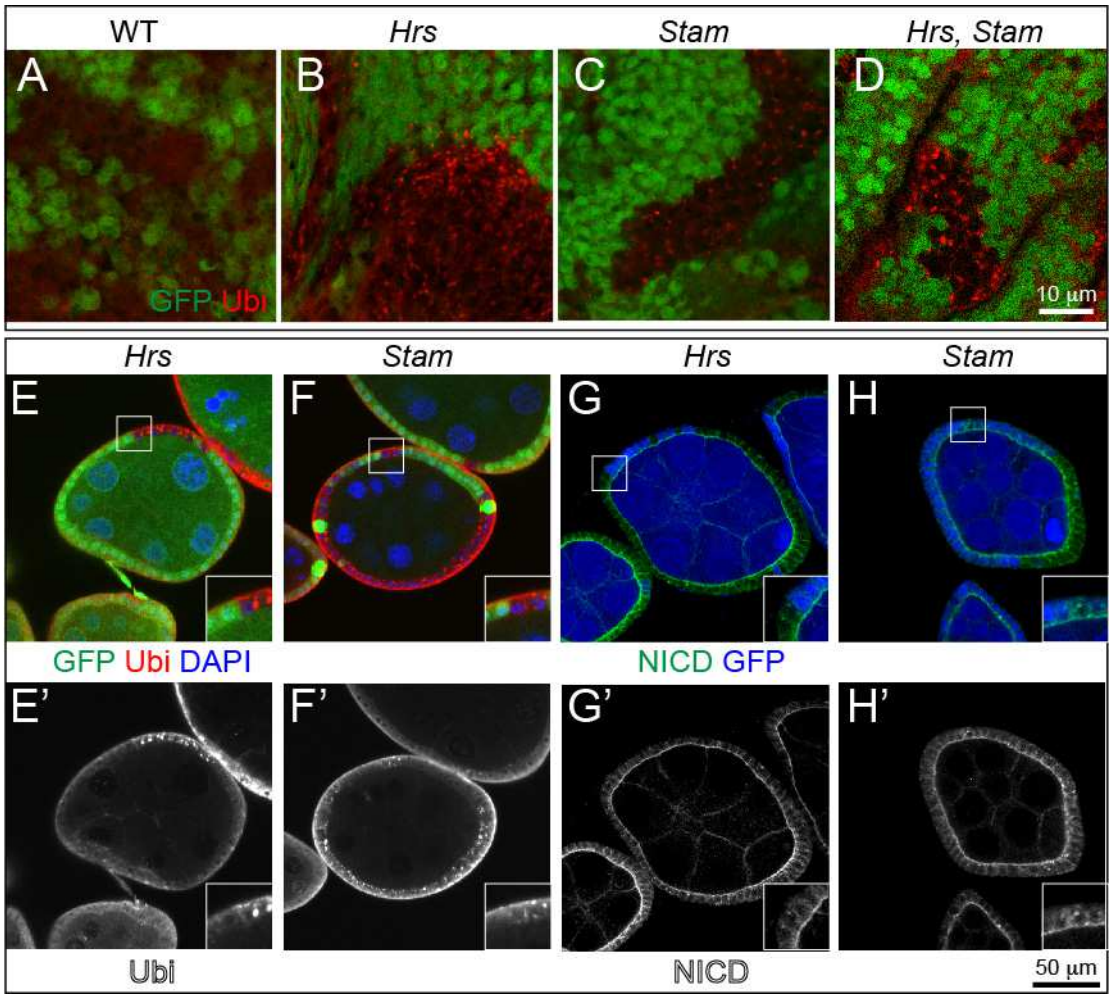

Figure 19 Single mutant cells for *Hrs* or *Stam* or double mutant cells for *Hrs* and *Stam* accumulates ubiquitin.

A-D) Higher magnification of a region of mosaic eye imaginal discs of the indicated genotypes stained using an antibody for mono- and poly-ubiquitin chains (Ubi). E-F) Mosaic clones mutant for *Hrs* or *Stam* in FE cells stained for ubiquitin (E'-F' show the splited channel for ubiquitin. G-H) Clones of mutant cells (GFP-negative) for *Hrs* or *Stam* stained for intracellular domain of Notch NICD. G'H') show the splitted channel for NICD. High magnification of the boxed areas is shown in insets.

Notch is among the cargoes subjected to endosomal sorting in *Drosophila* discs and FE cells (Moberg et al., 2005; Thompson et al., 2005; Vaccari & Bilder, 2005). To assess whether Notch is sorted and degraded in endosomes of ESCRT-0 mutant cells, we immunolocalized Notch in *Hrs* mutant cells or *Stam* mutant cells or both *Hrs, Stam* double mutant cells. Compared to WT cells, double mutant eye disc cells display accumulation of Notch, as we assess with an antibody that recognizes the extracellular domain of Notch (NECD) **(Fig.20 A-B)**.

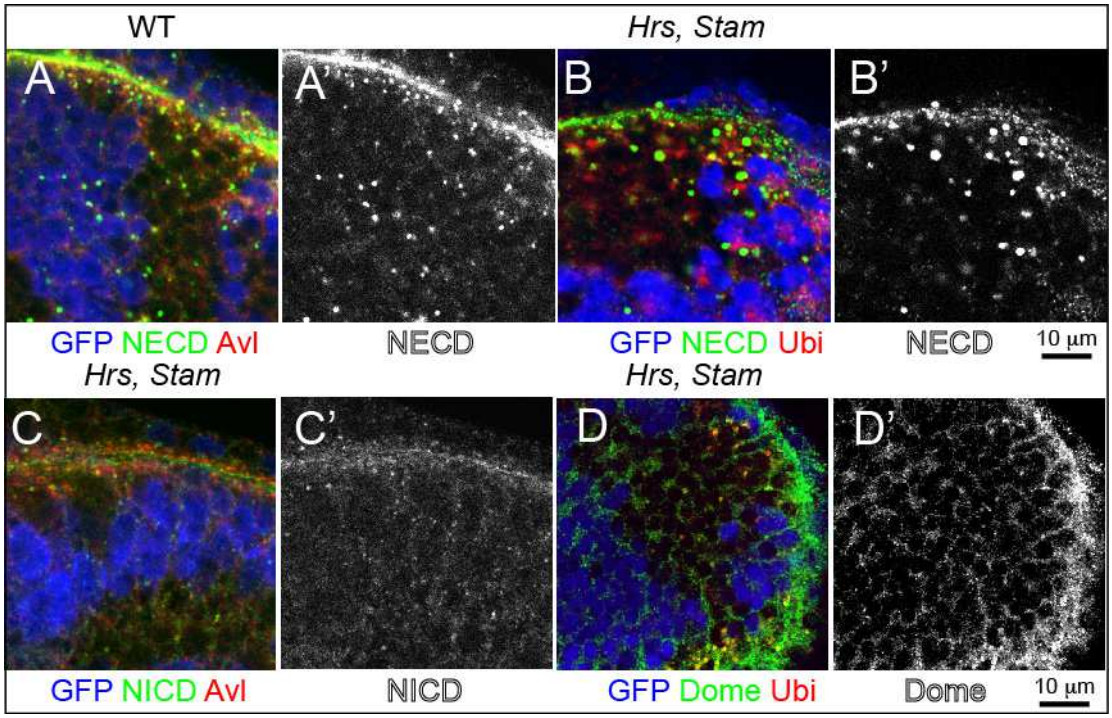

Figure 20 Hrs, Stam or double mutant for Hrs and Stam accumulates endocytic cargoes including Notch and Domeless receptor.

A-C) Co-localization of Notch, revealed either by an antibody that recognizes the extracellular domain of Notch (NECD) or the intracellular part (NICD) with Avl, a marker of early endosomes, in mosaic eye imaginal discs. Note that accumulation is less evident using NICD antibody B-B') Co-localization of NECD with an antibody that recognizes ubiquitin shows that in mutant *Hrs, Stam* clones NECD is accumulated in large intracellular puncta, some of which also positive for ubiquitin. D-D') Co-localization of Domeless (Dome) receptor with ubiquitin. *Hrs, Stam* mutant cells (GFP-negative) accumulate ubiquitinated cargoes and moderate levels of Dome, compared to WT tissue (GFP-positive).

Accumulation is less evident using an antibody to the intracellular portion of Notch (NICD) both in mosaic FE cells or eye imaginal discs **(Fig.19 G-H and Fig.20 C-C')**. Similarly we found a moderate accumulation of Domeless (Dome), the single-pass non-tyrosine-kinase receptor for JAK/STAT signaling **(Fig.20D-D')**.

9.1.3 ESCRT-0 is not required for endosome maturation

Due to the fact that ESCRTs are involved in endosome maturation (Doyotte, Russell, Hopkins, & Woodman, 2005; Razi & Futter, 2006; Rieder, Banta, Köhrer, McCaffery, & Emr, 1996; Stuffers, Sem Wegner, Stenmark, & Brech, 2009), we next assayed whether ESCRT-0 mutant cells possess mature endosomes. An aspect of endosome maturation is MVE biogenesis that involves formation of ILVs. We therefore analyzed the morphology of mutant cells at the ultra-structural level to determine whether ESCRT-0 components are able to form mature MVE containing

ILVs. To this end, we generated mutant eye discs containing a minimal amount of non-homozygous cells (Newsome et al., 2000).

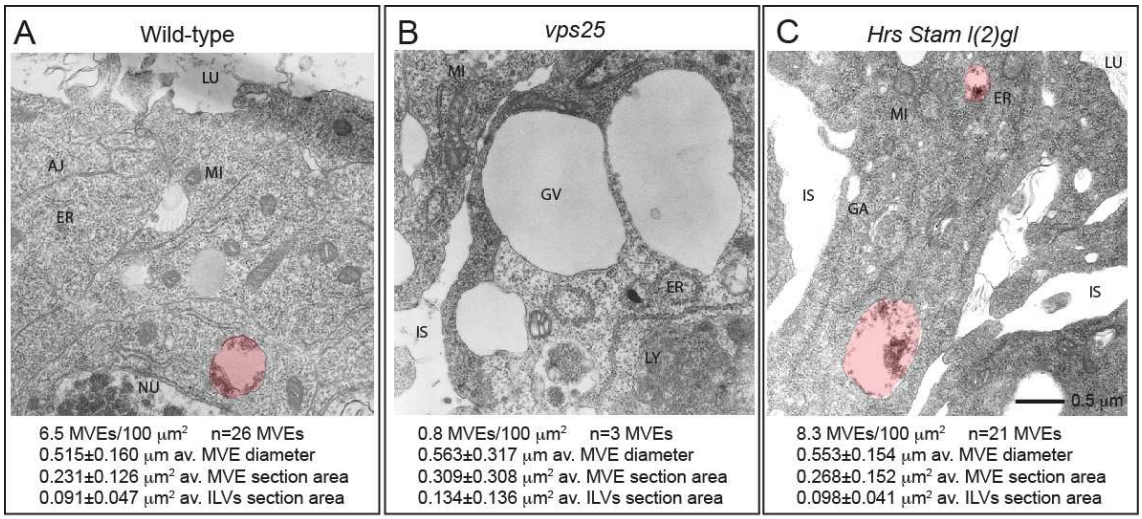

Figure 21 ESCRT-0 is not required for ILVs maturation

A-C) Electron micrograph of sections of eye tissue of the indicated genotype. A portion of the apical part of 2-3 epithelial cells above the level of the basal nuclei is shown. While MVE (highlighted in red) are absent in *Vps25* mutant cells, they are present in ESCRT-0 mutant cells. Quantification of MVE density, diameter, section area and ILV content is presented below each panel. Labels are as follows: PM: peripodial membrane, DT:disc tissue, LU: apical lumen, AJ Adherens Junctions, ER: Endoplasmic Reticulum, GA: Golgi.

In sections from control discs, we could observe several MVEs with an average diameter of approximately 500 nm and a little less than half of their section represented by ILVs **(Fig. 21A)**. As previously reported, in mutant cells for Vps25, a ESCRT-II component that is required for MVE biogenesis (Vaccari & Bilder, 2005), we detected very few MVEs **(Fig. 21B)**. In these cells, we often observe the presence of very large (diameter>1500nm) clear vacuoles, which are likely to be immature enlarged endosomes. Due to loss of apico-basal polarity of *Vps25* mutant cells, we also find large interstitial spaces. In tissue mutant for *Hrs*, *Stam*, *l(2)gl* we find MVEs that are indistinguishable in abundance and features to those of WT cells **(Fig. 21C)**, despite the presence of tissue disorganization similar to that of *Vps25* cells due to the *l(2)gl* mutation, which *per se*, does not affect trafficking (data not shown). These analyses indicate that ESCRT-0 components are dispensable for MVE biogenesis in epithelial tissue.

Another aspect of endosomal maturation is the progressive acidification of the lumen of endosomes (Maxfield & Yamashiro, 1987). To test whether *Hrs* or *Stam* or both *Hrs* and *Stam* mutant cells possess acidic organelles, we cultured mosaic discs in presence of Lysotracker, a vital dye that concentrates in acidic compartments. Compared to WT cells and consistent with what was previously reported (Vaccari et al., 2010), clones of *Hrs* mutant cells incorporate normal levels of Lysotracker **(Fig.22 A-C)**. Similarly, *Stam* or both *Hrs* and *Stam* mutant cells are indistinguishable to surrounding WT cells, indicating no impairment of the ability to acidify endocytic organelles.

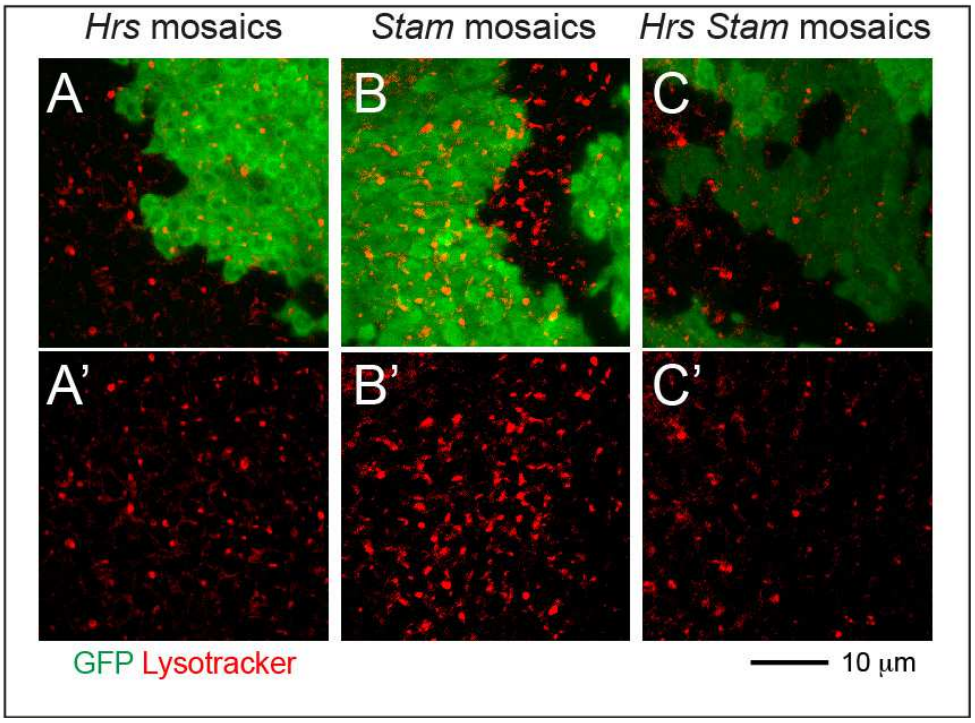

Figure 22*Hrs, Stam* or *Hrs* and *Stam* mutations do not impaired acidification.

Incorporation of Lysotracker in mosaic discs. A single subapical confocal cross-section is shown in each panel, showing no difference in acidification in WT (GFP-positive) versus mutant cells.

Taken together, these data indicate that loss of *Hrs, Stam* or of both do not affect endosomal maturation.

9.1.4 ESCRT-0 is not required for Notch signaling activation or downregulation

Accumulation of Notch in endosomes of ESCRT-I, -II, -III mutants correlates with ectopic and ligand-independent Notch signaling (Vaccari et al., 2009). In contrast, mutations that disrupt earlier steps of endocytic vesicle trafficking such as those affecting *Rab5* and *avl* inhibit activation of Notch (Vaccari et al., 2008). To test Notch activation in ESCRT-0 mutants, we monitored expression of the transcription factor Hnt and Cut in FE cells. Hnt and cut expression is modulated by Notch activation at mid-oogenesis. In particular, at stage 6 of oogenesis, Notch signaling is activated in FE cells. As a result, FE cells downregulate Cut expression, upregulate Hnt expression, arrest mitotic cell cycles and begin to endoreplicate (Deng, Althauser, & Ruohola-Baker, 2001; López-Schier & St Johnston, 2001). Surprisingly, the pattern of Hnt and Cut expression detected by immunofluorescence in small clones of *Hrs* or *Stam* or both *Hrs* and *Stam* mutant FE cells is unchanged, when compared to WT cells, indicating that Notch activation is not altered in ESCRT-0 mutants **(Fig.23 A-F)**. Overall, our data confirm and extend the notion that ESCRT-0 activity is not required to prevent ectopic ligand-independent Notch signaling activity, as is the case of ESCRT-I, -II, -III (Thompson et al., 2005; Vaccari & Bilder, 2005; Vaccari et al., 2009).

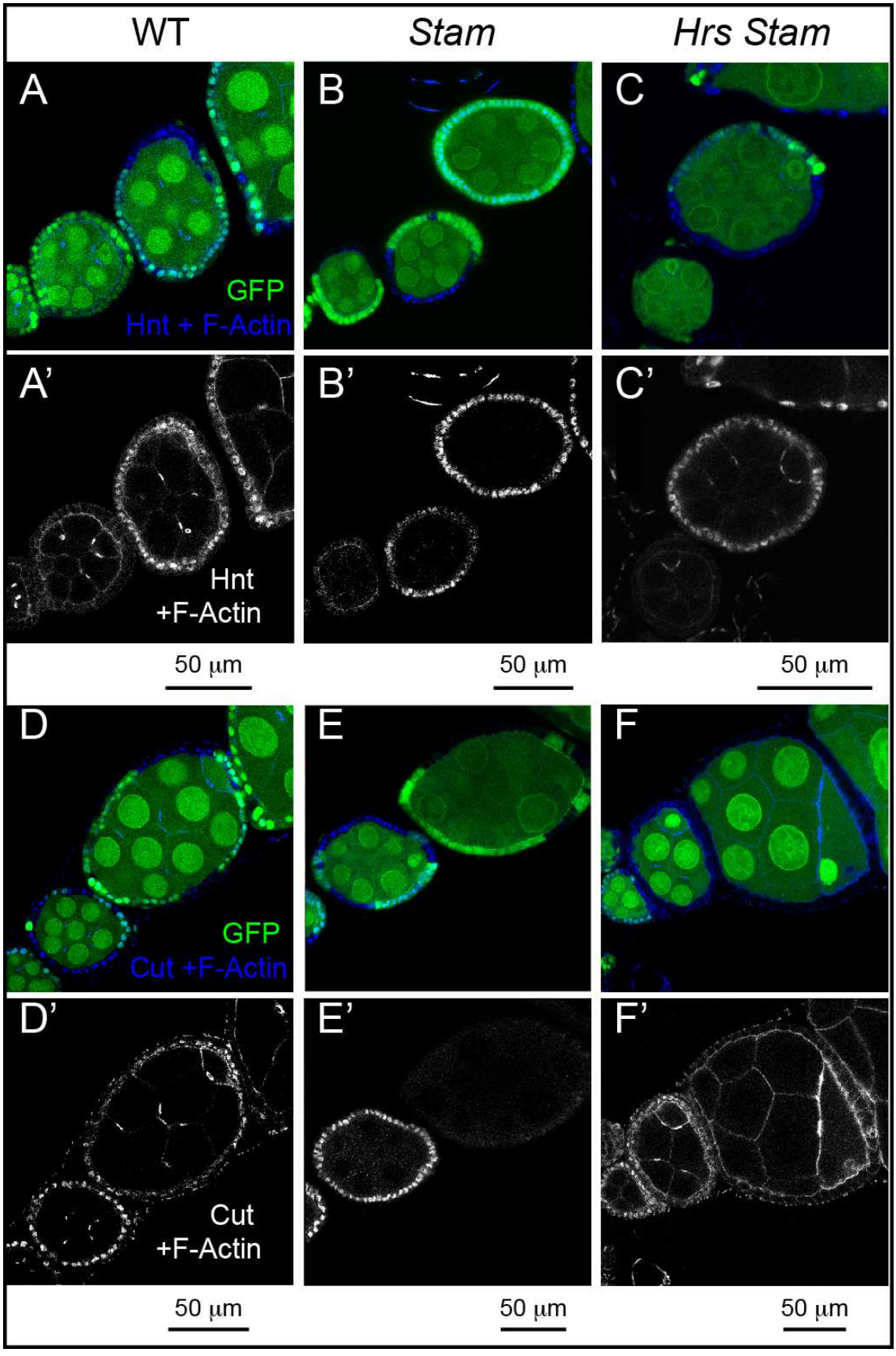

Figure 23 ESCRT-0 is not required for Notch signaling activation or downregulation

Mosaic egg chambers at stages 5-7 oogenesis stained to detect the Notch target Hnt (A-C) and Cut (D-F) and F-Actin. *Stam* or *Hrs, Stam* mutant cells are marked by absence of GFP. In both *Stam* and *Hrs, Stam* mutant FE cells, Hnt is normally expressed and Cut normally downregulated after stage 6, indicating no impairment of Notch signaling activation (A-F' show single channels).

9.2 Results Project 2

9.2.1 Mitf protein localizes in lysosomes and in the nucleus of WDs.

To explore the function of *Drosophila* Mitf in *vivo,* we first characterized whether it is expressed in the WD. We carried out *in situ* hybridizations using a probe for Mitf that lacks the bHLH-Zip region to avoid cross-reaction with bHLH transcription factors expressed in the WD. To control for the specificity of the probe, we performed the *in situ* experiment in WD overexpressing a WT Mitf form (Jón H Hallsson et al., 2004) using the GAL4/UAS system [**see** Material and Methods for more details (Duffy, 2000)]. We used ms1096-Gal4 (ms1096>), which drives expression in the wing pouch, the central part of the wing disc, and found that specifically recognize Mitf **(Fig.24)**. Hybridization in WT discs revealed that endogenous Mitf mRNA is uniformly expressed at low but detectable levels in the WD **(Fig.24).**

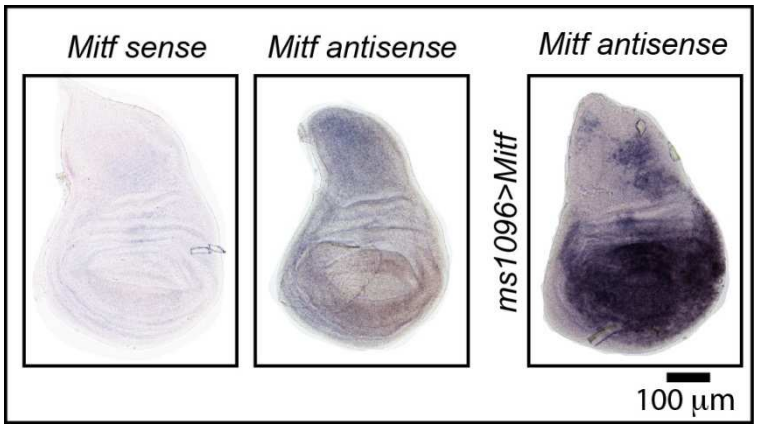

Figure 24 Expression of endogenous Mitf in *Drosophila* WDs

***In situ* experiment using labeled sense and antisense RNA probe for Mitf transcripts in WD from yellow white (control) animals and from animals overexpressing Mitf in the WD. The sense probe has been used as a negative control. Dorsal is up, anterior to the left. All WDs shown in figures are oriented as such.**

To quantify the level of Mitf overexpression in WDs we performed a qPCR. WDs overexpressing functional Mitf or a Mitf dominant negative form which is unable to bind the DNA (MitfDN; (Jón H Hallsson et al., 2004))showed 18-22 folds increased in mRNA levels of Mitf compared to control discs **(Fig.25A)**.

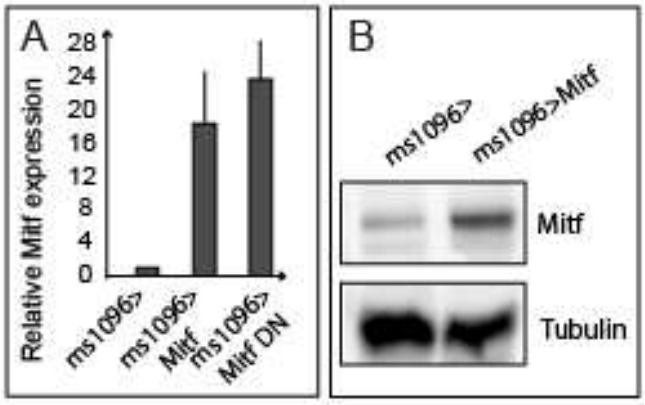

Figure 25 Expression of mRNA and protein levels of Mitf in WT as well as Mitf overexpressing WDs.

A) qPCR analysis showed levels of Mitf mRNA in WDs overexpressing both forms of Mitf compared to control. RPL32 has been used as housekeeping control. The values represent the means ± s.d. of two independent experiments B) Detection of the *Drosophila* Mitf protein by Western blot using an anti-Mitf antibody and tubulin as loading control in WT WDs and WDs overexpressing Mitf. The antibody recognizes a band of around 90 kDa, the expected size for Mitf.

We then studied the localization of Mitf at the protein level in WDs. To this end, we first raised an antibody specific for *Drosophila* Mitf by immunizing rabbits with a purified GST-tagged recombinant portion of Mitf protein (**see** Material and Methods for details). Western blot analysis shows that the antibody we generated specifically recognizes a band of the expected size in WT WDs, which is increased in WDs overexpressing Mitf **(Fig.25B)**.

To detect Mitf localization at the subcellular level, we performed an immunostaining in the WDs. As a control for specificity of the antibody for immune-localization analyses, we stained WDs overexpressing Mitf or MitfDN in the wing pouch**.** Consistent with our in situ hybridization findings, also at the protein level Mitf is uniformly expressed at low levels in WT WD **(Fig. 26A-B)**.

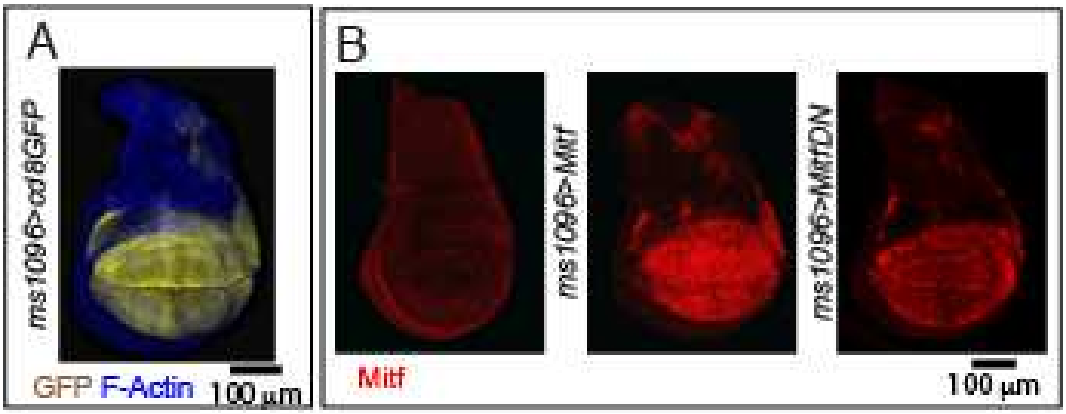

Figure 26 Mitf protein distribution in WDs.

A) A WD overexpressing the transmembrane protein CD8-GFP shows the expression pattern of MS1096-GAL4 driver. The GFP region (shown in yellow) is the part of the disc in which constructs used in this study have been overexpressed. B) Control WD and WDs overexpressing Mitf or MitfDN stained with anti-*Drosophila* Mitf antibody.

At higher magnification, we observed that Mitf localizes in cytoplasmic puncta in WT tissue. In contrast overexpression of both Mitf and MitfDN leads to a prominent localization in the nucleus of discs cells **(Fig.27).**

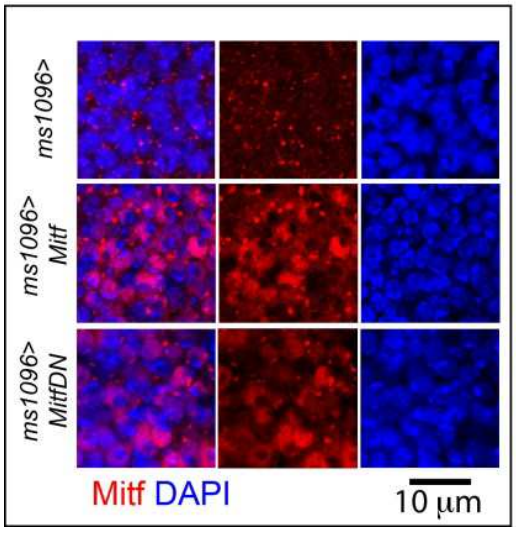

Figure 27 Mitf protein localizes in the nucleus in the WD.

High magnifications of portions of WT or overexpressing WDs for Mitf or MitfDN stained with Dapi.

Because mammalian TFEB shuttles between lysosomes and the nucleus (Jose A Martina, Chen, Gucek, & Puertollano, 2012; Settembre et al., 2012), we sought to determine whether the observed punctate cytoplasmic localization corresponds to lysosomes. To this end, we stained discs expressing YFP-lamp1, which has been shown to be a *bona fide* marker for lysosomes (Takáts et al., 2013)**(Fig.28A)**.

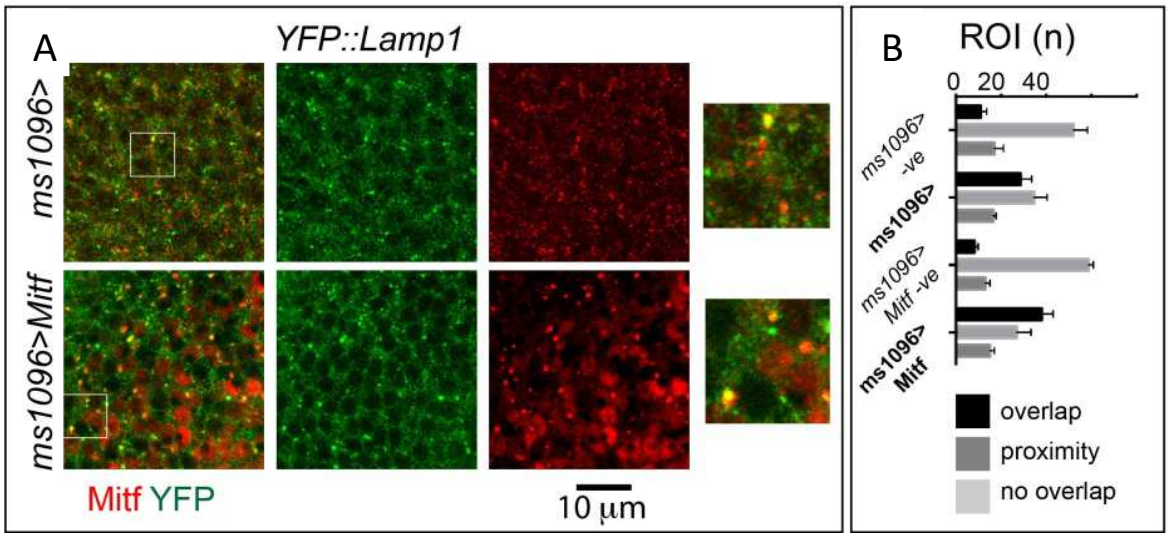

Figure 28 Mitf protein localizes also in the lysosomes of WDs.

A) High magnifications of portions of WT or overexpressing WDs for Mitf in the background of the *YFP::Lamp1* trapped line. Note that Mitf is present in the nucleus when overexpressed and in a fraction of lysosomes. B) Quantification of the experiment shown in A) ms1096>-ve and ms1096>mitf-ve are negative controls (see material and methods for more details).

In this analysis, we found that approximately half of the puncta are positive for YFP-Lamp1, with a slight increase when Mitf is overexpressed **(see quantification in Fig.28B)**. Thus, Mitf localizes to lysosomes and possibly to additional cytoplasmic compartments.

9.2.2 Mitf regulates lysosomal biogenesis

To test whether *Drosophila* Mitf promotes lysosomal biogenesis as its mammalian counterpart does, we labeled lysosomes in WT and Mitf-overexpressing WDs with the acidophilic dye Lysotracker. Upon overexpression in the wing epithelium, Mitf leads to an expansion of the acidic compartments, which are significantly increased in size **(Fig. 29A quantification in B).** Conversely, overexpression of MitfDN or NICD, the active form of Notch does not show similar expansion of acidified compartments.

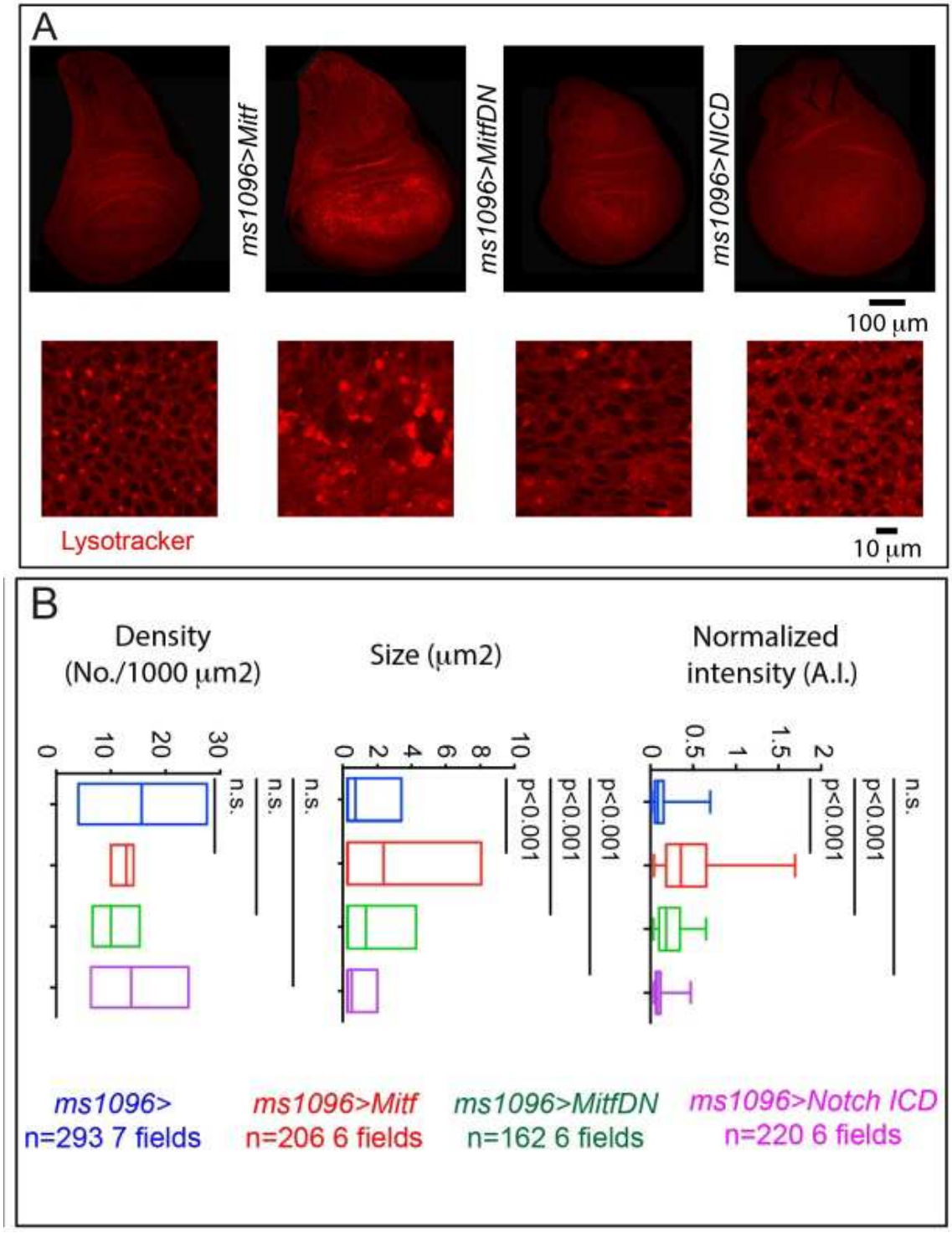

Figure 29 Mitf regulates lysosomal biogenesis and in some extent also autophagy.

A) Lysotracker analysis in WT WDs or WDs overexpressing Mitf, MitfDN or Nicd. High magnifications of portions of the WDs are shown below the discs. B) Quantification of lysotracker puncta density, size and normalized intensity of the experiment shown in A).

To determine whether Mitf regulates autophagy, we labeled discs to detect ref(2)P (the *Drosophila* homolog of human p62/SQSTM1), and Atg8a (human LC3). Overexpression of Mitf leads to a mild increase in ref(2)P and Atg8a signal

(Fig. 30A-B), relative to the basal low levels observed in control discs, suggesting that Mitf might stimulate autophagy.

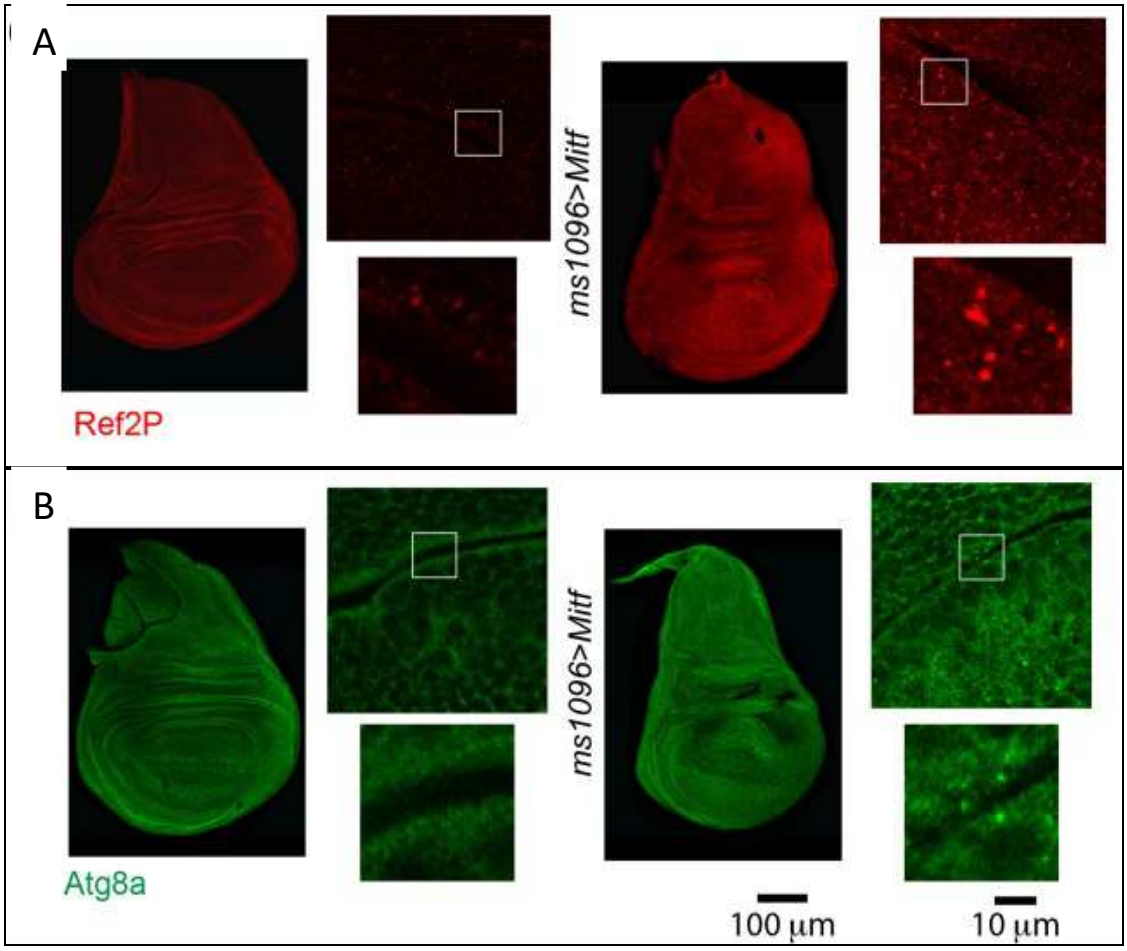

Figure 30 Mitf might affect autophagy.

A) Immunolocalization of ref(2) or B) ATG8a, both markers of the autophagic pathway in discs of the indicated genotype. Side panels are higher magnifications of the tissue with insets shown below them.

Finally, we find that overexpression of Mitf in the WDs leads to formation of a low number of apoptotic cells, as shown by expression of activated product of the gene Decay (Caspase 3), which is not normally present in control discs. Smaller amount of apoptotic cells are also detectable on MitfDN overexpressing WDs **(Fig.31)**. Combined, these data indicate that misexpression of Mitf leads to activation of catabolic processes as observed for mammalian TFEB (Settembre et al., 2011).

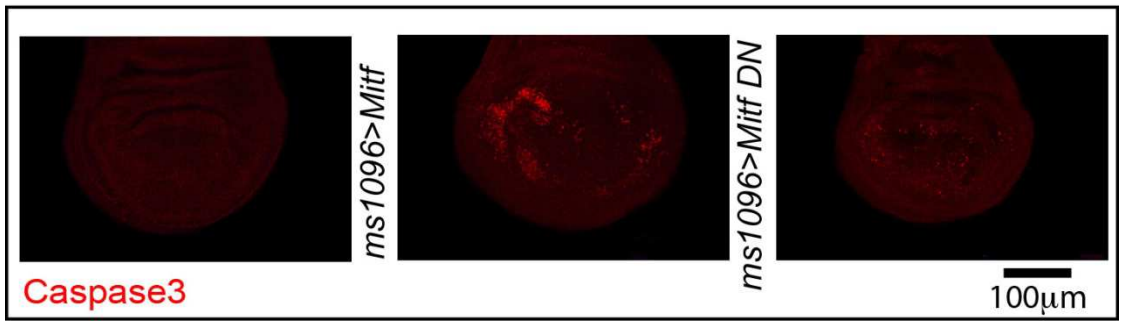

Figure 31 Mitf overexpression leads to apoptotic cells.

Control WD or WDs overexpressing either WT or DN forms of Mitf stained for cleaved-Caspase 3, a marker for apoptosis. WDs overexpressing either forms of Mitf show some apoptotic cells compared to control.

9.2.3 Mitf positively regulates V-ATPase subunit expression

To assess whether Mitf acts as a master regulator of lysosomal gene expression in *Drosophila*, we performed qPCR on extracts from WT discs and discs overexpressing Mitf or MitfDN to detect expression levels for a panel of *Drosophila* homologs of TFEB target genes that includes V-ATPase subunit genes, lysosomal genes and autophagy genes. In this analysis we found that expression of endogenous mRNA of the V-ATPase subunits is increased 4 to 5 folds upon Mitf overexpression, compared to control WDs expressing MitfDN. In contrast, expression of the lysosomal gene *Lamp1* and of the autophagy gene *ref(2)P* is not upregulated upon Mitf overexpression in WDs **(Fig.32)**.

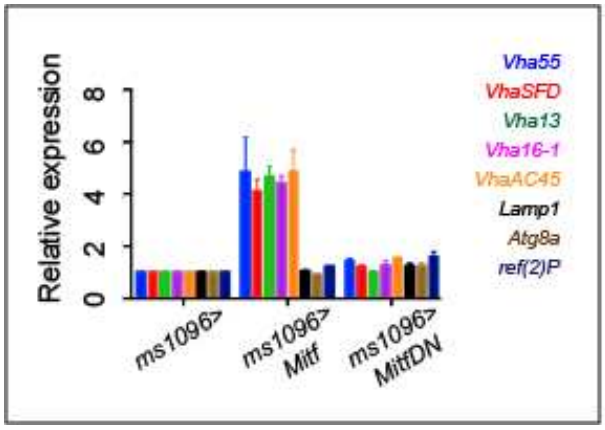

Figure 32 qPCR analysis of putative Mitf target genes in WDs.

RPL32 has been used as housekeeping control. The values represent means ± s.d. of two independent experimets. All the V-ATPase subunits but not Lamp1, Atg8a and Ref(2)p are transcriptional targets of Mitf.

These data indicate that *Drosophila* Mitf regulates transcription of lysosomal genes as its mammalian counterpart. However the set of genes regulated by Mitf, at least in the WD might be limited when compared to mammals.

We confirmed these data by studying the expression in WD of available GFP and YFP knock-in lines for some of the genes that we have analyzed by qPCR. In particular, we used three lines with insertions in genes encoding components of the cytoplasmic V_1 sector of V-ATPase (*YFP::Vha55* tagging the gene encoding subunit B, *GFP::VhaSFD* tagging the gene encoding subunit H, *GFP::Vha13* tagging the gene encoding subunit G). One line (*GFP::Vha16-1*) with a GFP insertion within the gene encoding the c subunit of the membrane-embedded V_0 sector and one line (*GFP::VhaAC45*) tagging the gene encoding for the accessory subunit AC45, which has been shown to be associated with the V_0 sector (J.R. Jansen & J.M. Martens, 2012). Finally, we used *YFP::Lamp1,* tagging the single *Drosophila* homolog of mammalian Lamp1/2 (Buszczak et al., 2007; Morin et al., 2001; Takáts et al., 2013) (**see** Material and Methods for details).

Upon Mitf overexpression, all lines displayed variable up-regulation with the exception of *YFP::Lamp1* **(Fig. 33A).**

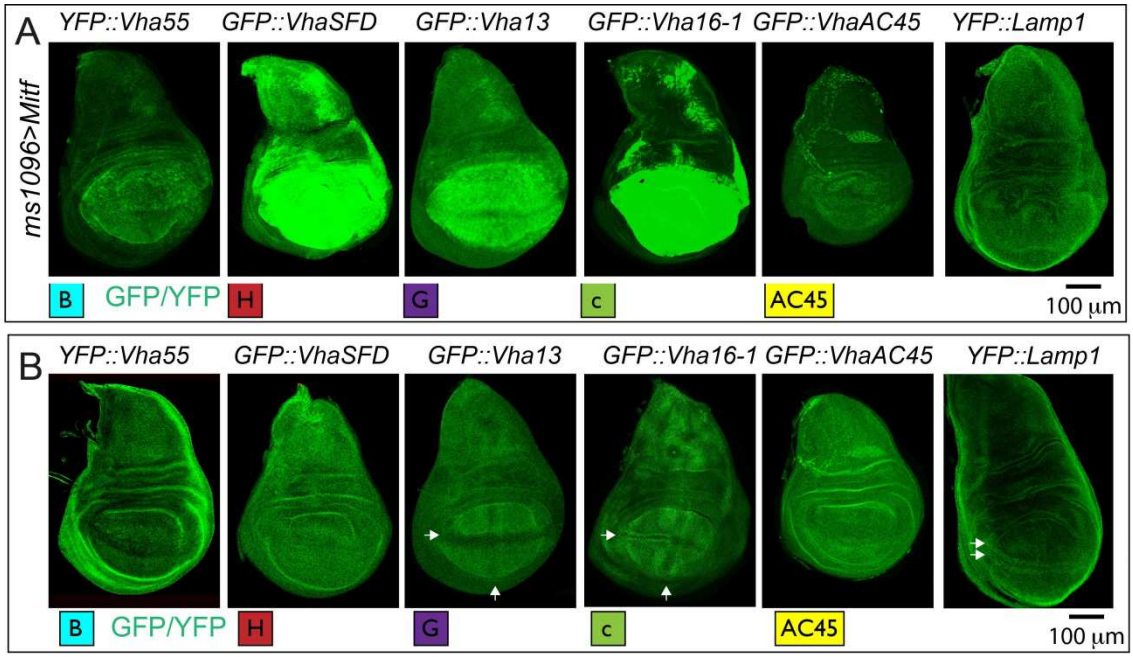

Figure 33 Mitf regulates V-ATPase expression.

A) Pattern of expression in WDs of the tagged lines for indicated subset of *Drosophila* homologs of TFEB target genes upon overexpression of Mitf. Note that V-ATPase subunit expression but not Lamp1 expression is controlled by Mitf. B) Pattern of expression in WDs of tagged lines for the indicated subset of *Drosophila* homologs of TFEB target genes.

9.2.4 Vha16-1 and Vha13 expression is modulated by Notch signaling

In the course of the study of V-ATPase subunit expression, we observed that the expression pattern of *GFP::Vha16-1, GFP::Vha13* and *YFP::Lamp1* appears patterned. This is not the case for expression of *YFP::Vha55*, *GFP::VhaSFD*, *GFP::AC45* **(Fig. 33B).** Expression of *GFP::Vha16-1, GFP::Vha13* and *YFP::Lamp1* appeared distinctive mostly at the dorso-ventral (D/V) boundary and anterior-posterior (A/P) boundary of the WD **(Fig. 33B, arrows)**, suggesting that these genes might be controlled by developmental signaling pathways occurring at the boundaries. Among others, a prominent developmental pathway operating at tissue boundaries in the wing pouch is Notch signaling. To explore a possible correlation between lysosomal genes and developmental signaling, we analyzed *GFP::Vha16-1* in discs expressing the Notch signaling reporter *E(spl)mβ-LacZ* (Bailey & Posakony, 1995). We observed that expression of the reporter is complementary to that of *GFP::Vha16-1* **(Fig. 34).**

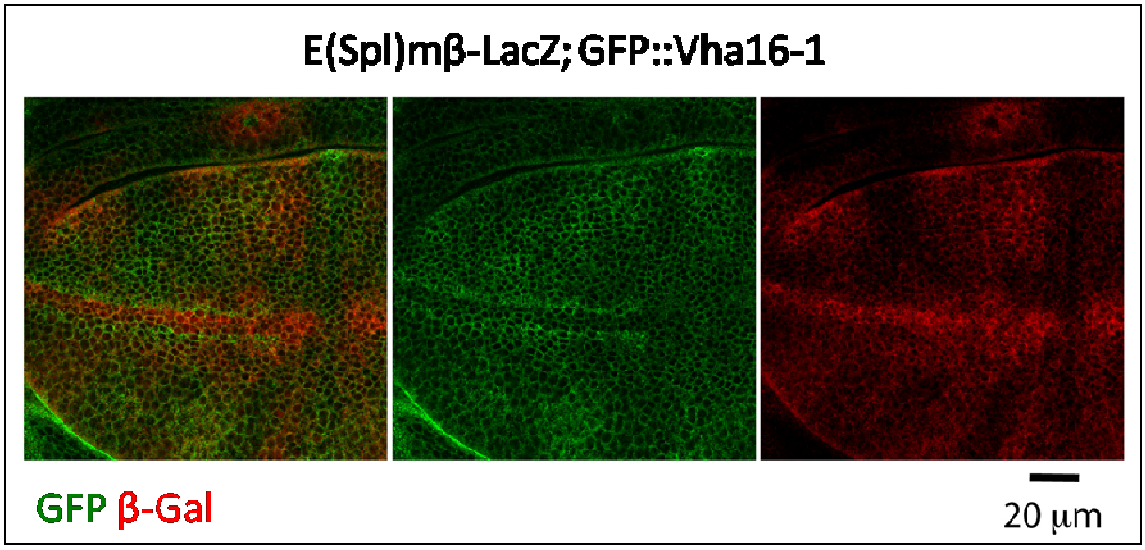

Figura 34 GFP::Vha16-1 expression pattern is complementary to the expression pattern of the E(spl)mβ.

E(spl)mβ-LacZ GFP::Vha16-1 WDs stained for β-Gal.

To test whether Notch signaling might control V-ATPase subunit expression, we overexpressed NICD or NEXT, two activated forms of Notch, in the wing pouch with ms1096-Gal4 driver and assessed changes in expression of Vha16-1 by *in situ* hybridization. Ectopic overexpression of NICD or NEXT causes tissue overgrowth as previously reported (Go et al., 1998). Moreover, qPCR analysis shows that overexpression of NICD is quite efficient with 5 fold increased in mRNA Notch levels compared to control, indicating that Notch signaling was ectopically activated **(Fig.35A)**.

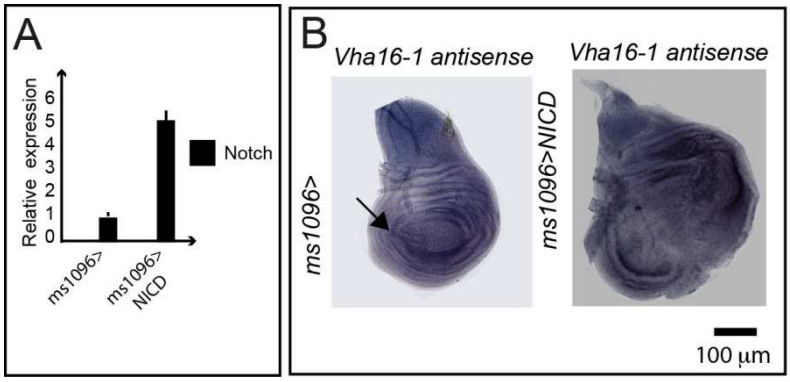

Figure 35 Upon NICD overexpression, Vha16 mRNA level is reduced compared to control.

A) Notch expression levels in WT WDs and WDs overexpressing NICD tested by qPCR. WDs overexpressing NICD showed 5 fold increased in Notch mRNA levels. B) In situ experiment in WT WD and WDs overexpressing NICD using labeled Vha16-1 antisense probe revealed changes in the transcriptional mRNA Vha16-1 pattern upon NICD overexpression.

Interestingly, under these conditions, we observed that *Vha16-1* expression in the wing pouch of overexpressing discs is reduced compared to control **(Fig.35B).** Such reduction was confirmed upon analysis of *GFP::Vha16-1* and it is observed also in *GFP:Vha13* discs overexpressing NICD **(Fig.36A-D)**. However, this is not the case for *YFP::Vha55*, *GFP::VhaSFD*, *GFP::VhaAC45* **(Fig 36E)** These data suggest that Notch could modulate the expression of a subset of V-ATPase subunits. To exclude that changes that we observe could be due to stability of the GFP tag, we repeated the experiment and detected the expression of the unrelated protein GFP::CG8668. *CG8668* encodes a transmembrane glycosyl-transferase, unrelated to Notch pathway. GFP::CG8668 is expressed in a uniform pattern in the WD that is not changed by ectopic Notch activation **(Fig.36F)**, confirming that effects observed are not due to nature of the tag. Overall these data suggest that Notch is able to modulate expression of a subset of V-ATPase subunits.

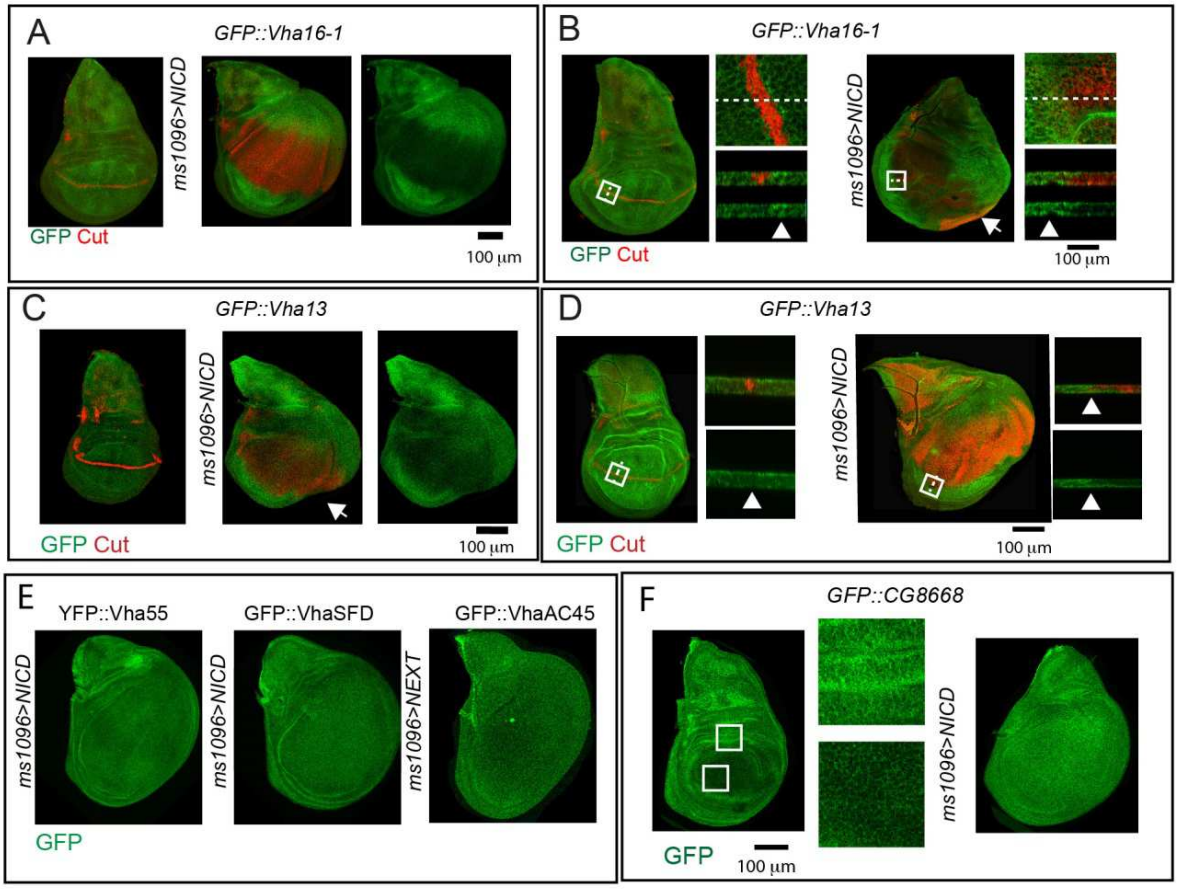

Figure 36 *GFP::Vha16-1* and *GFP::Vha13* expression is downregulated by activation of Notch signaling.

A-D) Discs of the indicated genotype stained to detect the Notch target Cut. Note that upon NICD overexpression, *GFP::Vha16-1* and *GFP::Vha13* expression are very low in Cut-positive cells. In B) e D) xy and z-section of the boxed areas are shown to indicate the complementarity of Cut and GFP expression (arrowheads). E) WDs overexpressing NICD or NEXT in the background of *YFP::Vha55*, *GFP::VhaSFD*, *GFP::VhaAC45*. Note that expression pattern of these V-ATPase subunits do not change upon Notch overexpression. F) WT WD or WD overexpressing NICD showing the expression pattern of *GFP::CG8668.* Expression of GFP-CG8668 is uniform in the disc. Enlargements of the indicated areas of the dorsal hinge and of the pouch are shown beside the disc.

9.2.5 PNCs show elevated expression of GFP::Vha16-1

One exclusive feature of *GFP::Vha16-1* expression that was not displayed by *GFP::Vha13* or other trapped lines is elevated expression in the PNCs of the WDs, such as those that straddle the anterior D/V boundary **(Fig.33B arrows).** These PNCs are instructed by the high levels of wg signaling occurring at the boundary. Wg is expressed by boundary cells downstream of Notch signaling. PNCs will gradually develop into SOPs by the Notch-dependent lateral inhibition process (Diaz-Benjumea & Cohen, 1995; Hartenstein & Posakony, 1990; Rulifson, Micchelli, Axelrod, Perrimon, & Blair, 1996). We find elevation of *GFP::Vha16-1* expression appears restricted to cells positive for the SOP marker *neur-lacZ* **(Fig.37A)**. Interestingly, expression of *GFP::Vha16-1* is low in cells positive for *E(Spl)m4-LacZ* **(Fig.37B)** a Notch target that identifies non-SOP cells, in which Notch signaling is active, within differentiated PNC cluster (Bailey & Posakony, 1995)

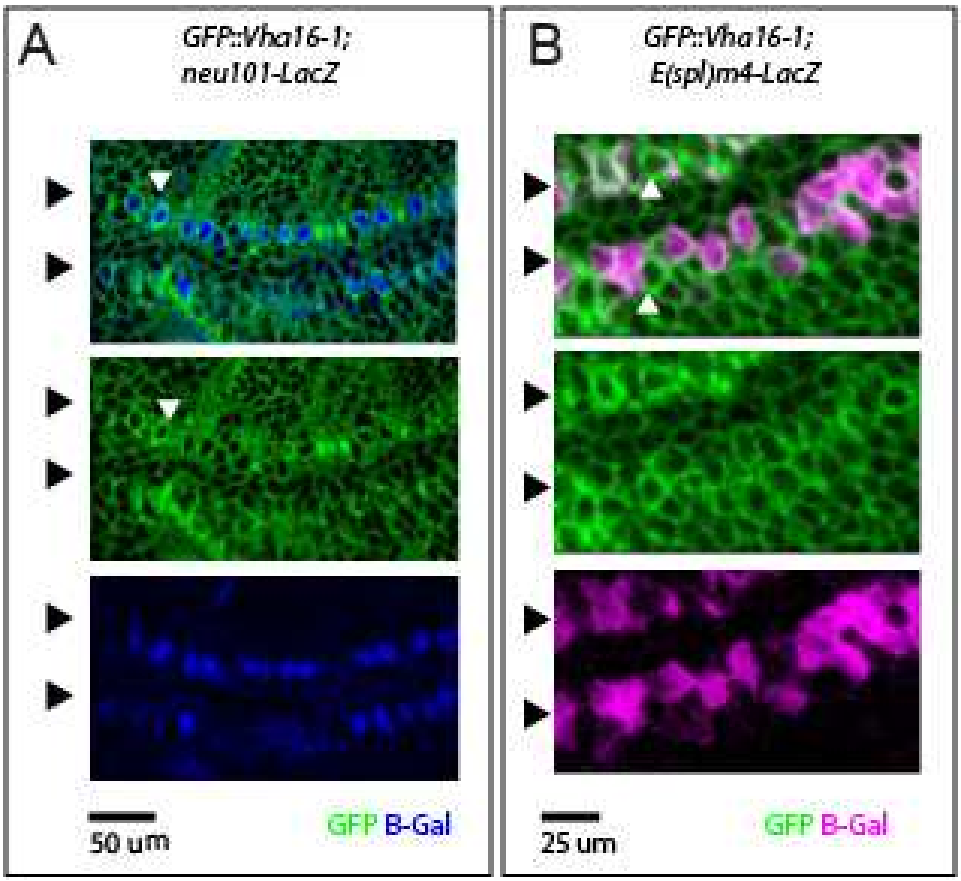

Figure 37 Vha16-1 expression is elevated in SOPs

A-B A high magnification of the anterior part of the wing pouch of the WDs of the indicated genotypes stained as indicated. Note that *GFP::Vha16-1* expression is elevated in *neur-LacZ* positive cell and low in *E(Spl)m4* positive cell.

Elevated expression of Vha16-1 in the SOPs of the anterior part of the D/V boundary was also detected by *in situ* hybridization with a probe that recognizes endogenous Vha16-1 mRNA **(Fig.38A)**, indicating that it is not due to GFP tagging of the Vha16-1 gene.

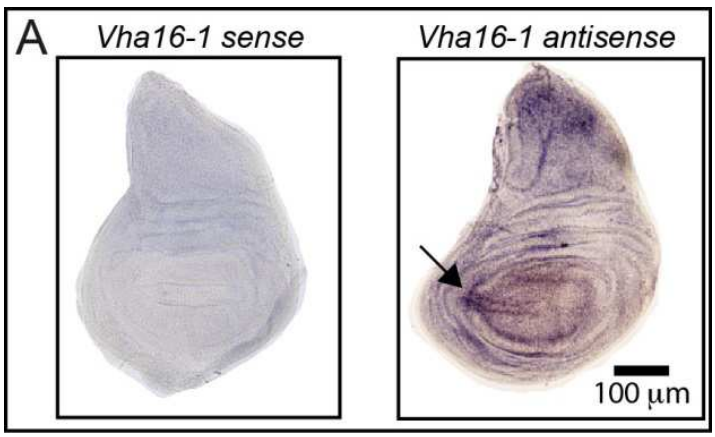

Figure 38 Vha16-1 mRNA distribution in WDs revealed by *in situ* hybridization experiment.

Labeled sense and antisense RNA probe for Vha16-1 transcripts in *yellow white* (control) WDs. Sense probe has been used as negative control. Note that mRNA Vha16-1 expression is higher in two stripes of the anterior part of the D/V boundary.

To further characterized Vha16-1 expression in the forming SOPs, we next studied *GFP::Vha16-1* localization in discs stained for the early PNC marker Ac (Cubas, de Celis, Campuzano, & Modolell, 1991). We find that not all the cells positive for Ac display elevated levels of *GFP::Vha16-1* expression neither elevated *GFP::Vha16-1* expression is a characteristic seen exclusively by Ac-positive cells **(Fig.39)**.

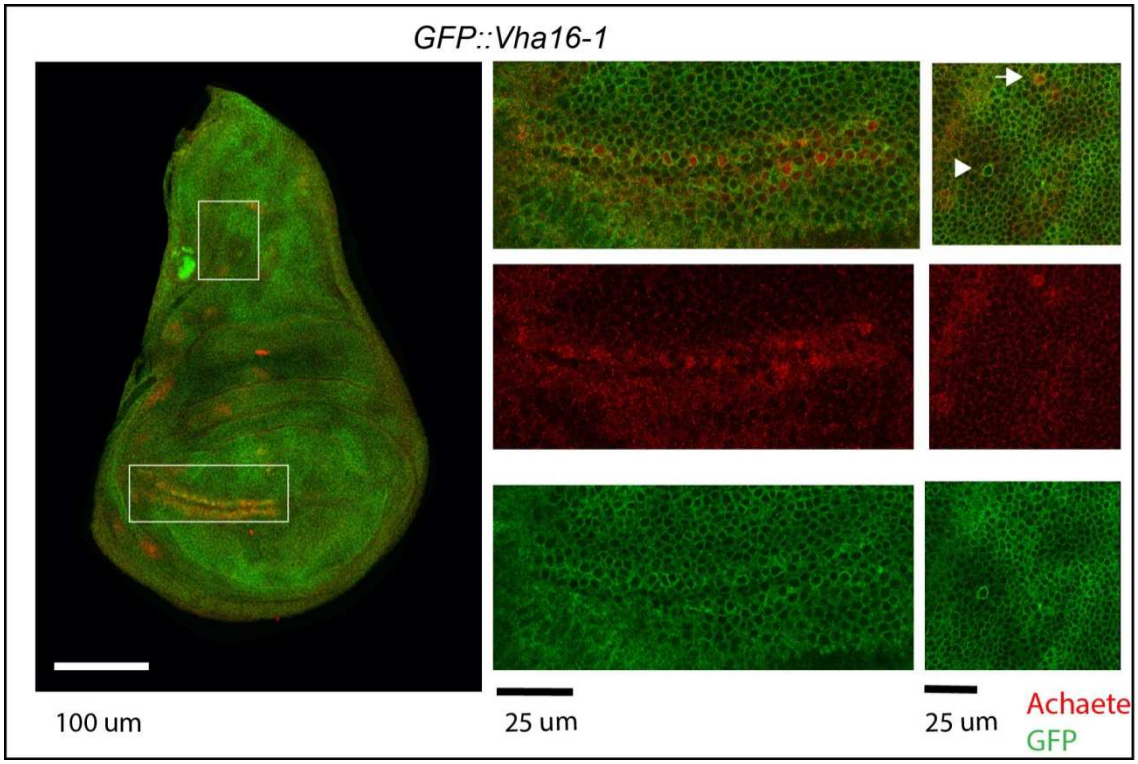

Figure 39 Vha16-1 expression is elevated in the PNCs of WDs.

***GFP::Vha16-1* WD stained for Achaete protein and GFP. In the middle and on the left side higher magnifications with splitted channels of the anterior part of the wing pouch and the dorsal hinge of the notum are shown. Note that *GFP::Vha16-1* expression is elevated in Ac-expressing tissue. Note that some Ac-positive cells do not show elevated *GFP::Vha16* expression (Arrows). Conversely, elevated *GFP::Vha16-1* expression is seen in cells not positive for Ac (arrowhead).**

A possible explanation for such finding is that *GFP::Vha16-1* is expressed in the PNCs transiently and at late stages of PNC development when Ac expression is starting to fade. Remarkably, expression of CD8GFP, a membrane-tagged form of GFP, under the control of two independent GAL4 elements inserted in the 5'UTR of *Vha16-1* (*Vha16-1::Gal4* **Fig.14A**) can be detected in variable subsets of SOPs,

stained with the SOP marker hindsight (Hnt) **(Fig. 40 A-B)**. Although expression of CD8GFP only partially recapitulate the pattern of *GFP::Vha16-1,* these data indicate that expression in SOPs is likely to be controlled by the *GFP::Vha16-1* promoter. This together with the fact that not all Ac positive cells show elevated *GFP::Vha16-1* expression and vice-versa **(Fig. 39 arrow and arrowhead)** suggest that Vha16-1 expression in SOPs might be tightly temporarily regulated during SOP development.

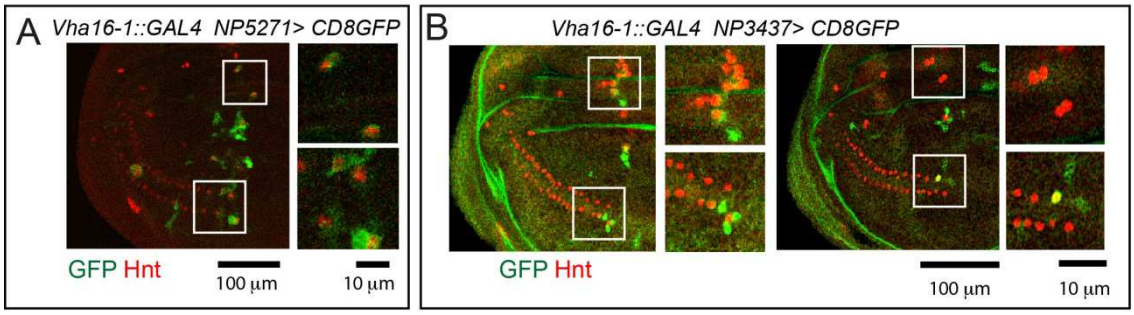

Figure 40 Vha16::Gal4>CD8GFP recapitulate GFP::Vha16-1 expression in some SOPs.

Vha16-1^{NP5271}Gal4> and Vha16-1^{NP3437}Gal4> UAS-CD8GFP WDs stained for Hnt and GFP. Close-ups of the boxed regions are shown on the right. Note GFP expression in some Hnt- positive SOPs of the margin and hinge (insets) and that the two discs of the same genotype in panel E have a slightly different expression pattern suggesting a temporal and developmental control of Vha16-1 expression.

9.2.6 Elevation in SOP is part of the pro-neural cascade

To test whether Vha16-1 follows SOP determination that is instructed by Notch signaling by lateral inhibition, we generated ectopic SOPs by ectopically expressing the Notch target *E(spl)m4*, which antagonizes Notch signaling activation (Apidianakis, Nagel, Chalkiadaki, Preiss, & Delidakis, 1999).

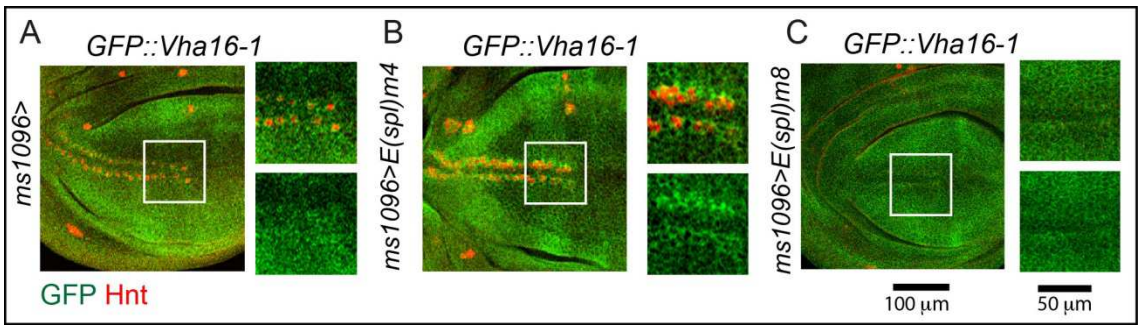

Figure 41 Elevated Vha16-1 expression follows SOP differentiation.

A-C) GFP::Vha16-1 WD or GFP::Vha16-1 WD overexpressing the Notch target E(Spl) genes m8 and m4 under ms1096-Gal4. Note that overexpression of m8 results in loss of sensory organs and of GFP::Vha16-1 expression at the anterior margin, while overexpression of m4 leads to formation of

ectopic SOPs expressing GFP::Vha16-1. Insets corresponding to areas of the pouch are shown on the sides of each disc.

We found that expression of *GFP::Vha16-1* is elevated in ectopic clusters **(Fig. 41A-B)**. In contrast, ectopic expression of *E(spl)m8*, a Notch target gene that is known to enforce lateral inhibition, leads to disappearance of SOPs differentiation and associated *GFP::Vha16-1* expression **(Fig. 41C)**. Together this evidence indicates that *GFP::Vha16-1* expression follows Notch-dependent PNC differentiation.

Changes in V-ATPase subunit expression induced by Notch activation might correlate with lysosomal functionality. In fact we have found that in NICD overexpressing WDs lysotracker puncta are slightly smaller compared to control **(Fig.29A-B).** However, this is unlikely due to control of Mitf by Notch signaling. Indeed when we monitored expression of endogenous mRNA Mitf by qPCR upon overexpression of NICD we found no change **(Fig.42A)**. At protein level, Mitf protein shows a uniform expression pattern upon NICD **(Fig.42B)**.

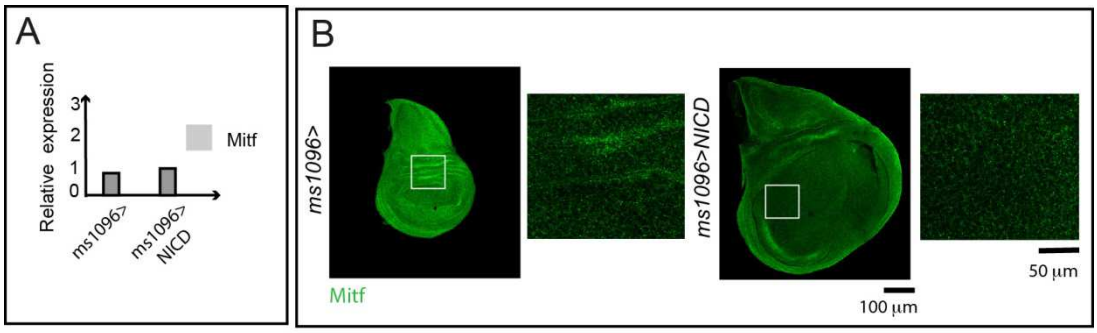

Figure 42 Mitf expression does not change upon NICD expression.

A) Mitf transcript levels assessed by qPCR in WT WDs or WDs overexpressing NICD. B) WT WDs and WDs overexpressing NICD stained for Mitf protein. Beside each disc is shown an inset of a region of the wing pouch.

To test whether elevation of Vha16-1 expression in SOPs depends on Mitf we then overexpressed MitfDN and studied Vha16-1 expression. Interestingly, we found a reduction of *GFP::Vha16-1* expression at the anterior boundary SOPs,which are marked with Hnt **(Fig.43)**. Together with our Mitf localization analysis in the disc, these data indicate that basal levels of Mitf play a permissive role in the upregulation of Vha16-1 during SOP development. In the course of this analysis we

also found that the stereotypic pattern of SOPs was altered in discs expressing MitfDN **(Fig.43 arrowheads)**, prompting us to evaluate the importance of Mitf in SOP differentiation.

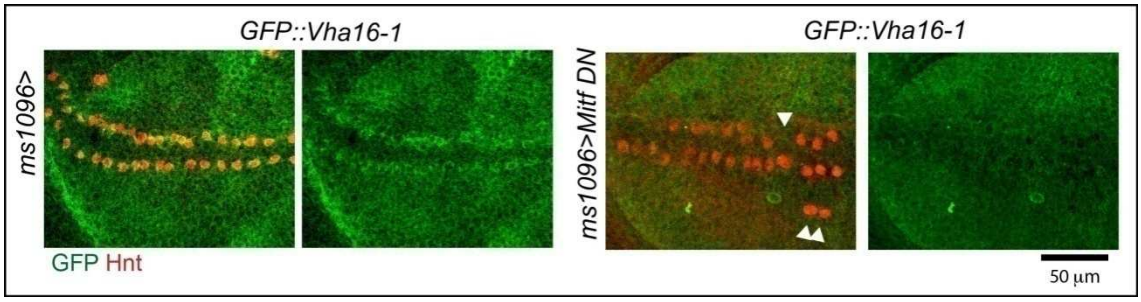

Figure 43 MitfDN overexpression disrupts Vha16-1 expression pattern in SOPs.

High magnifications of the anterior part of the wing pouch of *GFP::Vha16-1* WDs or *GFP::Vha16-1* overexpressing MitfDN. The image is a maximal projection of several sections. Note that overexpression of MitfDN disrupts the pattern of *GFP::Vha16-1* expression in SOPs and leads to missing and ectopic SOPs (arrowheads).

9.2.7 Proneural development is supported by TFEB/V-ATPase axis.

To determine whether *Mitf* might play a role in the proneural differentiation cascade that leads to SOP formation, we overexpressed Mitf and MitfDN in the wing pouch and assessed in detail the alteration of PNCs patterning of the SOPs straddling the anterior D/V boundary. These SOPs will give rise to the chemo-sensory bristles of the adult wing margin (Hartenstein & Posakony, 1990). Upon Mitf misexpression, we found perturbation of PNC patterning, as revealed by broadening of expression of the PNC marker Ac, compared to control **(Fig.44A-C).** This is unlikely to be due to changes in wg or Notch signaling because overexpression of Mitf does not change expression of wg **(Fig.44D-F)** and of the Notch target Cut at the D/V margin compared to control WDs **(Fig.44G-I).**

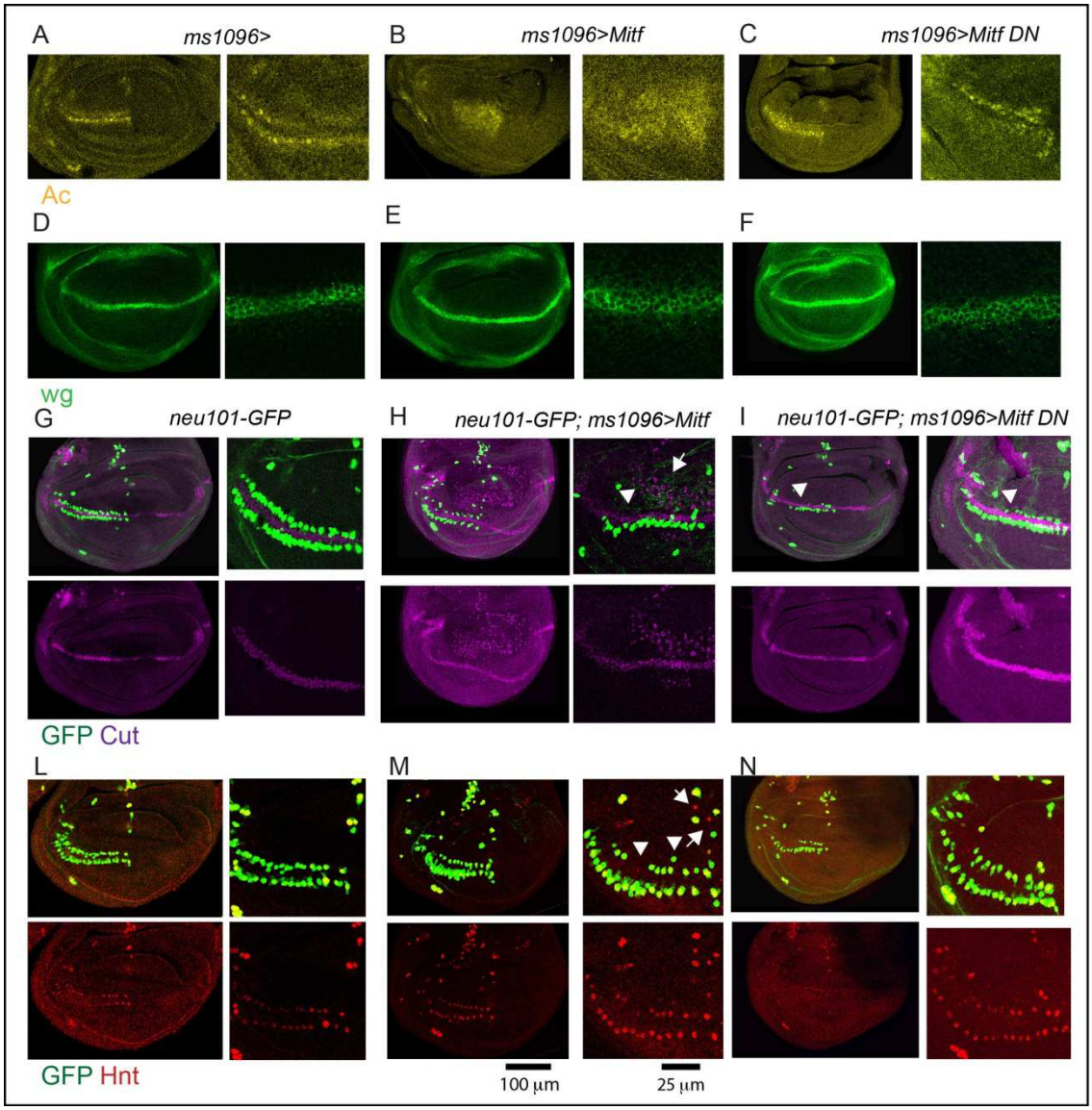

Figure 44 Mitf misexpression perturbs SOP development.

A-N) Wing pouches and higher magnifications of the anterior part of the WDs of the indicated genotype stained as indicated. Note that Mitf and MitfDN overexpression results in (A-C) perturbation of the expression of Ac protein; (D-I) no perturbation of Wg and Cut expression at the D/V boundary; G-I) Formation of misplaced or ectopic Neur-GFP and Cut positive cells and L-N) misplaced or ectopic Hnt positive cells. Some of the ectopic Cut and Hnt-positive cells were not Neur-GFP positive (white arrows) and could represent incomplete SOP commitment.

To assess SOP differentiation, we analyzed discs expressing *Neur-GFP* or stained for Hnt. Interestingly, mis-expression of Mitf or MitfDN leads to loss and ectopic Hnt- and Neur-positive cells **(Fig.44G-N)**. In addition, overexpression of Mitf results also in formation of ectopic cells positive for Cut, which marks sense organs and non-neuronal cells in the hinge and notum (Blochlinger, Jan, & Jan, 1991). Consistent with this, the wing margin of adult animals is disrupted and it displays missing or ectopic mechano-sensory bristles **(Fig.45)**.

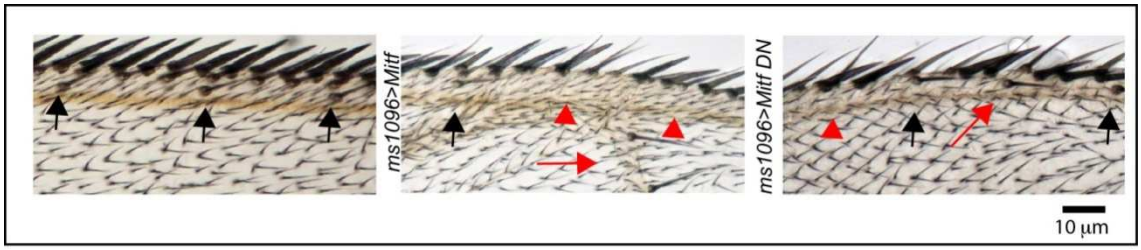

Figure 45 Functional Mitf or MitfDN disrupts formation of adult sensory organs.

High magnification of the antero-distal dorsal area of the margin of adult wings of the indicated genotypes. Normal sensory margin bristle position is shown by black arrows. Expression of both Mitf and MitfDN in WDs results in loss (red arrowheads) or misplacement and ectopic sensory bristles (red arrows).

9.2.8 Vha16-1 is crucial for correct SOP establishment.

During pupal life, SOPs undergo Notch-dependent asymmetric cell divisions to generate the differentiated cells that compose the adult mechano-sensory organ (Hartenstein & Posakony, 1990). Interestingly, elevated *GFP::Vha16-1* expression is present in the SOP lineage also during pupal development **(Fig.46A)**. Together with the evidence presented above, these data suggest that high levels of *Vha16-1* might be crucial for correct SOP establishment and also for subsequent development of mechano-sensory organs. To test whether this is the case, we used *in vivo* RNAi (See **Fig.14A** for details). Expression of a Vha16-1 RNAi hairpin in the whole wing pouch leads to specific reduction of endogenous Vha16-1 expression and of GFP expression in *GFP::Vha16-1* WD, indicating that the RNAi line is on target **(Fig. 46 B-C)**. Interestingly, expression of Vha16-1 RNAi in the notum with *Pannier-Gal4* (pnr>) leads to a decrease in size of the adult thorax, which is formed by the fusion of the left and right nota. This phenotype is coupled with depigmentation and misorientation of bristles, a known effect in *Drosophila* of reduced V-ATPase and lysosomal activity (Akbar, Ray, & Krämer, 2009; Hermle et al., 2010) **(Fig.46D)**. Importantly, the density of microchaeta, which derive from pupal SOPs, is also increased independent of thorax size **(Fig.46D; quantification**

in E), suggesting that reduction of *Vha16-1* might weaken Notch-mediated lateral inhibition during PNC development.

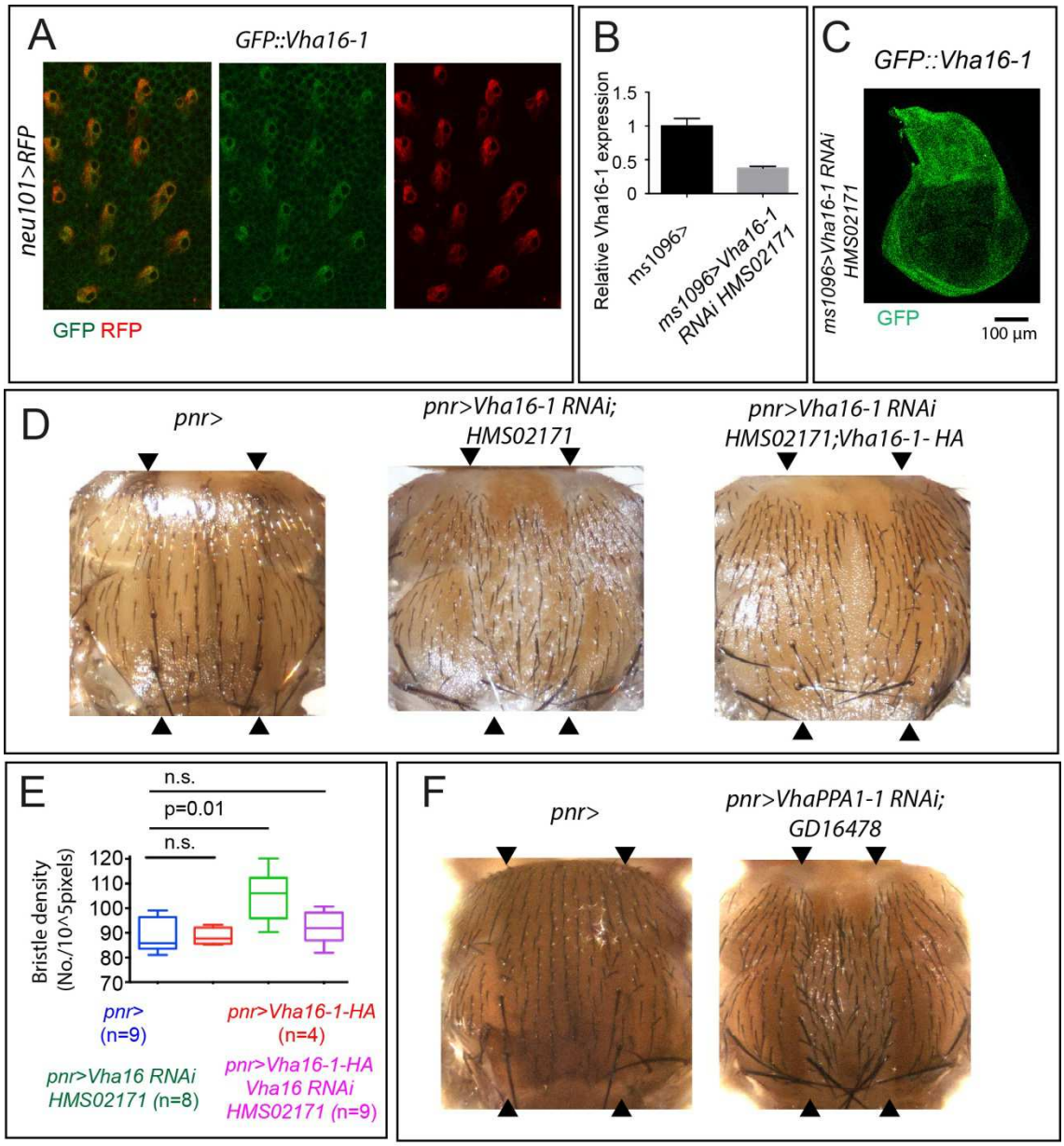

Figure 46 Vha16-1 is expressed in pupal SOPs, and is required for proper SOP differentiation.

A) Pupal nota of the indicated genotype dissected 20 hours APF. Note that elevated GFP::Vha16-1 expression is maintained along the SOP lineage (cells of the SOP lineage in the pupae are marked by Neur101gal4>RFP) B) Vha16-1 transcripts levels tested by qPCR in WT WDs and WDs expressing the Vha16-1RNAi construct HMS02171. Note that upon expression of this construct Vha16-1 expression is downregulated of almost 70%. C) WDs overexpressing the Vha16-1RNAi construct in the background of *GFP::Vha16-1* show downregulation of GFP signal, suggesting that the Vha16-1RNAi targets the Vha16-1 gene. D) Phenotypic defects associated with RNAi-mediated knock-down of Vha16-1 expression with the indicated RNAi line, compared to control (pnr>). Defects are rescued by concomitant expression of the RNAi lines and a RNAi-resistant Vha16-1HA construct. The domain of PannierGal4 expression is delimited by arrowheads. E) Quantification of the number of bristle/Area (Bristle density) relative to the experiment shown in D. Statistical analysis is based on Kruskal Wallis Test with Dunn's multiple comparison relative to control. F) Phenotypic defects associated with RNAi-mediated knock-down of VhaPPA1, another component of the membrane-embedded V0 sector. Note that knock-down of VhaPPA1 resulted in a similar phenotype of that shown upon Vha16-1 knock-down.

These effects are specific to depletion of *Vha16-1*, as they are rescued by concomitant overexpression of RNAi-resistant Vha16-1 tagged with HA (Vha16-1-HA, **Fig46D**). Similar results were obtained by downregulating *VhaPPA1-1,* the gene encoding the component of the membrane-embedded V_0 sector c'' **(Fig. 46F)**, as previously reported (Mummery-Widmer et al., 2009). However, Vha16-1 is not sufficient to promote ectopic PNC formation. In fact, overexpression of Vha16-1-HA *per se* in the wing pouch or notum does not perturb microchaeta formation (not shown), suggesting that the patterning activity of *Vha16-1* requires additional factors. Overall these data indicate that Mitf and its target Vha16-1 might be functional elements of the proneural patterning machinery in WDs epithelia.

9.2.9 PNCs possess a distinctive lysosomal compartment

Is the function of V-ATPase and Mitf in pro-neural development linked to regulation of endo-lysosomal system? To assess this, we tested whether PNCs possess an endo-lysosomal compartment that is different to that of surrounding cells. Consistent with observations in **Fig. 33 B**, expression of *YFP::Lamp1* is mildly upregulated in PNC region abutting the D/V margin, while we did not detect significant differences in endogenous expression or localization of Mitf across the wing pouch **(Fig.47A)**. To further assess lysosomal abundance, we labeled acidified compartments in the disc with lysotracker. We found that lysotracker incorporation is high in PNCs compared to other epithelial cells of the disc, suggesting that PNCs might possess more lysosomes than surrounding cells **(Fig.47B)**. These lysosomes might be less acidified and active than those of surrounding cells. In fact, upon ubiquitous expression of GFP-hLamp1 in the disc with actin-Gal4, we found that PNCs are more GFP-positive than surrounding cells **(Fig.47C)**. GFP-hLAMP1 is a lysosome-anchored GFP form that has been developed as a sensor for lysosomal acidification, because the GFP is exposed to the

lysosomal lumen, where it gets unfolded under low pH (Pulipparacharuvil et al., 2005). In contrast, localization of Syx7, a marker of early endosomes (Lu & Bilder, 2005) is uniform across the disc tissue **(Fig.47D)**. Consistent with previous evidence indicating transcriptional down-regulation of Notch in PNCs (Bray, 1997; de Celis et al., 1996), we found that overall Notch protein levels in the endolysosomal system of PNCs are lower than in the rest of the disc **(Fig.47D)**.

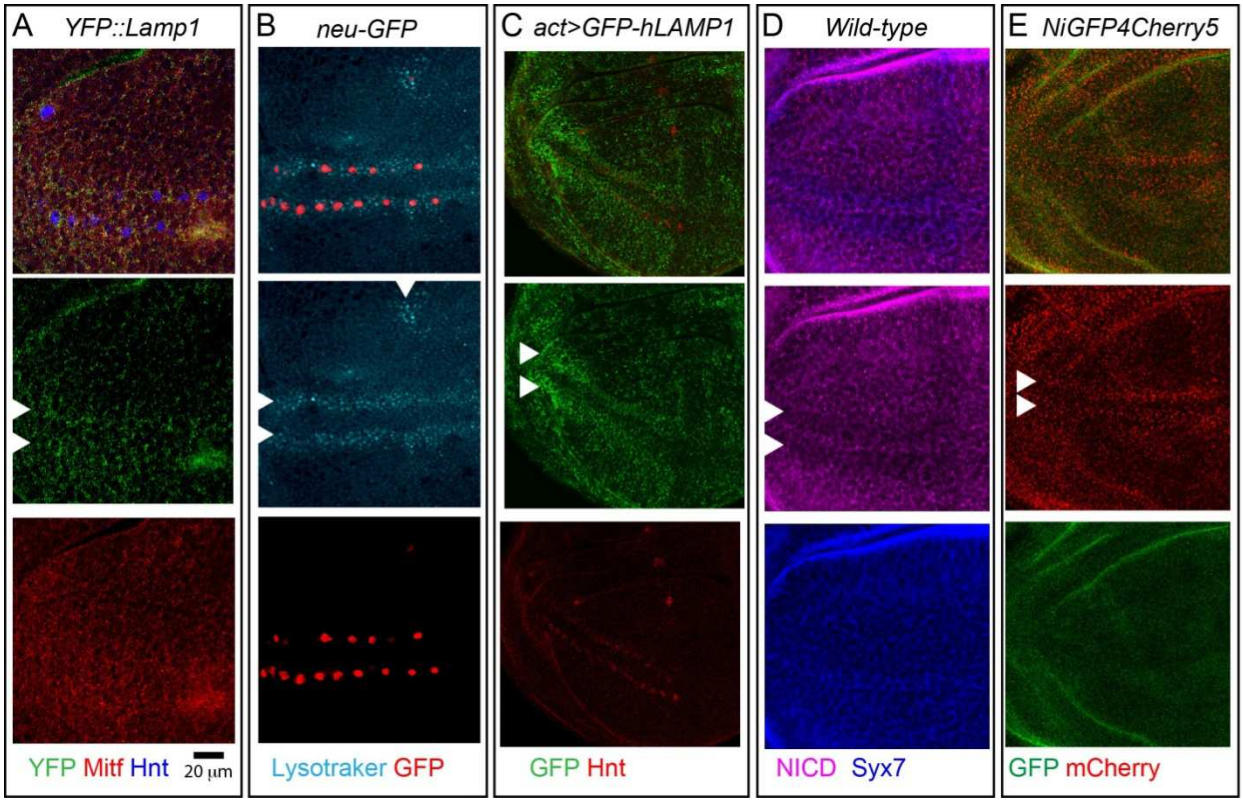

Figure 47 PNCs possess a distinctive lysosomal compartment

High magnification of the anterior part of the wing pouch of the WDs of the indicated genotypes, stained as indicated. Arrowheads point to approximate location of PNC. Note that compared to surrounding epithelial cells, PNC cells show a slightly higher amount of YFP-LAMP1 positive lysosomes (A), a higher number of acidified organelles (B) and of GFP-hLAMP1 puncta (C), overall less Notch protein (D) and more endo-lysosomal Notch (E).

We next determined Notch stability in the endo-lysosomal system of PNCs. To this end, we analyzed expression of NiGFP4Cherry5, a functional Notch form tagged with fast-maturing, pH-sensitive GFP and a slow-maturing pH-insensitive mCherry. It has been recently reported that the GFP signal of such Notch form indicates the newly-synthetized Notch found at the plasma membrane, while the mCherry signal highlights old Notch molecules that reach the endo-lysosomal

compartment on their way to degradation (Couturier et al., 2014). Using this sensor, we found that the amount of mCherry-positive Notch in the endo-lysosomal compartment is increased in the PNCs **(Fig.47E)**. Overall, these data indicate that PNCs might possess an expanded, less degradative and more Notch-rich lysosomal system than surrounding cells.

10 DISCUSSION

10.1 Discussion Project1

10.1.1 The ESCRT-0 complex is dispensable for tumor suppression in *Drosophila*.

In the first part of my Ph.D work, I reported the effects of impairment of ESCRT-0 function on *Drosophila* epithelial tissue development *in vivo*. In particular I have analyzed *Hrs* and *Stam* mutations in eye imaginal discs and FE cells, and I showed that homozygous mutations for either one or both components of the ESCRT-0 do not affect tissue architecture, do not cause neoplastic growth or loss of epithelial organization. Therefore, ESCRT-0 function *per se* is not tumor suppressive in *Drosophila*. This is a striking difference compared to what observed for downstream ESCRT I-II-III components.(Herz et al., 2006, 2009; Menut et al., 2007; Moberg et al., 2005; Thompson et al., 2005; Vaccari & Bilder, 2005; Vaccari et al., 2009). The possible reasons for the fact that the ESCRT-0 complex does not possess tumor suppressive activity are discussed below.

The first possibility is that the tumor suppressor function of ESCRTs might not be linked to endosomal sorting. Indeed, ESCRTs components have a more ancestral function than that in endosomal sorting and phylogenetic analysis indicates that orthologs of ESCRT-III and Vps4 are present in archaebacteria (Leung, Dacks, & Field, 2008), an organism that lacks the endomembrane system. In these organisms, ESCRT-III and Vps4 function in plasma-membrane abscission during cytokinesis (Samson, Obita, Freund, Williams, & Bell, 2008). Such function is conserved in higher eukaryotes (reviewed in (Bhutta, McInerny, & Gould, 2014). Whether the tumor suppressor activity of some ESCRTs correlates with their

involvement in cytokinesis cannot be excluded. For instance, the role of the ESCRT-I component Tsg101 in cytokinesis has been associated with the tumor suppressor BRCA2, a major breast cancer susceptibility gene (Foulkes & Shuen, 2013). However, the ESCRT-II complex also behaves as tumor suppressor in *Drosophila* but appear dispensable for cytokinesis, suggesting that the tumorigenic potential in this case is primarily due to defects in the MVE pathway (Agromayor & Martin-Serrano, 2013; Carlton & Martin-Serrano, 2007; Morita, Sandrin, Chung, et al., 2007).

ESCRT-0 is dispensable for cytokinesis function and it is the most recently evolved ESCRT complex (Leung et al., 2008). Thus, an alternative possibility is that ESCRT-0 evolved specifically for sorting purposes and perhaps it engages only a subset of cargoes that might not be tumorigenic. Although ESCRT-0 complex is important for ubiquitinated cargo recognition and recruitment to endosomal membranes, there are likely to be one or more alternative ESCRT-0 proteins that function either in parallel with or instead of Hrs and Stam. Some organisms such as plants (Winter & Hauser, 2006) do not even express Hrs and therefore different proteins might have evolved to replace Hrs function. Tom and GGA proteins are good candidates for such function and they are both conserved in *Drosophila*. Like ESCRT-0, these proteins interact with ESCRT-I and contain VHS, ubiquitin-binding and clathrin-binding domains and may associates with PtdIns(3)P-binding proteins that target them to endosome membranes (Blanc et al., 2009; Katoh et al., 2004; Puertollano & Bonifacino, 2004; Puertollano, 2005). Thus, ESCRT-0 complex could be dispensable for sorting of proteins required for tumor suppression. One of the striking phenotypes observed in ESCRT-I, II, III mutants is the loss of epithelial polarity. Thus, it is possible that polarity proteins and adhesion molecules might not traffic through the ESCRT-0 complex. Although we have not

directly tested this hypothesis, a study showed that mutation in *Drosophila* Hrs does not affect localization of DE-Cadherin, a junctional adhesion protein involved in the regulation of polarity in *Drosophila* epithelial cells (Jékely and Rørth, 2003; Leibfried et al., 2008). On the other hand, clonal inactivation of ESCRT-I or II resulted in mis-distribution of polarized proteins and junctional proteins, thus loss of epithelial polarity (Moberg et al., 2005; Vaccari & Bilder, 2005). Interestingly, even in mammalian epithelial cells, inhibition of ESCRT-I function resulted in accumulation of the tight junction protein Claudin-1 into intracellular vesicles and disruption of polarity (Dukes et al., 2011).

Finally, cargoes that contribute to tumor suppression might be sorted by ESCRT-0 but they might not become ectopically activated in the absence of ESCRT-0. Consistent with this, in this and other studies, it has been shown that mutation in ESCRT-0 results in accumulation of multiple signaling receptors. However, it was also shown that most of them are largely derived form the pool of unliganded receptors and therefore are not *per se* active (Jékely and Rørth, 2003). A study of *Drosophila* Hrs showed that its mutation results in failure to degrade active EGF and the receptor tyrosine kinase (RTK) *Torso* (Lloyd et al., 2002). However, RTK signaling activation was not found sufficient to promote tumorigenesis in *Hrs* mutant tissue. This suggests that the tumor suppression activity might not originate from failure to downregulate small amounts of physiologically activated receptors but rather from ectopic activation of receptors already engaged by defective ESCRT pathway.

10.1.2 ESCRT-0 is dispensable for Notch signaling activation in endosomes

The latter scenario presented above is consistent with our findings and with evidence in literature. Indeed, we observed that mutations in *Hrs* or *Stam* or both *Hrs* and *Stam* resulted in accumulation of ubiquitinated cargoes, which suggests

that both Hrs and Stam are required as other ESCRTs for efficient removal of ubiquitinated proteins as previously observed (Herz et al., 2009; Jékely and Rørth, 2003; Tamai et al., 2008). In ESCRT-0 mutants we also observed accumulation of Notch receptor in endosomes, especially when immunolocalizing with an anti-Notch ECD, which recognizes the extracellular portion of Notch. It is not clear why the accumulation is less evident by immunolocalization of the intracellular portion of Notch with anti Notch, ICD. One possibility might be that NICD accumulated less then NECD, perhaps due to the fact that Notch is normally activated in mutant cells, alternatively, the two antibodies might possess different efficiency in recognizing their epitopes. Whichever the case, accumulation of Notch and Dome receptors that we observed in ESCRT-0 mutants is consistent with what has been reported for other ESCRTs and what has been observed for mutation in *Hrs* for several other signaling molecules including Notch, Dl, EGFR, Patched, Smoothened and thickveins (the Drosophila TGFβ type 1 receptor) (Jékely and Rørth, 2003). However, Notch signaling is normal when either one component of ESCRT-0 or both are mutated, in sheer contrast with ESCRT –I, -II, -III mutations in which Notch signaling is ectopically activated. This phenotype is remarkably distinct from that of mutations in upstream components of the early endosome such as Dynamin and Rab5, in which despite strong accumulation at the cell surface Notch signaling activation is almost abolished (Vaccari et al., 2008). Reduction in Notch signaling activation in *dynamin*, *avl* or *rab5* mutants is consistent with a general impairment in the internalization of Notch in endosomes, in which cleavage and activation of Notch is thought to occur efficiently (Pasternak et al., 2003; Vaccari et al., 2008). However unsorted Notch in ESCRT-0 defective endosomes might not yield ectopic ligand-independent activation because Notch does not become clustered by ESCRT-0 on the limiting membrane of endosomes. We have shown

that endosomes of ESCRT-0 mutant cells are otherwise mature because they are acidified and possess ILVs. Notably, Dx-mediated endosomal Notch signaling requires Hrs (Childress et al., 2006; Yamada et al., 2011) suggesting that ligand-independent Notch signaling activation might occurs downstream ESCRT-0 recruitment and might require gathering of Notch in the clathrin coated subdomain on the limiting membrane of sorting endosomes (C Raiborg, Bache, Mehlum, Stang, & Stenmark, 2001).

In summary, our comparative analysis of Hrs and Stam in epithelial tissue *in vivo* reveals that both proteins are essential for efficient removal of ubiquitinated cargoes and receptors. Unexpectedly, ESCRT-0 is dispensable for control of cell polarity and proliferation, a major tumor suppressive event. We therefore predict that ESCRT-0 might be essential for clustering of Notch and other cargoes on the limiting membrane of endosomes, a process that might be necessary for tumorigenic activation of Notch signaling.

10.2 Discussion Project 2

10.2.1 Mitf is the functional homolog of TFEB

In addition to its previously known role in eye development (Jón H Hallsson et al., 2004) in the second part of my Ph.D work, we reported that the *Drosophila* Mitf regulates lysosomal biogenesis and expression of subunits of the V-ATPase pump. In epithelial tissue, we find that a fraction of Mitf resides in lysosomes and, when overexpressed, in the nucleus, where it is transcriptionally active. These observations are in accordance with findings in mice and *C. elegans* in which TFEB (HLH-30 in *C. elegans*) shuttles from the cytoplasm to the nucleus to induce lysosomal biogenesis and autophagy (Lapierre et al., 2013; José A Martina, Diab, Li, et al., 2014; O'Rourke & Ruvkun, 2013; Settembre et al., 2011, 2012). In non-overexpressing conditions, however, we were unable to detect nuclear localization

of Mitf in WDs. This could be due to a low or transient expression of Mitf in the nucleus, or to a limited efficiency of the antibody to detect small amounts of Mitf. Alternatively, the nature of the tissue, or the experimental conditions, might have not been optimal to detect nuclear Mitf. For instance, one could need to starve animals or could need to analyze specialized *Drosophila* tissues involved in nutrient metabolism, such as the larval fat body, to observed endogenous Mitf in the nucleus.

Mis-expression of the functional Mitf resulted in a transcriptional upregulation of several V-ATPase subunits confirming the conserved role of Mitf/TFEB in the transcriptional control of the holoenzyme complex (Palmieri et al., 2011). Interestingly, we show that differently from mammalian cells (Palmieri et al., 2011; Settembre et al., 2011), *Drosophila* Lamp1, Atg8a and ref(2)P/p62 are not modulated by Mitf in WDs. This is consistent with the fact that their promoters do not contain as many and as conserved E-Boxes as V-ATPase subunits (Federico De Masi, personal communication). In addition, we find only slight changes in the protein level of Atg8a and ref(2)P in the wing tissue in overexpressing discs. This evidence suggests that the set of Mitf/TFEB target genes in *Drosophila* might be limited compared to other metazoans and mostly restricted to V-ATPase subunit genes. Despite this, overall these observations strongly indicate that *Drosophila* Mitf is the functional homolog of TFEB.

10.2.2 Components of the lysosomes are developmentally regulated

Using several GFP-insertion lines to track expression of potential Mitf target in WDs, we observed that *Lamp1*, encoding a protein that localizes in the lysosomes (Chen, Murphy, Willingham, Pastan, & August, 1985), and Vha16-1 and Vha13 encoding two subunits of the V-ATPase display a distinctive expression pattern that follows a subset of known patterning events occurring in WDs. This

indicates that key components of the lysosomes might be regulated during development to correctly shape the pattern of the WDs. Consistently, we observed that expression of both Vha16-1 and Vha13 is upregulated upon mis-expression of Mitf and downregulated upon activation of Notch signaling.

10.2.3 Mitf contributes to early step of PNC development

Our mis-expression experiments *in vivo* indicated that Mitf acts downstream of developmental signaling and is required to regulate expression of V-ATPase subunits such as Vha16-1, eventually ensuring correct differentiation of PNCs. During PNC development, cell fate commitment involves the activity of a number of bHLH transcription factors, suggesting that Mitf might add to an already complex combinatorial code contributing to specify neuronal identity. A more trivial possibility is that Mitf might have unspecific effects on regulation by known bHLH factors involved in PNC development. However, we find this unlikely because patterning perturbations are observed also by overexpression of Mitf DN, which is unable to bind DNA (Jón H Hallsson et al., 2004). Thus, our findings strongly suggest that *Drosophila* Mitf performs functions in development that might in large part coincide with modulation of lysosomal biogenesis. Such implication might be useful to understand the functions in mammals, which are complicated by the existence of multiple family members (Jose A Martina & Puertollano, 2013; José A Martina, Diab, Lishu, et al., 2014). Further experiments will be needed to address the molecular nature of the interplay between Mitf with factors involved in proneural development.

10.2.4 Different V-ATPase subunits show differential expression pattern in WDs

A complication to the scenario proposed above, is our finding that expression patterns of different subunits of the V-ATPase vary considerably within

the same tissue. The expression pattern of Vha55, VhaSFD and VhaAC45 is uniform in the disc and unchanged by modulation of Notch signaling. Vha55 and VhaSFD are part of the V_1 sector, which can reversibly associates with the V_0 sector upon low nutrition status in both yeast and insects (Kane, 1995; Sumner et al., 1995). Recent *in vivo* yeast experiments and *in vitro* experiments in mammals argue against a complete separation of the V-ATPase, suggesting exclusive release of V_1C, a known regulator of nutrient-mediated coupling of the V_1 and V_0 sector (Tabke et al., 2014). *VhaAc45* encodes a subunit that has been recently suggested to cap the proteolipid ring on the luminal side and presumably associates with the V_0 sector (Rawson et al., 2015), whereas *Vha13* encodes subunit V_1G that forms with V_0a and V_1E the 3 peripheral stalks that prevent undesired rotation of the V_1 sector (Marshansky et al., 2014). Thus, the barring effects of the GFP tag, which we have excluded with a number of control experiments, it is not clear whether the differences in expression that we observe reflect localization of the pump, association of V_1 to V_0, activity of the pump or finally moonlighting functions of the single subunits. Interestingly, we have recently shown that mis-expression of *Drosophila* Vha44, encoding for V_1C, results in a sharp increase of *GFP::Vha16-1* and decrease in *GFP::VhaSFD* expression in WDs (Petzoldt, Gleixner, Fumagalli, Vaccari, & Simons, 2013), indicating that pump functionality *in vivo* involves complex and currently unclear regulation of subunit expression and/or turnover. Despite this, the common aspect of Vha16-1 and Vha13 patterned expression, and the similar phenotypes of downregulation of Vha16-1 and VhaPPA1-1 suggest that pump activity, rather than a moonlighting function of the single subunits, might be developmentally regulated. In contrast, the strong elevation of expression in SOPs, which is exclusively observed for Vha16-1 and which is maintained during pupal life, could hint to additional function of the Vha16-1 or of the V_0 sector that might

not involve the V-ATPase pump activity. Concerning this, the proteolipid ring is thought to assist membrane fusion processes (Liégeois, Benedetto, Garnier, Schwab, & Labouesse, 2006; Strasser, Iwaszkiewicz, Michielin, & Mayer, 2011), while Vha16-1 has been reported to be part of the connexons in the gap junctions (Dunlop et al., 1995; Finbow et al., 1994).

10.2.5 V-ATPase may act during PNC development to regulate Notch signaling

When we reduced expression of two components of the V_0 sector of the V-ATPase i.e. Vha16-1 and VhaPPA1-1, the thorax of adult flies presented supernumerary bristle. Such a neurogenic phenotype might arise from defects in enforcing lateral inhibition by Notch signaling. If so, developmental control of Vha16-1 expression might be required to modulate Notch signaling activation during lateral inhibition processes. This is in agreement with previous reports in *Drosophila* which have shown that V-ATPase activity is required for Notch signaling activation and for bristle specification (Mummery-Widmer et al., 2009; Vaccari et al., 2010; Yan et al., 2009).

10.2.6 Changes in V-ATPase expression reflect changes in lysosomal functionality and distribution

A possible reason to modulate V-ATPase subunit expression might be the necessity to change functionality of endo-lysosomal compartment of differentiating cells perhaps to support signaling processes that control cell fate, such as Notch. In mammals, cell fate differentiation from monocyte to macrophages results in a large expansion of the lysosomal compartment and increased V-ATPase expression (Lee et. al 1995). *In vivo*, we observed differences in the distribution and functionality of endo-lysosomal compartments in the PNC regions that in part correlate with changes in expression of V-ATPase components. In particular, we observed increased lysotracker uptake and accumulation of

GFP-hLAMP1, a sensor for lysosomal functionality, in the PNC regions. Thus, these regions may possess an increased number of lysosomes with slightly less capability to degrade compared to those of non-neurogenic regions.

10.2.7 Changes in the distribution and functionality of lysosomes may affect Notch signaling activation or degradation

Several studies have demonstrated that Notch activation is exquisitely sensitive to endo-lysosomal events (Hori et al., 2004; Shimizu et al., 2014; Vaccari & Bilder, 2005). For instance, the establishment of low luminal pH could be important for optimal γ-secretase activity, and/or for maturation and localization of the γ-secretase holoenzyme, a process that could boost signaling activation at early steps of PNC development. Consistent with this, it has been shown that γ-secretase works more efficiently in the lysosomes, where the pH is more acidic (Pasternak et al., 2003). Moreover, in rats mutations that affect V-ATPase activity also show reduced γ-secretase function and ultimately reduced Notch signaling (Valapala et al., 2013). Thus, changes in the V-ATPase function and luminal pH may affect the efficiency of Notch receptor cleavage and activation.

Differences in lysosomal compartment distribution and activity could be a mode of biasing signaling and selectively altering endocytic trafficking, a major route of signaling regulation (Sigismund et al., 2012). Thus, differences in endo-lysosomal content could channel Notch into specific compartments. Using a dual tagged Notch receptor, we observed that in the PNC regions Notch receptor molecules are abundant in the endo-lysosomal compartment, a place where Notch can be subjected to either receptor degradation ultimately reducing signaling or stabilization and signaling activation, depending on the activity of factors such as Dx (Hori et al., 2004; A. Mukherjee et al., 2005; M. Wilkin et al., 2008). Thus, it is possible that a certain basal level of Notch signaling output may originate at the

level of the endo-lysosomal compartments, perhaps independently of ligands, as recently shown during development of different *Drosophila* organs, such as follicle cells, blood cells and WDs (Mukherjee et al., 2011; Palmer et al., 2014; Shimizu et al., 2014). Overexpression in *Drosophila* WDs of Mucolipin, a lysosomal calcium channel that is target of TFEB (Sardiello et al., 2009), strongly enhances ligand-independent activation of Notch, which is calcium-sensitive (Rand et al., 2000; Shimizu et al., 2014). Interestingly, lysosomal calcium regulation has been recently implicated in regulation of TFEB activity in mammalian cells (Medina et al., 2015). Thus, it is possible that ligand-independent basal activation of Notch might be an integral part of the TFEB regulatory loop that regulates lysosomal biogenesis. Consistent with this, one of the consequences of ectopic activation of Notch in WD is decrease of Vha16-1 and Vha13 expression and a slight reduction of the lysosomal compartment.

Interestingly, in mammals TFEB senses amino acid levels from protein degradation in lysosomes, as part of a feedback loop with mTOR and V-ATPase that adjusts lysosomal biogenesis to match the cell energy needs (Roczniak-Ferguson et al., 2012; Settembre et al., 2012; Zoncu et al., 2011). Whether and how Notch phenotypes are dependent on mTor and nutrient metabolism at the endo-lysosome is not known and is the focus of our current investigations.

In summary, we propose a model **(Fig. 48)** for early step of PNCs development in which the Mitf/V-ATPase axis might be important to set the correct level of Notch signaling activity by modulating lysosomal biogenesis and associated signaling. Once Notch is activated correctly, it could decrease V-ATPase expression and revert the lysosomal compartment to a predifferentiative state. Although it requires further testing, such model integrates the developmental and lysosomal functions of the TFEB/Mift family of bHLH transcription factors and

might provide a framework for our understanding of lysosomal Notch signaling and of mis-regulation of the TFEB/V-ATPase axis in cancer.

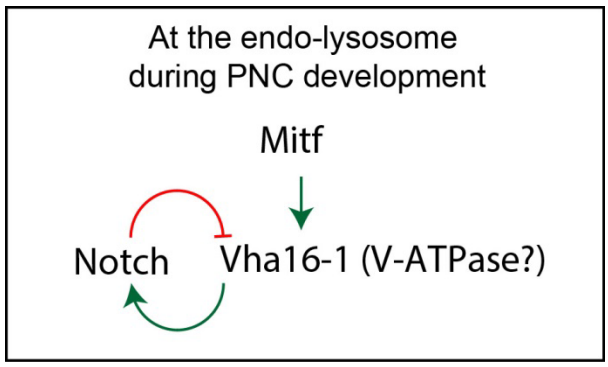

Figure 48 Proposed model for the activity of Mitf and V-ATPase in PNC regions.

***Drosophila* Mitf/V-ATPase axis might operate at the endo-lysosome as a conserved unit that supports Notch signaling during cell fate specification during WD development.**

11 ACKNOWLEDGEMENTS

I would like to express my sincere gratitude to my PhD advisor, Dr. Thomas Vaccari for his continous supervision of my project, for his patience, support and immense knowledge.

I would also like to thank the members of my thesis committee, Dr. Christos Delidakis and Simona Polo for their insightful comments, very helpful discussion and their willingness in reading my thesis.

My sincere gratitude goes to the IFOM institute and all the facilities which provide cutting-edge technologies and excellent research.

My sincere thanks to all my group members and the members of Ciliberto's group for their everyday support and for sharing tears and laughs. They all are great scientists and very good friends.

Last but not the least, a big thanks to my boyfriend Marcello, to my closest friend Valeria, to my spiritual and psychological mentors, Antonella Memmo and Martina Bergomi, and to my family. All of them have been essential to my success.They have been my rocks especially during this last very challenging year.

12 REFERENCES

Adams, D. S., Masi, A., & Levin, M. (2007). H+ pump-dependent changes in membrane voltage are an early mechanism necessary and sufficient to induce Xenopus tail regeneration. *Development*, *134*(7), 1323–1335. http://doi.org/10.1242/dev.02812

Adams, D. S., Robinson, K. R., Fukumoto, T., Yuan, S., Albertson, R. C., Yelick, P., … Levin, M. (2006). Early, H+-V-ATPase-dependent proton flux is necessary for consistent left-right patterning of non-mammalian vertebrates. *Development (Cambridge, England)*, *133*(9), 1657–71. http://doi.org/10.1242/dev.02341

Agrawal, N., Kango, M., Mishra, A., & Sinha, P. (1995). Neoplastic transformation and aberrant cell-cell interactions in genetic mosaics of lethal(2)giant larvae (lgl), a tumor suppressor gene of Drosophila. *Developmental Biology*, *172*(1), 218–29. http://doi.org/10.1006/dbio.1995.0017

Agromayor, M., & Martin-Serrano, J. (2013). Knowing when to cut and run: mechanisms that control cytokinetic abscission. *Trends in Cell Biology*, *23*(9), 433–41. http://doi.org/10.1016/j.tcb.2013.04.006

Akbar, M. A., Ray, S., & Krämer, H. (2009). The SM protein Car/Vps33A regulates SNARE-mediated trafficking to lysosomes and lysosome-related organelles. *Molecular Biology of the Cell*, *20*(6), 1705–14. http://doi.org/10.1091/mbc.E08-03-0282

Allan, A. K., Du, J., Davies, S. A., & Dow, J. A. T. (2005). Genome-wide survey of V-ATPase genes in Drosophila reveals a conserved renal phenotype for lethal alleles. *Physiological Genomics*, *22*(2), 128–38. http://doi.org/10.1152/physiolgenomics.00233.2004

Apidianakis, Y., Nagel, A. C., Chalkiadaki, A., Preiss, A., & Delidakis, C. (1999). Overexpression of the m4 and mα genes of the E(spl)-Complex antagonizes Notch mediated lateral inhibition. *Mechanisms of Development*, *86*(1-2), 39–50. http://doi.org/10.1016/S0925-4773(99)00099-4

Bailey, A. M., & Posakony, J. W. (1995). Suppressor of hairless directly activates transcription of enhancer of split complex genes in response to Notch receptor activity. *Genes & Development*, *9*(21), 2609–2622. http://doi.org/10.1101/gad.9.21.2609

Baron, M. (2012). Endocytic routes to Notch activation. *Seminars in Cell & Developmental Biology*, *23*(4), 437–442. http://doi.org/10.1016/j.semcdb.2012.01.008

Beth S. Lee, David M. Underhill, Monica K. Crane and Stephen L. Gluck, D. M. (1995).

Transcriptional Regulation of the Vacuolar H-ATPase B2 Subunit Gene in Differentiating THP-1 Cells. *Journal of Biological Chemistry*, *270*(13), 7320–7329. http://doi.org/10.1074/jbc.270.13.7320

Bhutta, M. S., McInerny, C. J., & Gould, G. W. (2014). ESCRT function in cytokinesis: location, dynamics and regulation by mitotic kinases. *International Journal of Molecular Sciences*, *15*(12), 21723–39. http://doi.org/10.3390/ijms151221723

Blanc, C., Charette, S. J., Mattei, S., Aubry, L., Smith, E. W., Cosson, P., & Letourneur, F. (2009). Dictyostelium Tom1 participates to an ancestral ESCRT-0 complex. *Traffic (Copenhagen, Denmark)*, *10*(2), 161–71. http://doi.org/10.1111/j.1600-0854.2008.00855.x

Blochlinger, K., Jan, L. Y., & Jan, Y. N. (1991). Transformation of sensory organ identity by ectopic expression of Cut in Drosophila. *Genes & Development*, *5*(7), 1124–35. Retrieved from http://www.ncbi.nlm.nih.gov/pubmed/1676691

Bray, S. J. (1997). Expression and function of Enhancer of split bHLH proteins during Drosophila neurogenesis. *Perspectives on Developmental Neurobiology*, *4*(4), 313–23. Retrieved from http://www.ncbi.nlm.nih.gov/pubmed/9171445

Brennan, K., Tateson, R., Lieber, T., Couso, J. P., Zecchini, V., & Arias, A. M. (1999). The abruptex mutations of notch disrupt the establishment of proneural clusters in Drosophila. *Developmental Biology*, *216*(1), 230–42. http://doi.org/10.1006/dbio.1999.9501

Brook, W. J., Diaz-Benjumea, F. J., & Cohen, S. M. (1996). Organizing spatial pattern in limb development. *Annual Review of Cell and Developmental Biology*, *12*, 161–80. http://doi.org/10.1146/annurev.cellbio.12.1.161

Brown, D., Smith, P. J., & Breton, S. (1997). Role of V-ATPase-rich cells in acidification of the male reproductive tract. *The Journal of Experimental Biology*, *200*(Pt 2), 257–62. Retrieved from http://www.ncbi.nlm.nih.gov/pubmed/9050233

Buechling, T., Bartscherer, K., Ohkawara, B., Chaudhary, V., Spirohn, K., Niehrs, C., & Boutros, M. (2010). Wnt/Frizzled signaling requires dPRR, the Drosophila homolog of the prorenin receptor. *Current Biology : CB*, *20*(14), 1263–8. http://doi.org/10.1016/j.cub.2010.05.028

Burcklé, C., & Bader, M. (2006). Prorenin and its ancient receptor. *Hypertension*, *48*(4), 549–51. http://doi.org/10.1161/01.HYP.0000241132.48495.df

Buszczak, M., Paterno, S., Lighthouse, D., Bachman, J., Planck, J., Owen, S., … Spradling, A. C. (2007). The carnegie protein trap library: a versatile tool for Drosophila developmental studies. *Genetics*, *175*(3), 1505–31. http://doi.org/10.1534/genetics.106.065961

Carlton, J. G., & Martin-Serrano, J. (2007). Parallels between cytokinesis and retroviral budding: a role for the ESCRT machinery. *Science (New York, N.Y.)*, *316*(5833), 1908–12. http://doi.org/10.1126/science.1143422

Castro, B., Barolo, S., Bailey, A. M., & Posakony, J. W. (2005). Lateral inhibition in proneural clusters: cis-regulatory logic and default repression by Suppressor of Hairless. *Development (Cambridge, England)*, *132*(15), 3333–44. http://doi.org/10.1242/dev.01920

Chanut-Delalande, H., Jung, A. C., Baer, M. M., Lin, L., Payre, F., & Affolter, M. (2010). The Hrs/Stam complex acts as a positive and negative regulator of RTK signaling during Drosophila development. *PloS One*, *5*(4), e10245. http://doi.org/10.1371/journal.pone.0010245

Chatterjee, D., Chakraborty, M., Leit, M., Neff, L., Jamsa-Kellokumpu, S., Fuchs, R., & Baron, R. (1992). Sensitivity to vanadate and isoforms of subunits A and B distinguish the osteoclast proton pump from other vacuolar H+ ATPases. *Proceedings of the National Academy of Sciences of the United States of America*, *89*(14), 6257–61. Retrieved from http://www.pubmedcentral.nih.gov/articlerender.fcgi?artid=49479&tool=pmcentrez&rendertype=abstract

Chen, J. W., Murphy, T. L., Willingham, M. C., Pastan, I., & August, J. T. (1985). Identification of two lysosomal membrane glycoproteins. *The Journal of Cell Biology*, *101*(1), 85–95. Retrieved from http://www.pubmedcentral.nih.gov/articlerender.fcgi?artid=2113627&tool=pmcentrez&rendertype=abstract

Childress, J. L., Acar, M., Tao, C., & Halder, G. (2006). Lethal giant discs, a novel C2-domain protein, restricts notch activation during endocytosis. *Current Biology : CB*, *16*(22), 2228–33. http://doi.org/10.1016/j.cub.2006.09.031

Chu, T., Sun, J., Saksena, S., & Emr, S. D. (2006). New component of ESCRT-I regulates endosomal sorting complex assembly. *The Journal of Cell Biology*, *175*(5), 815–23. http://doi.org/10.1083/jcb.200608053

Coonrod, E. M., Graham, L. A., Carpp, L. N., Carr, T. M., Stirrat, L., Bowers, K., … Stevens, T. H. (2013). Homotypic vacuole fusion in yeast requires organelle acidification and not the V-ATPase membrane domain. *Developmental Cell*, *27*(4), 462–8. http://doi.org/10.1016/j.devcel.2013.10.014

Cordle, J., RedfieldZ, C., Stacey, M., van der Merwe, P. A., Willis, A. C., Champion, B. R., … Handford, P. A. (2008). Localization of the Delta-like-1-binding Site in Human Notch-1 and Its Modulation by Calcium Affinity. *Journal of Biological Chemistry*, *283*(17), 11785–11793. http://doi.org/10.1074/jbc.M708424200

Cornell, M., Evans, D. A., Mann, R., Fostier, M., Flasza, M., Monthatong, M., … Baron, M. (1999). The Drosophila melanogaster Suppressor of deltex gene, a regulator of the Notch receptor signaling pathway, is an E3 class ubiquitin

ligase. *Genetics*, *152*(2), 567–76. Retrieved from http://www.pubmedcentral.nih.gov/articlerender.fcgi?artid=1460625&tool=pmcentrez&rendertype=abstract

Couso, J. P., Bishop, S. A., & Martinez Arias, A. (1994). The wingless signalling pathway and the patterning of the wing margin in Drosophila. *Development (Cambridge, England)*, *120*(3), 621–36. Retrieved from http://www.ncbi.nlm.nih.gov/pubmed/8162860

Couturier, L., Trylinski, M., Mazouni, K., Darnet, L., & Schweisguth, F. (2014). A fluorescent tagging approach in Drosophila reveals late endosomal trafficking of Notch and Sanpodo. *The Journal of Cell Biology*, *207*(3), 351–63. http://doi.org/10.1083/jcb.201407071

Cruciat, C.-M., Ohkawara, B., Acebron, S. P., Karaulanov, E., Reinhard, C., Ingelfinger, D., … Niehrs, C. (2010). Requirement of prorenin receptor and vacuolar H+-ATPase-mediated acidification for Wnt signaling. *Science (New York, N.Y.)*, *327*(5964), 459–63. http://doi.org/10.1126/science.1179802

Cubas, P., de Celis, J. F., Campuzano, S., & Modolell, J. (1991). Proneural clusters of achaete-scute expression and the generation of sensory organs in the Drosophila imaginal wing disc. *Genes & Development*, *5*(6), 996–1008. http://doi.org/10.1101/gad.5.6.996

D'Souza, B., Meloty-Kapella, L., & Weinmaster, G. (2010). Canonical and non-canonical Notch ligands. *Current Topics in Developmental Biology*, *92*, 73–129. http://doi.org/10.1016/S0070-2153(10)92003-6

de Celis, J. F., Garcia-Bellido, A., & Bray, S. J. (1996). Activation and function of Notch at the dorsal-ventral boundary of the wing imaginal disc. *Development (Cambridge, England)*, *122*(1), 359–69. Retrieved from http://www.ncbi.nlm.nih.gov/pubmed/8565848

del Álamo, D., Rouault, H., & Schweisguth, F. (2011). Mechanism and significance of cis-inhibition in Notch signalling. *Current Biology : CB*, *21*(1), R40–7. http://doi.org/10.1016/j.cub.2010.10.034

Deng, W. M., Althauser, C., & Ruohola-Baker, H. (2001). Notch-Delta signaling induces a transition from mitotic cell cycle to endocycle in Drosophila follicle cells. *Development (Cambridge, England)*, *128*(23), 4737–46. Retrieved from http://www.ncbi.nlm.nih.gov/pubmed/11731454

Devergne, O., Ghiglione, C., & Noselli, S. (2007). The endocytic control of JAK/STAT signalling in Drosophila. *Journal of Cell Science*, *120*(Pt 19), 3457–64. http://doi.org/10.1242/jcs.005926

Diaz-Benjumea, F. J., & Cohen, S. M. (1995). Serrate signals through Notch to establish a Wingless-dependent organizer at the dorsal/ventral compartment boundary of the Drosophila wing. *Development (Cambridge, England)*, *121*(12), 4215–25. Retrieved from

http://www.ncbi.nlm.nih.gov/pubmed/8575321

Diederich, R., Matsuno, K., Hing, H., & Artavanis-Tsakonas, S. (1994). Cytosolic interaction between deltex and Notch ankyrin repeats implicates deltex in the Notch signaling pathway. *Development*, *120*(3), 473–481. Retrieved from http://dev.biologists.org/content/120/3/473.short

Djiane, A., Krejci, A., Bernard, F., Fexova, S., Millen, K., & Bray, S. J. (2013). Dissecting the mechanisms of Notch induced hyperplasia. *The EMBO Journal*, *32*(1), 60–71. http://doi.org/10.1038/emboj.2012.326

Dow, J. A. (1999). The multifunctional Drosophila melanogaster V-ATPase is encoded by a multigene family. *Journal of Bioenergetics and Biomembranes*, *31*(1), 75–83. Retrieved from http://www.ncbi.nlm.nih.gov/pubmed/10340851

Doyotte, A., Russell, M. R. G., Hopkins, C. R., & Woodman, P. G. (2005). Depletion of TSG101 forms a mammalian "Class E" compartment: a multicisternal early endosome with multiple sorting defects. *Journal of Cell Science*, *118*(Pt 14), 3003–17. http://doi.org/10.1242/jcs.02421

Duffy, J. B. (2000). GAL4 system in Drosophila: a fly geneticist's Swiss army knife. *Genesis (New York, N.Y. : 2000)*, *34*(1-2), 1–15. http://doi.org/10.1002/gene.10150

Dukes, J. D., Fish, L., Richardson, J. D., Blaikley, E., Burns, S., Caunt, C. J., … Whitley, P. (2011). Functional ESCRT machinery is required for constitutive recycling of claudin-1 and maintenance of polarity in vertebrate epithelial cells. *Molecular Biology of the Cell*, *22*(17), 3192–205. http://doi.org/10.1091/mbc.E11-04-0343

Dunlop, J., Jones, P. C., & Finbow, M. E. (1995). Membrane insertion and assembly of ductin: a polytopic channel with dual orientations. *The EMBO Journal*, *14*(15), 3609–16. Retrieved from http://www.pubmedcentral.nih.gov/articlerender.fcgi?artid=394434&tool=pmcentrez&rendertype=abstract

Finbow, M. E., Goodwin, S. F., Meagher, L., Lane, N. J., Keen, J., Findlay, J. B., & Kaiser, K. (1994a). Evidence that the 16 kDa proteolipid (subunit c) of the vacuolar H(+)-ATPase and ductin from gap junctions are the same polypeptide in Drosophila and Manduca: molecular cloning of the Vha16k gene from Drosophila. *Journal of Cell Science*, *107 (Pt 7*, 1817–24. Retrieved from http://www.ncbi.nlm.nih.gov/pubmed/7983150

Fiúza, U.-M., & Arias, A. M. (2007). Cell and molecular biology of Notch. *The Journal of Endocrinology*, *194*(3), 459–74. http://doi.org/10.1677/JOE-07-0242

Flannery, A. R., Graham, L. A., & Stevens, T. H. (2004). Topological Characterization of the c, c', and c'' Subunits of the Vacuolar ATPase from the Yeast Saccharomyces cerevisiae. *Journal of Biological Chemistry*, *279*(38), 39856–

39862. http://doi.org/10.1074/jbc.M406767200

Forgac, M. (2007a). Vacuolar ATPases: rotary proton pumps in physiology and pathophysiology. *Nature Reviews. Molecular Cell Biology*, *8*(11), 917–29. http://doi.org/10.1038/nrm2272

Fortini, M. E., & Artavanis-Tsakonas, S. (1994). The suppressor of hairless protein participates in notch receptor signaling. *Cell*, *79*(2), 273–82. Retrieved from http://www.ncbi.nlm.nih.gov/pubmed/7954795

Fostier, M., Evans, D. A., Artavanis-Tsakonas, S., & Baron, M. (1998). Genetic characterization of the Drosophila melanogaster Suppressor of deltex gene: A regulator of notch signaling. *Genetics*, *150*(4), 1477–85. Retrieved from http://www.genetics.org/content/150/4/1477.abstract

Foulkes, W. D., & Shuen, A. Y. (2013). In brief: BRCA1 and BRCA2. *The Journal of Pathology*, *230*(4), 347–9. http://doi.org/10.1002/path.4205

Fre, S., Huyghe, M., Mourikis, P., Robine, S., Louvard, D., & Artavanis-Tsakonas, S. (2005). Notch signals control the fate of immature progenitor cells in the intestine. *Nature*, *435*(7044), 964–8. http://doi.org/10.1038/nature03589

Fre, S., Pallavi, S. K., Huyghe, M., Lae, M., Janssen, K.-P., Robine, S., … Louvard, D. (2009). Notch and Wnt signals cooperatively control cell proliferation and tumorigenesis in the intestine. *Proceedings of the National Academy of Sciences*, *106*(15), 6309–6314. http://doi.org/10.1073/pnas.0900427106

Fürthauer, M., & González-Gaitán, M. (2009). Endocytic regulation of notch signalling during development. *Traffic (Copenhagen, Denmark)*, *10*(7), 792–802. http://doi.org/10.1111/j.1600-0854.2009.00914.x

Gallagher, C. M., & Knoblich, J. A. (2006). The Conserved C2 Domain Protein Lethal (2) Giant Discs Regulates Protein Trafficking in Drosophila. *Developmental Cell*, *11*(5), 641–653. http://doi.org/10.1016/j.devcel.2006.09.014

Gho, M., Bellaïche, Y., & Schweisguth, F. (1999). Revisiting the Drosophila microchaete lineage: a novel intrinsically asymmetric cell division generates a glial cell. *Development (Cambridge, England)*, *126*(16), 3573–84. Retrieved from http://www.ncbi.nlm.nih.gov/pubmed/10409503

Go, M. J., Eastman, D. S., & Artavanis-Tsakonas, S. (1998). Cell proliferation control by Notch signaling in Drosophila development. *Development (Cambridge, England)*, *125*(11), 2031–40. Retrieved from http://www.ncbi.nlm.nih.gov/pubmed/9570768

Goentoro, L. A., Yakoby, N., Goodhouse, J., Schüpbach, T., & Shvartsman, S. Y. (2006). Quantitative analysis of the GAL4/UAS system in Drosophila oogenesis. *Genesis (New York, N.Y. : 2000)*, *44*(2), 66–74. http://doi.org/10.1002/gene.20184

Gordon, W. R., Vardar-Ulu, D., L'Heureux, S., Ashworth, T., Malecki, M. J., Sanchez-

Irizarry, C., … Blacklow, S. C. (2009). Effects of S1 cleavage on the structure, surface export, and signaling activity of human Notch1 and Notch2. *PloS One*, *4*(8), e6613. http://doi.org/10.1371/journal.pone.0006613

Goriely, A., Dumont, N., Dambly-Chaudière, C., & Ghysen, A. (1991). The determination of sense organs in Drosophila: effect of the neurogenic mutations in the embryo. *Development (Cambridge, England)*, *113*(4), 1395–404. Retrieved from http://www.ncbi.nlm.nih.gov/pubmed/1811951

Graham, L. A., Hill, K. J., & Stevens, T. H. (1998). Assembly of the yeast vacuolar H+-ATPase occurs in the endoplasmic reticulum and requires a Vma12p/Vma22p assembly complex. *The Journal of Cell Biology*, *142*(1), 39–49. Retrieved from http://www.pubmedcentral.nih.gov/articlerender.fcgi?artid=2133036&tool=pmcentrez&rendertype=abstract

Guo, M., Jan, L. Y., & Jan, Y. N. (1996). Control of Daughter Cell Fates during Asymmetric Division: Interaction of Numb and Notch. *Neuron*, *17*(1), 27–41. http://doi.org/10.1016/S0896-6273(00)80278-0

Gupta-Rossi, N., Le Bail, O., Gonen, H., Brou, C., Logeat, F., Six, E., … Israël, A. (2001). Functional interaction between SEL-10, an F-box protein, and the nuclear form of activated Notch1 receptor. *The Journal of Biological Chemistry*, *276*(37), 34371–8. http://doi.org/10.1074/jbc.M101343200

Guruharsha, K. G., Kankel, M. W., & Artavanis-Tsakonas, S. (2012). The Notch signalling system: recent insights into the complexity of a conserved pathway. *Nature Reviews. Genetics*, *13*(9), 654–66. http://doi.org/10.1038/nrg3272

Hallsson, J. H., Haflidadóttir, B. S., Schepsky, A., Arnheiter, H., & Steingrímsson, E. (2007). Evolutionary sequence comparison of the Mitf gene reveals novel conserved domains. *Pigment Cell Research / Sponsored by the European Society for Pigment Cell Research and the International Pigment Cell Society*, *20*(3), 185–200. http://doi.org/10.1111/j.1600-0749.2007.00373.x

Hallsson, J. H., Haflidadóttir, B. S., Stivers, C., Odenwald, W., Arnheiter, H., Pignoni, F., & Steingrímsson, E. (2004). The basic helix-loop-helix leucine zipper transcription factor Mitf is conserved in Drosophila and functions in eye development. *Genetics*, *167*(1), 233–41. Retrieved from http://www.pubmedcentral.nih.gov/articlerender.fcgi?artid=1470875&tool=pmcentrez&rendertype=abstract

Hartenstein, V., & Posakony, J. W. (1990). A dual function of the Notch gene in Drosophila sensillum development. *Developmental Biology*, *142*(1), 13–30. Retrieved from http://www.ncbi.nlm.nih.gov/pubmed/2227090

Hayek, S. R., Lee, S. A., & Parra, K. J. (2014). Advances in targeting the vacuolar proton-translocating ATPase (V-ATPase) for anti-fungal therapy. *Frontiers in Pharmacology*, *5*, 4. http://doi.org/10.3389/fphar.2014.00004

Hayward, P., Brennan, K., Sanders, P., Balayo, T., DasGupta, R., Perrimon, N., &

Martinez Arias, A. (2005). Notch modulates Wnt signalling by associating with Armadillo/beta-catenin and regulating its transcriptional activity. *Development (Cambridge, England)*, *132*(8), 1819–30. http://doi.org/10.1242/dev.01724

Heitzler, P., Bourouis, M., Ruel, L., Carteret, C., & Simpson, P. (1996). Genes of the Enhancer of split and achaete-scute complexes are required for a regulatory loop between Notch and Delta during lateral signalling in Drosophila. *Development (Cambridge, England)*, *122*(1), 161–71. Retrieved from http://www.ncbi.nlm.nih.gov/pubmed/8565827

Hemesath, T. J., Steingrímsson, E., McGill, G., Hansen, M. J., Vaught, J., Hodgkinson, C. A., … Fisher, D. E. (1994). microphthalmia, a critical factor in melanocyte development, defines a discrete transcription factor family. *Genes & Development*, *8*(22), 2770–80. Retrieved from http://www.ncbi.nlm.nih.gov/pubmed/7958932

Hermle, T., Saltukoglu, D., Grünewald, J., Walz, G., & Simons, M. (2010). Regulation of Frizzled-dependent planar polarity signaling by a V-ATPase subunit. *Current Biology : CB*, *20*(14), 1269–76. http://doi.org/10.1016/j.cub.2010.05.057

Herz, H.-M., Chen, Z., Scherr, H., Lackey, M., Bolduc, C., & Bergmann, A. (2006). vps25 mosaics display non-autonomous cell survival and overgrowth, and autonomous apoptosis. *Development (Cambridge, England)*, *133*(10), 1871–80. http://doi.org/10.1242/dev.02356

Herz, H.-M., Woodfield, S. E., Chen, Z., Bolduc, C., & Bergmann, A. (2009). Common and distinct genetic properties of ESCRT-II components in Drosophila. *PloS One*, *4*(1), e4165. http://doi.org/10.1371/journal.pone.0004165

Hiesinger, P. R., Fayyazuddin, A., Mehta, S. Q., Rosenmund, T., Schulze, K. L., Zhai, R. G., … Bellen, H. J. (2005). The v-ATPase V0 subunit a1 is required for a late step in synaptic vesicle exocytosis in Drosophila. *Cell*, *121*(4), 607–20. http://doi.org/10.1016/j.cell.2005.03.012

Ho, M., Hirata, R., Umemoto, N., Ohya, Y., Takatsuki, A., Stevens, T., & Anraku, Y. (1993). VMA13 encodes a 54-kDa vacuolar H(+)-ATPase subunit required for activity but not assembly of the enzyme complex in Saccharomyces cerevisiae. *J. Biol. Chem.*, *268*(24), 18286–18292. Retrieved from http://www.jbc.org/content/268/24/18286.short

Hori, K., Fostier, M., Ito, M., Fuwa, T. J., Go, M. J., Okano, H., … Matsuno, K. (2004). Drosophila deltex mediates suppressor of Hairless-independent and late-endosomal activation of Notch signaling. *Development (Cambridge, England)*, *131*(22), 5527–37. http://doi.org/10.1242/dev.01448

Hori, K., Sen, A., Kirchhausen, T., & Artavanis-Tsakonas, S. (2011). Synergy between the ESCRT-III complex and Deltex defines a ligand-independent Notch signal.

The Journal of Cell Biology, *195*(6), 1005–15. http://doi.org/10.1083/jcb.201104146

Hori, K., Sen, A., Kirchhausen, T., & Artavanis-Tsakonas, S. (2012). Regulation of ligand-independent Notch signal through intracellular trafficking. *Communicative & Integrative Biology*, *5*(4), 374–6. http://doi.org/10.4161/cib.19995

Huppert, S. S., Jacobsen, T. L., & Muskavitch, M. A. (1997). Feedback regulation is central to Delta-Notch signalling required for Drosophila wing vein morphogenesis. *Development (Cambridge, England)*, *124*(17), 3283–91. Retrieved from http://www.ncbi.nlm.nih.gov/pubmed/9310323

Im, Y. J., & Hurley, J. H. (2008). Integrated Structural Model and Membrane Targeting Mechanism of the Human ESCRT-II Complex. *Developmental Cell*, *14*(6), 902–913. http://doi.org/10.1016/j.devcel.2008.04.004

Irvine, K. D., & Vogt, T. F. (1997). Dorsal—ventral signaling in limb development. *Current Opinion in Cell Biology*, *9*(6), 867–876. http://doi.org/10.1016/S0955-0674(97)80090-7

Itoh, M., Kim, C.-H., Palardy, G., Oda, T., Jiang, Y.-J., Maust, D., … Chitnis, A. B. (2003). Mind bomb is a ubiquitin ligase that is essential for efficient activation of Notch signaling by Delta. *Developmental Cell*, *4*(1), 67–82. Retrieved from http://www.ncbi.nlm.nih.gov/pubmed/12530964

J.R. Jansen, E., & J.M. Martens, G. (2012). Novel Insights into V-ATPase Functioning: Distinct Roles for its Accessory Subunits ATP6AP1/Ac45 and ATP6AP2/(pro) Renin Receptor. *Current Protein & Peptide Science*, *13*(2), 124–133. http://doi.org/10.2174/138920312800493160

Jaekel, R., & Klein, T. (2006). The Drosophila Notch inhibitor and tumor suppressor gene lethal (2) giant discs encodes a conserved regulator of endosomal trafficking. *Developmental Cell*, *11*(5), 655–69. http://doi.org/10.1016/j.devcel.2006.09.019

Jafar-Nejad, H., Tien, A.-C., Acar, M., & Bellen, H. J. (2006). Senseless and Daughterless confer neuronal identity to epithelial cells in the Drosophila wing margin. *Development (Cambridge, England)*, *133*(9), 1683–92. http://doi.org/10.1242/dev.02338

Jansen, E. J. R., van Bakel, N. H. M., Olde Loohuis, N. F. M., Hafmans, T. G. M., Arentsen, T., Coenen, A. J. M., … Martens, G. J. M. (2012). Identification of domains within the V-ATPase accessory subunit Ac45 involved in V-ATPase transport and Ca2+-dependent exocytosis. *The Journal of Biological Chemistry*, *287*(33), 27537–46. http://doi.org/10.1074/jbc.M112.356105

Jékely, G., & Rørth, P. (2003a). Hrs mediates downregulation of multiple signalling receptors in Drosophila. *EMBO Reports*, *4*(12), 1163–1168. http://doi.org/10.1038/sj.embor.7400019

Jennings, B., Preiss, A., Delidakis, C., & Bray, S. (1994). The Notch signalling pathway is required for Enhancer of split bHLH protein expression during neurogenesis in the Drosophila embryo. *Development (Cambridge, England)*, *120*(12), 3537–48. Retrieved from http://www.ncbi.nlm.nih.gov/pubmed/7821220

Kaether, C., Haass, C., & Steiner, H. (2006). Assembly, Trafficking and Function of γ-Secretase. *Neurodegenerative Diseases*, *3*(4-5), 275–283. http://doi.org/10.1159/000095267

Kane, P. M. (1995). Disassembly and Reassembly of the Yeast Vacuolar H+-ATPase in Vivo. *J. Biol. Chem.*, *270*(28), 17025–17032. Retrieved from http://www.jbc.org/content/270/28/17025.short

Katoh, Y., Shiba, Y., Mitsuhashi, H., Yanagida, Y., Takatsu, H., & Nakayama, K. (2004). Tollip and Tom1 form a complex and recruit ubiquitin-conjugated proteins onto early endosomes. *The Journal of Biological Chemistry*, *279*(23), 24435–43. http://doi.org/10.1074/jbc.M400059200

Kidd, S., & Lieber, T. (2002). Furin cleavage is not a requirement for Drosophila Notch function. *Mechanisms of Development*, *115*(1-2), 41–51. http://doi.org/10.1016/S0925-4773(02)00120-X

Kim, J., Sebring, A., Esch, J. J., Kraus, M. E., Vorwerk, K., Magee, J., & Carroll, S. B. (1996). Integration of positional signals and regulation of wing formation and identity by Drosophila vestigial gene. *Nature*, *382*(6587), 133–8. http://doi.org/10.1038/382133a0

Kopan, R., & Ilagan, M. X. G. (2009). The canonical Notch signaling pathway: unfolding the activation mechanism. *Cell*, *137*(2), 216–33. http://doi.org/10.1016/j.cell.2009.03.045

Lapierre, L. R., De Magalhaes Filho, C. D., McQuary, P. R., Chu, C.-C., Visvikis, O., Chang, J. T., … Hansen, M. (2013). The TFEB orthologue HLH-30 regulates autophagy and modulates longevity in Caenorhabditis elegans. *Nature Communications*, *4*, 2267. http://doi.org/10.1038/ncomms3267

Le Borgne, R., Bardin, A., & Schweisguth, F. (2005). The roles of receptor and ligand endocytosis in regulating Notch signaling. *Development (Cambridge, England)*, *132*(8), 1751–62. http://doi.org/10.1242/dev.01789

Le Bras, S., Loyer, N., & Le Borgne, R. (2011). The multiple facets of ubiquitination in the regulation of notch signaling pathway. *Traffic (Copenhagen, Denmark)*, *12*(2), 149–61. http://doi.org/10.1111/j.1600-0854.2010.01126.x

Lecourtois, M., & Schweisguth, F. (1995). The neurogenic suppressor of hairless DNA-binding protein mediates the transcriptional activation of the enhancer of split complex genes triggered by Notch signaling. *Genes & Development*, *9*(21), 2598–608. Retrieved from http://www.ncbi.nlm.nih.gov/pubmed/7590238

Lee, T., & Luo, L. (2001). Mosaic analysis with a repressible cell marker (MARCM) for Drosophila neural development. *Trends in Neurosciences*, *24*(5), 251–4. Retrieved from http://www.ncbi.nlm.nih.gov/pubmed/11311363

Lehmann, R., Jimnez, F., Dietrich, U., & Campos-Ortega, J. A. (1983). On the phenotype and development of mutants of early neurogenesis inDrosophila melanogaster. *Wilhelm Roux's Archives of Developmental Biology*, *192*(2), 62–74. http://doi.org/10.1007/BF00848482

Leibfried, A., Fricke, R., Morgan, M. J., Bogdan, S., & Bellaiche, Y. (2008). Drosophila Cip4 and WASp define a branch of the Cdc42-Par6-aPKC pathway regulating E-cadherin endocytosis. *Current Biology : CB*, *18*(21), 1639–48. http://doi.org/10.1016/j.cub.2008.09.063

Leung, K. F., Dacks, J. B., & Field, M. C. (2008). Evolution of the multivesicular body ESCRT machinery; retention across the eukaryotic lineage. *Traffic (Copenhagen, Denmark)*, *9*(10), 1698–716. http://doi.org/10.1111/j.1600-0854.2008.00797.x

Liégeois, S., Benedetto, A., Garnier, J.-M., Schwab, Y., & Labouesse, M. (2006). The V0-ATPase mediates apical secretion of exosomes containing Hedgehog-related proteins in Caenorhabditis elegans. *The Journal of Cell Biology*, *173*(6), 949–61. http://doi.org/10.1083/jcb.200511072

Lissemore, J. L., & Starmer, W. T. (1999). Phylogenetic analysis of vertebrate and invertebrate Delta/Serrate/LAG-2 (DSL) proteins. *Molecular Phylogenetics and Evolution*, *11*(2), 308–19. http://doi.org/10.1006/mpev.1998.0588

Lloyd, T. E., Atkinson, R., Wu, M. N., Zhou, Y., Pennetta, G., & Bellen, H. J. (2002). Hrs regulates endosome membrane invagination and tyrosine kinase receptor signaling in Drosophila. *Cell*, *108*(2), 261–9. Retrieved from http://www.ncbi.nlm.nih.gov/pubmed/11832215

López-Schier, H., & St Johnston, D. (2001). Delta signaling from the germ line controls the proliferation and differentiation of the somatic follicle cells during Drosophila oogenesis. *Genes & Development*, *15*(11), 1393–405. http://doi.org/10.1101/gad.200901

Lowe, N., Rees, J. S., Roote, J., Ryder, E., Armean, I. M., Johnson, G., … St Johnston, D. (2014). Analysis of the expression patterns, subcellular localisations and interaction partners of Drosophila proteins using a pigP protein trap library. *Development (Cambridge, England)*, *141*(20), 3994–4005. http://doi.org/10.1242/dev.111054

Lu, H., & Bilder, D. (2005). Endocytic control of epithelial polarity and proliferation in Drosophila. *Nature Cell Biology*, *7*(12), 1232–9. http://doi.org/10.1038/ncb1324

Ludwig, J., Kerscher, S., Brandt, U., Pfeiffer, K., Getlawi, F., Apps, D. K., & Schägger, H. (1998). Identification and characterization of a novel 9.2-kDa membrane

sector-associated protein of vacuolar proton-ATPase from chromaffin granules. *The Journal of Biological Chemistry*, *273*(18), 10939–47. Retrieved from http://www.ncbi.nlm.nih.gov/pubmed/9556572

Manolson, M. F., Wu, B., Proteau, D., Taillon, B. E., Roberts, B. T., Hoyt, M. A., & Jones, E. W. (1994). STV1 gene encodes functional homologue of 95-kDa yeast vacuolar H(+)-ATPase subunit Vph1p. *The Journal of Biological Chemistry*, *269*(19), 14064–74. Retrieved from http://www.ncbi.nlm.nih.gov/pubmed/7514599

Marjuki, H., Gornitzky, A., Marathe, B. M., Ilyushina, N. A., Aldridge, J. R., Desai, G., … Webster, R. G. (2011). Influenza A virus-induced early activation of ERK and PI3K mediates V-ATPase-dependent intracellular pH change required for fusion. *Cellular Microbiology*, *13*(4), 587–601. http://doi.org/10.1111/j.1462-5822.2010.01556.x

Marshansky, V., Rubinstein, J. L., & Grüber, G. (2014). Eukaryotic V-ATPase: novel structural findings and functional insights. *Biochimica et Biophysica Acta*, *1837*(6), 857–79. http://doi.org/10.1016/j.bbabio.2014.01.018

Martina, J. A., Chen, Y., Gucek, M., & Puertollano, R. (2012). MTORC1 functions as a transcriptional regulator of autophagy by preventing nuclear transport of TFEB. *Autophagy*, *8*(6), 903–14. http://doi.org/10.4161/auto.19653

Martina, J. A., Diab, H. I., Li, H., & Puertollano, R. (2014). Novel roles for the MiTF/TFE family of transcription factors in organelle biogenesis, nutrient sensing, and energy homeostasis. *Cellular and Molecular Life Sciences : CMLS*, *71*(13), 2483–97. http://doi.org/10.1007/s00018-014-1565-8

Martina, J. A., Diab, H. I., Lishu, L., Jeong-A, L., Patange, S., Raben, N., & Puertollano, R. (2014). The nutrient-responsive transcription factor TFE3 promotes autophagy, lysosomal biogenesis, and clearance of cellular debris. *Science Signaling*, *7*(309), ra9. http://doi.org/10.1126/scisignal.2004754

Martina, J. A., & Puertollano, R. (2013). Rag GTPases mediate amino acid-dependent recruitment of TFEB and MITF to lysosomes. *The Journal of Cell Biology*, *200*(4), 475–91. http://doi.org/10.1083/jcb.201209135

Martinez-Zaguilan, R., Lynch, R. M., Martinez, G. M., & Gillies, R. J. (1993). Vacuolar-type H(+)-ATPases are functionally expressed in plasma membranes of human tumor cells. *Am J Physiol Cell Physiol*, *265*(4), C1015–1029. Retrieved from http://ajpcell.physiology.org/content/265/4/C1015.short

Matsuno, K., Diederich, R. J., Go, M. J., Blaumueller, C. M., & Artavanis-Tsakonas, S. (1995). Deltex acts as a positive regulator of Notch signaling through interactions with the Notch ankyrin repeats. *Development (Cambridge, England)*, *121*(8), 2633–44. Retrieved from http://www.ncbi.nlm.nih.gov/pubmed/7671825

Maxfield, F. R., & Yamashiro, D. J. (1987). Endosome acidification and the pathways

of receptor-mediated endocytosis. *Advances in Experimental Medicine and Biology*, *225*, 189–98. Retrieved from http://www.ncbi.nlm.nih.gov/pubmed/2839960

Mazaleyrat, S. L., Fostier, M., Wilkin, M. B., Aslam, H., Evans, D. A. P., Cornell, M., & Baron, M. (2003). Down-regulation of Notch target gene expression by Suppressor of deltex. *Developmental Biology*, *255*(2), 363–72. Retrieved from http://www.ncbi.nlm.nih.gov/pubmed/12648496

Medina, D. L., Di Paola, S., Peluso, I., Armani, A., De Stefani, D., Venditti, R., … Ballabio, A. (2015). Lysosomal calcium signalling regulates autophagy through calcineurin and TFEB. *Nature Cell Biology*, *17*(3), 288–299. http://doi.org/10.1038/ncb3114

Meloty-Kapella, L., Shergill, B., Kuon, J., Botvinick, E., & Weinmaster, G. (2012). Notch Ligand Endocytosis Generates Mechanical Pulling Force Dependent on Dynamin, Epsins, and Actin. *Developmental Cell*, *22*(6), 1299–1312. http://doi.org/10.1016/j.devcel.2012.04.005

Menut, L., Vaccari, T., Dionne, H., Hill, J., Wu, G., & Bilder, D. (2007). A mosaic genetic screen for Drosophila neoplastic tumor suppressor genes based on defective pupation. *Genetics*, *177*(3), 1667–77. http://doi.org/10.1534/genetics.107.078360

Micchelli, C. A., & Blair, S. S. (1999). Dorsoventral lineage restriction in wing imaginal discs requires Notch. *Nature*, *401*(6752), 473–6. http://doi.org/10.1038/46779

Micchelli, C. A., Rulifson, E. J., & Blair, S. S. (1997). The function and regulation of cut expression on the wing margin of Drosophila: Notch, Wingless and a dominant negative role for Delta and Serrate. *Development (Cambridge, England)*, *124*(8), 1485–95. Retrieved from http://www.ncbi.nlm.nih.gov/pubmed/9108365

Moberg, K. H., Schelble, S., Burdick, S. K., & Hariharan, I. K. (2005). Mutations in erupted, the Drosophila ortholog of mammalian tumor susceptibility gene 101, elicit non-cell-autonomous overgrowth. *Developmental Cell*, *9*(5), 699–710. http://doi.org/10.1016/j.devcel.2005.09.018

Morgan, T. H. (1917). The Theory of the Gene. http://doi.org/doi:10.1086/279629.

Morin, X., Daneman, R., Zavortink, M., & Chia, W. (2001). A protein trap strategy to detect GFP-tagged proteins expressed from their endogenous loci in Drosophila. *Proceedings of the National Academy of Sciences of the United States of America*, *98*(26), 15050–5. http://doi.org/10.1073/pnas.261408198

Morita, E., Sandrin, V., Alam, S. L., Eckert, D. M., Gygi, S. P., & Sundquist, W. I. (2007). Identification of human MVB12 proteins as ESCRT-I subunits that function in HIV budding. *Cell Host & Microbe*, *2*(1), 41–53. http://doi.org/10.1016/j.chom.2007.06.003

Morita, E., Sandrin, V., Chung, H.-Y., Morham, S. G., Gygi, S. P., Rodesch, C. K., & Sundquist, W. I. (2007). Human ESCRT and ALIX proteins interact with proteins of the midbody and function in cytokinesis. *The EMBO Journal*, *26*(19), 4215–27. http://doi.org/10.1038/sj.emboj.7601850

Muench, S. P., Trinick, J., & Harrison, M. A. (2011). Structural divergence of the rotary ATPases. *Quarterly Reviews of Biophysics*, *44*(3), 311–56. http://doi.org/10.1017/S0033583510000338

Mukherjee, A., Veraksa, A., Bauer, A., Rosse, C., Camonis, J., & Artavanis-Tsakonas, S. (2005). Regulation of Notch signalling by non-visual beta-arrestin. *Nature Cell Biology*, *7*(12), 1191–201. http://doi.org/10.1038/ncb1327

Mukherjee, T., Kim, W. S., Mandal, L., & Banerjee, U. (2011a). Interaction between Notch and Hif-alpha in development and survival of Drosophila blood cells. *Science (New York, N.Y.)*, *332*(6034), 1210–3. http://doi.org/10.1126/science.1199643

Mumm, J. S., Schroeter, E. H., Saxena, M. T., Griesemer, A., Tian, X., Pan, D. J., … Kopan, R. (2000). A ligand-induced extracellular cleavage regulates gamma-secretase-like proteolytic activation of Notch1. *Molecular Cell*, *5*(2), 197–206. Retrieved from http://www.ncbi.nlm.nih.gov/pubmed/10882062

Mummery-Widmer, J. L., Yamazaki, M., Stoeger, T., Novatchkova, M., Bhalerao, S., Chen, D., … Knoblich, J. A. (2009). Genome-wide analysis of Notch signalling in Drosophila by transgenic RNAi. *Nature*, *458*(7241), 987–92. http://doi.org/10.1038/nature07936

Musse, A. A., Meloty-Kapella, L., & Weinmaster, G. (2012). Notch ligand endocytosis: mechanistic basis of signaling activity. *Seminars in Cell & Developmental Biology*, *23*(4), 429–36. http://doi.org/10.1016/j.semcdb.2012.01.011

Nelson, H., & Nelson, N. (1990). Disruption of genes encoding subunits of yeast vacuolar H(+)-ATPase causes conditional lethality. *Proceedings of the National Academy of Sciences*, *87*(9), 3503–3507. http://doi.org/10.1073/pnas.87.9.3503

Neumann, C. J., & Cohen, S. M. (1996). A hierarchy of cross-regulation involving Notch, wingless, vestigial and cut organizes the dorsal/ventral axis of the Drosophila wing. *Development (Cambridge, England)*, *122*(11), 3477–85. Retrieved from http://www.ncbi.nlm.nih.gov/pubmed/8951063

Newsome, T. P., Asling, B., & Dickson, B. J. (2000). Analysis of Drosophila photoreceptor axon guidance in eye-specific mosaics. *Development (Cambridge, England)*, *127*(4), 851–60. Retrieved from http://www.ncbi.nlm.nih.gov/pubmed/10648243

Nichols, J. T., Miyamoto, A., Olsen, S. L., D'Souza, B., Yao, C., & Weinmaster, G. (2007). DSL ligand endocytosis physically dissociates Notch1 heterodimers

before activating proteolysis can occur. *The Journal of Cell Biology*, *176*(4), 445–458. http://doi.org/10.1083/jcb.200609014

Nishi, T., & Forgac, M. (2000). Molecular Cloning and Expression of Three Isoforms of the 100-kDa a Subunit of the Mouse Vacuolar Proton-translocating ATPase. *Journal of Biological Chemistry*, *275*(10), 6824–6830. http://doi.org/10.1074/jbc.275.10.6824

O'Rourke, E. J., & Ruvkun, G. (2013). MXL-3 and HLH-30 transcriptionally link lipolysis and autophagy to nutrient availability. *Nature Cell Biology*, *15*(6), 668–76. http://doi.org/10.1038/ncb2741

Overstreet, E. (2004). Fat facets and Liquid facets promote Delta endocytosis and Delta signaling in the signaling cells. *Development*, *131*(21), 5355–5366. http://doi.org/10.1242/dev.01434

Pallavi, S. K., Ho, D. M., Hicks, C., Miele, L., & Artavanis-Tsakonas, S. (2012). Notch and Mef2 synergize to promote proliferation and metastasis through JNK signal activation in Drosophila. *The EMBO Journal*, *31*(13), 2895–2907. http://doi.org/10.1038/emboj.2012.129

Palmer, W. H., Jia, D., & Deng, W.-M. (2014). Cis-interactions between Notch and its ligands block ligand-independent Notch activity. *eLife*, *3*. http://doi.org/10.7554/eLife.04415

Palmer, W. H., Jia, D., & Deng, W.-M. (2015). Cis-interactions between Notch and its ligands block ligand-independent Notch activity. *eLife*, *4*, e04415. http://doi.org/10.7554/eLife.04415

Palmieri, M., Impey, S., Kang, H., di Ronza, A., Pelz, C., Sardiello, M., & Ballabio, A. (2011). Characterization of the CLEAR network reveals an integrated control of cellular clearance pathways. *Human Molecular Genetics*, *20*(19), 3852–66. http://doi.org/10.1093/hmg/ddr306

Parks, A. L., Klueg, K. M., Stout, J. R., & Muskavitch, M. A. (2000). Ligand endocytosis drives receptor dissociation and activation in the Notch pathway. *Development (Cambridge, England)*, *127*(7), 1373–85. Retrieved from http://www.ncbi.nlm.nih.gov/pubmed/10704384

Parks, A. L., Stout, J. R., Shepard, S. B., Klueg, K. M., Dos Santos, A. A., Parody, T. R., … Muskavitch, M. A. T. (2006). Structure-function analysis of delta trafficking, receptor binding and signaling in Drosophila. *Genetics*, *174*(4), 1947–61. http://doi.org/10.1534/genetics.106.061630

Parra, K. J., Keenan, K. L., & Kane, P. M. (2000). The H subunit (Vma13p) of the yeast V-ATPase inhibits the ATPase activity of cytosolic V1 complexes. *The Journal of Biological Chemistry*, *275*(28), 21761–7. http://doi.org/10.1074/jbc.M002305200

Pasternak, S. H., Bagshaw, R. D., Guiral, M., Zhang, S., Ackerley, C. A., Pak, B. J., …

Mahuran, D. J. (2003). Presenilin-1, nicastrin, amyloid precursor protein, and gamma-secretase activity are co-localized in the lysosomal membrane. *The Journal of Biological Chemistry*, *278*(29), 26687–94. http://doi.org/10.1074/jbc.M212192200

Pece, S., Serresi, M., Santolini, E., Capra, M., Hulleman, E., Galimberti, V., … Di Fiore, P. P. (2004). Loss of negative regulation by Numb over Notch is relevant to human breast carcinogenesis. *The Journal of Cell Biology*, *167*(2), 215–21. http://doi.org/10.1083/jcb.200406140

Peri, F., & Nüsslein-Volhard, C. (2008). Live imaging of neuronal degradation by microglia reveals a role for v0-ATPase a1 in phagosomal fusion in vivo. *Cell*, *133*(5), 916–27. http://doi.org/10.1016/j.cell.2008.04.037

Peters, C., Bayer, M. J., Bühler, S., Andersen, J. S., Mann, M., & Mayer, A. (2001). Trans-complex formation by proteolipid channels in the terminal phase of membrane fusion. *Nature*, *409*(6820), 581–8. http://doi.org/10.1038/35054500

Petzoldt, A. G., Gleixner, E. M., Fumagalli, A., Vaccari, T., & Simons, M. (2013). Elevated expression of the V-ATPase C subunit triggers JNK-dependent cell invasion and overgrowth in a Drosophila epithelium. *Disease Models & Mechanisms*, *6*(3), 689–700. http://doi.org/10.1242/dmm.010660

Philpott, A. (2010). Neural Development: bHLH Genes. Retrieved November 6, 2015, from http://www.els.net/WileyCDA/ElsArticle/refId-a0000827.html

Polo, S., Sigismund, S., Faretta, M., Guidi, M., Capua, M. R., Bossi, G., … Di Fiore, P. P. (2002). A single motif responsible for ubiquitin recognition and monoubiquitination in endocytic proteins. *Nature*, *416*(6879), 451–5. http://doi.org/10.1038/416451a

Poulton, J. S., Huang, Y.-C., Smith, L., Sun, J., Leake, N., Schleede, J., … Deng, W.-M. (2011). The microRNA pathway regulates the temporal pattern of Notch signaling in Drosophila follicle cells. *Development (Cambridge, England)*, *138*(9), 1737–45. http://doi.org/10.1242/dev.059352

Puertollano, R. (2005). Interactions of TOM1L1 with the multivesicular body sorting machinery. *The Journal of Biological Chemistry*, *280*(10), 9258–64. http://doi.org/10.1074/jbc.M412481200

Puertollano, R., & Bonifacino, J. S. (2004). Interactions of GGA3 with the ubiquitin sorting machinery. *Nature Cell Biology*, *6*(3), 244–51. http://doi.org/10.1038/ncb1106

Pulipparacharuvil, S., Akbar, M. A., Ray, S., Sevrioukov, E. A., Haberman, A. S., Rohrer, J., & Krämer, H. (2005). Drosophila Vps16A is required for trafficking to lysosomes and biogenesis of pigment granules. *Journal of Cell Science*, *118*(Pt 16), 3663–73. http://doi.org/10.1242/jcs.02502

Purves, D. C., & Brachmann, C. (2007). Dissection of imaginal discs from 3rd instar Drosophila larvae. *Journal of Visualized Experiments : JoVE*, (2), 140. http://doi.org/10.3791/140

Qiu, L., Joazeiro, C., Fang, N., Wang, H. Y., Elly, C., Altman, Y., … Liu, Y. C. (2000). Recognition and ubiquitination of Notch by Itch, a hect-type E3 ubiquitin ligase. *The Journal of Biological Chemistry*, *275*(46), 35734–7. http://doi.org/10.1074/jbc.M007300200

Raiborg, C., Bache, K. G., Mehlum, A., Stang, E., & Stenmark, H. (2001). Hrs recruits clathrin to early endosomes. *The EMBO Journal*, *20*(17), 5008–21. http://doi.org/10.1093/emboj/20.17.5008

Raiborg, C., Bremnes, B., Mehlum, A., Gillooly, D. J., D'Arrigo, A., Stang, E., & Stenmark, H. (2001). FYVE and coiled-coil domains determine the specific localisation of Hrs to early endosomes. *Journal of Cell Science*, *114*(Pt 12), 2255–63. Retrieved from http://www.ncbi.nlm.nih.gov/pubmed/11493665

Raiborg, C., & Stenmark, H. (2009). The ESCRT machinery in endosomal sorting of ubiquitylated membrane proteins. *Nature*, *458*(7237), 445–52. http://doi.org/10.1038/nature07961

Ramain, P., Khechumian, K., Seugnet, L., Arbogast, N., Ackermann, C., & Heitzler, P. (2001). Novel Notch alleles reveal a Deltex-dependent pathway repressing neural fate. *Current Biology : CB*, *11*(22), 1729–38. Retrieved from http://www.ncbi.nlm.nih.gov/pubmed/11719214

Rand, M. D., Grimm, L. M., Artavanis-Tsakonas, S., Patriub, V., Blacklow, S. C., Sklar, J., & Aster, J. C. (2000). Calcium depletion dissociates and activates heterodimeric notch receptors. *Molecular and Cellular Biology*, *20*(5), 1825–35. Retrieved from http://www.pubmedcentral.nih.gov/articlerender.fcgi?artid=85363&tool=pmcentrez&rendertype=abstract

Ranganathan, P., Weaver, K. L., & Capobianco, A. J. (2011). Notch signalling in solid tumours: a little bit of everything but not all the time. *Nature Reviews. Cancer*, *11*(5), 338–51. http://doi.org/10.1038/nrc3035

Rawson, S., Phillips, C., Huss, M., Tiburcy, F., Wieczorek, H., Trinick, J., … Muench, S. P. (2015). Structure of the Vacuolar H(+)-ATPase Rotary Motor Reveals New Mechanistic Insights. *Structure (London, England : 1993)*, *23*(3), 461–71. http://doi.org/10.1016/j.str.2014.12.016

Raymond, C. K., Howald-Stevenson, I., Vater, C. A., & Stevens, T. H. (1992). Morphological classification of the yeast vacuolar protein sorting mutants: evidence for a prevacuolar compartment in class E vps mutants. *Molecular Biology of the Cell*, *3*(12), 1389–402. Retrieved from http://www.pubmedcentral.nih.gov/articlerender.fcgi?artid=275707&tool=pmcentrez&rendertype=abstract

Razi, M., & Futter, C. E. (2006). Distinct roles for Tsg101 and Hrs in multivesicular body formation and inward vesiculation. *Molecular Biology of the Cell*, *17*(8), 3469–83. http://doi.org/10.1091/mbc.E05-11-1054

Rebay, I., Fleming, R. J., Fehon, R. G., Cherbas, L., Cherbas, P., & Artavanis-Tsakonas, S. (1991). Specific EGF repeats of Notch mediate interactions with Delta and Serrate: implications for Notch as a multifunctional receptor. *Cell*, *67*(4), 687–99. Retrieved from http://www.ncbi.nlm.nih.gov/pubmed/1657403

Rieder, S. E., Banta, L. M., Köhrer, K., McCaffery, J. M., & Emr, S. D. (1996). Multilamellar endosome-like compartment accumulates in the yeast vps28 vacuolar protein sorting mutant. *Molecular Biology of the Cell*, *7*(6), 985–99. Retrieved from http://www.pubmedcentral.nih.gov/articlerender.fcgi?artid=275948&tool=pmcentrez&rendertype=abstract

Roczniak-Ferguson, A., Petit, C. S., Froehlich, F., Qian, S., Ky, J., Angarola, B., … Ferguson, S. M. (2012). The transcription factor TFEB links mTORC1 signaling to transcriptional control of lysosome homeostasis. *Science Signaling*, *5*(228), ra42. http://doi.org/10.1126/scisignal.2002790

Roegiers, F., Kavaler, J., Tolwinski, N., Chou, Y.-T., Duan, H., Bejarano, F., … Lai, E. C. (2009). Frequent unanticipated alleles of lethal giant larvae in Drosophila second chromosome stocks. *Genetics*, *182*(1), 407–10. http://doi.org/10.1534/genetics.109.101808

Ross, D. A., & Kadesch, T. (2001). The notch intracellular domain can function as a coactivator for LEF-1. *Molecular and Cellular Biology*, *21*(22), 7537–44. http://doi.org/10.1128/MCB.21.22.7537-7544.2001

Rulifson, E. J., Micchelli, C. A., Axelrod, J. D., Perrimon, N., & Blair, S. S. (1996). wingless refines its own expression domain on the Drosophila wing margin. *Nature*, *384*(6604), 72–4. http://doi.org/10.1038/384072a0

Rusten, T. E., Vaccari, T., & Stenmark, H. (2011). Shaping development with ESCRTs. *Nature Cell Biology*, *14*(1), 38–45. http://doi.org/10.1038/ncb2381

Sakamoto, K., Ohara, O., Takagi, M., Takeda, S., & Katsube, K. (2002). Intracellular cell-autonomous association of Notch and its ligands: a novel mechanism of Notch signal modification. *Developmental Biology*, *241*(2), 313–26. http://doi.org/10.1006/dbio.2001.0517

Sakata, T., Sakaguchi, H., Tsuda, L., Higashitani, A., Aigaki, T., Matsuno, K., & Hayashi, S. (2004). Drosophila Nedd4 regulates endocytosis of notch and suppresses its ligand-independent activation. *Current Biology : CB*, *14*(24), 2228–36. http://doi.org/10.1016/j.cub.2004.12.028

Samson, R. Y., Obita, T., Freund, S. M., Williams, R. L., & Bell, S. D. (2008). A role for the ESCRT system in cell division in archaea. *Science (New York, N.Y.)*, *322*(5908), 1710–3. http://doi.org/10.1126/science.1165322

Sardiello, M., Palmieri, M., di Ronza, A., Medina, D. L., Valenza, M., Gennarino, V. A., … Ballabio, A. (2009). A gene network regulating lysosomal biogenesis and function. *Science (New York, N.Y.)*, *325*(5939), 473–7. http://doi.org/10.1126/science.1174447

Schneider, M., Troost, T., Grawe, F., Martinez-Arias, A., & Klein, T. (2013). Activation of Notch in lgd mutant cells requires the fusion of late endosomes with the lysosome. *Journal of Cell Science*, *126*(Pt 2), 645–56. http://doi.org/10.1242/jcs.116590

Schober, M., Schaefer, M., & Knoblich, J. A. (1999). Bazooka recruits Inscuteable to orient asymmetric cell divisions in Drosophila neuroblasts. *Nature*, *402*(6761), 548–51. http://doi.org/10.1038/990135

Selkoe, D. J., & Wolfe, M. S. (2007). Presenilin: running with scissors in the membrane. *Cell*, *131*(2), 215–21. http://doi.org/10.1016/j.cell.2007.10.012

Seol, J. H., Shevchenko, A., & Deshaies, R. J. (2001). Skp1 forms multiple protein complexes, including RAVE, a regulator of V-ATPase assembly. *Nature Cell Biology*, *3*(4), 384–91. http://doi.org/10.1038/35070067

Settembre, C., Di Malta, C., Polito, V. A., Garcia Arencibia, M., Vetrini, F., Erdin, S., … Ballabio, A. (2011). TFEB links autophagy to lysosomal biogenesis. *Science (New York, N.Y.)*, *332*(6036), 1429–33. http://doi.org/10.1126/science.1204592

Settembre, C., Zoncu, R., Medina, D. L., Vetrini, F., Erdin, S., Erdin, S., … Ballabio, A. (2012). A lysosome-to-nucleus signalling mechanism senses and regulates the lysosome via mTOR and TFEB. *The EMBO Journal*, *31*(5), 1095–108. http://doi.org/10.1038/emboj.2012.32

Seugnet, L., Simpson, P., & Haenlin, M. (1997). Requirement for dynamin during Notch signaling in Drosophila neurogenesis. *Developmental Biology*, *192*(2), 585–98. http://doi.org/10.1006/dbio.1997.8723

Shellenbarger, D. L., & Mohler, J. D. (1975). TEMPERATURE-SENSITIVE MUTATIONS OF THE NOTCH LOCUS IN DROSOPHILA MELANOGASTER. *Genetics*, *81*(1), 143–162. Retrieved from http://www.genetics.org/content/81/1/143.short

Shimizu, H., Woodcock, S. A., Wilkin, M. B., Trubenová, B., Monk, N. A. M., & Baron, M. (2014). Compensatory flux changes within an endocytic trafficking network maintain thermal robustness of Notch signaling. *Cell*, *157*(5), 1160–74. http://doi.org/10.1016/j.cell.2014.03.050

Shum, W. W. C., Da Silva, N., Brown, D., & Breton, S. (2009). Regulation of luminal acidification in the male reproductive tract via cell-cell crosstalk. *The Journal of Experimental Biology*, *212*(Pt 11), 1753–61. http://doi.org/10.1242/jeb.027284

Sigismund, S., Confalonieri, S., Ciliberto, A., Polo, S., Scita, G., & Di Fiore, P. P. (2012). Endocytosis and signaling: cell logistics shape the eukaryotic cell plan. *Physiological Reviews*, *92*(1), 273–366. http://doi.org/10.1152/physrev.00005.2011

Simpson, P. (1997). Notch signalling in development: on equivalence groups and asymmetric developmental potential. *Current Opinion in Genetics & Development*, *7*(4), 537–42. Retrieved from http://www.ncbi.nlm.nih.gov/pubmed/9309187

Skeath, J. B., & Carroll, S. B. (1991). Regulation of achaete-scute gene expression and sensory organ pattern formation in the Drosophila wing. *Genes & Development*, *5*(6), 984–995. http://doi.org/10.1101/gad.5.6.984

Skeath, J. B., Panganiban, G., Selegue, J., & Carroll, S. B. (1992). Gene regulation in two dimensions: the proneural achaete and scute genes are controlled by combinations of axis-patterning genes through a common intergenic control region. *Genes & Development*, *6*(12B), 2606–19. Retrieved from http://www.ncbi.nlm.nih.gov/pubmed/1340472

Steingrímsson, E., Tessarollo, L., Reid, S. W., Jenkins, N. A., & Copeland, N. G. (1998). The bHLH-Zip transcription factor Tfeb is essential for placental vascularization. *Development (Cambridge, England)*, *125*(23), 4607–16. Retrieved from http://www.ncbi.nlm.nih.gov/pubmed/9806910

Stevens, T. H., & Forgac, M. (1997a). Structure, function and regulation of the vacuolar (H+)-ATPase. *Annual Review of Cell and Developmental Biology*, *13*, 779–808. http://doi.org/10.1146/annurev.cellbio.13.1.779

Stevens, T. H., & Forgac, M. (1997b). Structure, function and regulation of the vacuolar (H+)-ATPase. *Annual Review of Cell and Developmental Biology*, *13*, 779–808. http://doi.org/10.1146/annurev.cellbio.13.1.779

Stransky, L. A., & Forgac, M. (2015). Amino Acid Availability Modulates Vacuolar H+-ATPase Assembly. *The Journal of Biological Chemistry*, M115.659128–. http://doi.org/10.1074/jbc.M115.659128

Strasser, B., Iwaszkiewicz, J., Michielin, O., & Mayer, A. (2011). The V-ATPase proteolipid cylinder promotes the lipid-mixing stage of SNARE-dependent fusion of yeast vacuoles. *The EMBO Journal*, *30*(20), 4126–41. http://doi.org/10.1038/emboj.2011.335

Struhl, G., & Adachi, A. (1998). Nuclear access and action of notch in vivo. *Cell*, *93*(4), 649–60. Retrieved from http://www.ncbi.nlm.nih.gov/pubmed/9604939

Stuffers, S., Sem Wegner, C., Stenmark, H., & Brech, A. (2009). Multivesicular endosome biogenesis in the absence of ESCRTs. *Traffic (Copenhagen, Denmark)*, *10*(7), 925–37. http://doi.org/10.1111/j.1600-0854.2009.00920.x

Sumner, J. P., Dow, J. A., Earley, F. G., Klein, U., Jäger, D., & Wieczorek, H. (1995). Regulation of plasma membrane V-ATPase activity by dissociation of peripheral subunits. *The Journal of Biological Chemistry*, *270*(10), 5649–53. Retrieved from http://www.ncbi.nlm.nih.gov/pubmed/7890686

Sun, X., & Artavanis-Tsakonas, S. (1996). The intracellular deletions of Delta and Serrate define dominant negative forms of the Drosophila Notch ligands. *Development (Cambridge, England)*, *122*(8), 2465–74. Retrieved from http://www.ncbi.nlm.nih.gov/pubmed/8756291

Sun, X., & Artavanis-Tsakonas, S. (1997). Secreted forms of DELTA and SERRATE define antagonists of Notch signaling in Drosophila. *Development (Cambridge, England)*, *124*(17), 3439–48. Retrieved from http://www.ncbi.nlm.nih.gov/pubmed/9310338

Sun-Wada, G.-H., Toyomura, T., Murata, Y., Yamamoto, A., Futai, M., & Wada, Y. (2006). The a3 isoform of V-ATPase regulates insulin secretion from pancreatic beta-cells. *Journal of Cell Science*, *119*(Pt 21), 4531–40. http://doi.org/10.1242/jcs.03234

Tabke, K., Albertmelcher, A., Vitavska, O., Huss, M., Schmitz, H.-P., & Wieczorek, H. (2014). Reversible disassembly of the yeast V-ATPase revisited under in vivo conditions. *The Biochemical Journal*, *462*(1), 185–97. http://doi.org/10.1042/BJ20131293

Takáts, S., Nagy, P., Varga, Á., Pircs, K., Kárpáti, M., Varga, K., … Juhász, G. (2013). Autophagosomal Syntaxin17-dependent lysosomal degradation maintains neuronal function in Drosophila. *The Journal of Cell Biology*, *201*(4), 531–9. http://doi.org/10.1083/jcb.201211160

Tamai, K., Toyoshima, M., Tanaka, N., Yamamoto, N., Owada, Y., Kiyonari, H., … Sugamura, K. (2008). Loss of hrs in the central nervous system causes accumulation of ubiquitinated proteins and neurodegeneration. *The American Journal of Pathology*, *173*(6), 1806–17. http://doi.org/10.2353/ajpath.2008.080684

Tapon, N., Ito, N., Dickson, B. J., Treisman, J. E., & Hariharan, I. K. (2001). The Drosophila tuberous sclerosis complex gene homologs restrict cell growth and cell proliferation. *Cell*, *105*(3), 345–55. Retrieved from http://www.ncbi.nlm.nih.gov/pubmed/11348591

Teis, D., Saksena, S., & Emr, S. D. (2008). Ordered assembly of the ESCRT-III complex on endosomes is required to sequester cargo during MVB formation. *Developmental Cell*, *15*(4), 578–89. http://doi.org/10.1016/j.devcel.2008.08.013

Teo, H., Perisic, O., González, B., & Williams, R. L. (2004). ESCRT-II, an Endosome-Associated Complex Required for Protein Sorting. *Developmental Cell*, *7*(4), 559–569. http://doi.org/10.1016/j.devcel.2004.09.003

Thompson, B. J., Mathieu, J., Sung, H.-H., Loeser, E., Rørth, P., & Cohen, S. M. (2005). Tumor suppressor properties of the ESCRT-II complex component Vps25 in Drosophila. *Developmental Cell*, *9*(5), 711–20. http://doi.org/10.1016/j.devcel.2005.09.020

Tiburcy, F., Beyenbach, K. W., & Wieczorek, H. (2013). Protein kinase A-dependent and -independent activation of the V-ATPase in Malpighian tubules of Aedes aegypti. *The Journal of Experimental Biology*, *216*(Pt 5), 881–91. http://doi.org/10.1242/jeb.078360

Tognon, E., & Vaccari, T. (2014). Immunohistochemical tools and techniques to visualize Notch in Drosophila melanogaster. *Methods in Molecular Biology (Clifton, N.J.)*, *1187*, 63–78. http://doi.org/10.1007/978-1-4939-1139-4_5

Tong, X., Zitserman, D., Serebriiskii, I., Andrake, M., Dunbrack, R., & Roegiers, F. (2010). Numb independently antagonizes Sanpodo membrane targeting and Notch signaling in Drosophila sensory organ precursor cells. *Molecular Biology of the Cell*, *21*(5), 802–10. http://doi.org/10.1091/mbc.E09-09-0831

Troost, T., Jaeckel, S., Ohlenhard, N., & Klein, T. (2012). The tumour suppressor Lethal (2) giant discs is required for the function of the ESCRT-III component Shrub/CHMP4. *Journal of Cell Science*, *125*(Pt 3), 763–76. http://doi.org/10.1242/jcs.097261

Usui, K., & Kimura, K. (1993). Sequential emergence of the evenly spaced microchaetes on the notum of Drosophila. *Roux's Archives of Developmental Biology*, *203*(3), 151–158. http://doi.org/10.1007/BF00365054

Vaccari, T., & Bilder, D. (2005). The Drosophila tumor suppressor vps25 prevents nonautonomous overproliferation by regulating notch trafficking. *Developmental Cell*, *9*(5), 687–98. http://doi.org/10.1016/j.devcel.2005.09.019

Vaccari, T., Duchi, S., Cortese, K., Tacchetti, C., & Bilder, D. (2010). The vacuolar ATPase is required for physiological as well as pathological activation of the Notch receptor. *Development (Cambridge, England)*, *137*(11), 1825–32. http://doi.org/10.1242/dev.045484

Vaccari, T., Lu, H., Kanwar, R., Fortini, M. E., & Bilder, D. (2008). Endosomal entry regulates Notch receptor activation in Drosophila melanogaster. *The Journal of Cell Biology*, *180*(4), 755–62. http://doi.org/10.1083/jcb.200708127

Vaccari, T., Rusten, T. E., Menut, L., Nezis, I. P., Brech, A., Stenmark, H., & Bilder, D. (2009). Comparative analysis of ESCRT-I, ESCRT-II and ESCRT-III function in Drosophila by efficient isolation of ESCRT mutants. *Journal of Cell Science*, *122*(Pt 14), 2413–23. http://doi.org/10.1242/jcs.046391

Valapala, M., Hose, S., Gongora, C., Dong, L., Wawrousek, E. F., Samuel Zigler, J., & Sinha, D. (2013). Impaired endolysosomal function disrupts Notch signalling in optic nerve astrocytes. *Nature Communications*, *4*, 1629.

http://doi.org/10.1038/ncomms2624

Vitavska, O., Wieczorek, H., & Merzendorfer, H. (2003). A novel role for subunit C in mediating binding of the H+-V-ATPase to the actin cytoskeleton. *The Journal of Biological Chemistry*, *278*(20), 18499–505. http://doi.org/10.1074/jbc.M212844200

Wang, W., & Struhl, G. (2004). Drosophila Epsin mediates a select endocytic pathway that DSL ligands must enter to activate Notch. *Development (Cambridge, England)*, *131*(21), 5367–80. http://doi.org/10.1242/dev.01413

Wang, W., & Struhl, G. (2005). Distinct roles for Mind bomb, Neuralized and Epsin in mediating DSL endocytosis and signaling in Drosophila. *Development (Cambridge, England)*, *132*(12), 2883–94. http://doi.org/10.1242/dev.01860

Wang, Y., Cipriano, D. J., & Forgac, M. (2007). Arrangement of Subunits in the Proteolipid Ring of the V-ATPase. *Journal of Biological Chemistry*, *282*(47), 34058–34065. http://doi.org/10.1074/jbc.M704331200

Wernet, M. F., Klovstad, M., & Clandinin, T. R. (2014). A Drosophila toolkit for the visualization and quantification of viral replication launched from transgenic genomes. *PloS One*, *9*(11), e112092. http://doi.org/10.1371/journal.pone.0112092

Westhoff, B., Colaluca, I. N., D'Ario, G., Donzelli, M., Tosoni, D., Volorio, S., … Di Fiore, P. P. (2009). Alterations of the Notch pathway in lung cancer. *Proceedings of the National Academy of Sciences of the United States of America*, *106*(52), 22293–8. http://doi.org/10.1073/pnas.0907781106

Wharton, K. A., Johansen, K. M., Xu, T., & Artavanis-Tsakonas, S. (1985). Nucleotide sequence from the neurogenic locus notch implies a gene product that shares homology with proteins containing EGF-like repeats. *Cell*, *43*(3 Pt 2), 567–81. Retrieved from http://www.ncbi.nlm.nih.gov/pubmed/3935325

Wilkin, M. B., & Baron, M. (2005). Endocytic regulation of Notch activation and down-regulation (review). *Molecular Membrane Biology*, *22*(4), 279–89. http://doi.org/10.1080/09687860500129778

Wilkin, M. B., Carbery, A.-M., Fostier, M., Aslam, H., Mazaleyrat, S. L., Higgs, J., … Baron, M. (2004). Regulation of notch endosomal sorting and signaling by Drosophila Nedd4 family proteins. *Current Biology : CB*, *14*(24), 2237–44. http://doi.org/10.1016/j.cub.2004.11.030

Wilkin, M., Tongngok, P., Gensch, N., Clemence, S., Motoki, M., Yamada, K., … Baron, M. (2008). Drosophila HOPS and AP-3 complex genes are required for a Deltex-regulated activation of notch in the endosomal trafficking pathway. *Developmental Cell*, *15*(5), 762–72. http://doi.org/10.1016/j.devcel.2008.09.002

Williams, R. L., & Urbé, S. (2007). The emerging shape of the ESCRT machinery.

Nature Reviews. Molecular Cell Biology, *8*(5), 355–68. http://doi.org/10.1038/nrm2162

Williamson, W. R., Wang, D., Haberman, A. S., & Hiesinger, P. R. (2010). A dual function of V0-ATPase a1 provides an endolysosomal degradation mechanism in Drosophila melanogaster photoreceptors. *The Journal of Cell Biology*, *189*(5), 885–99. http://doi.org/10.1083/jcb.201003062

Wilson, A., & Radtke, F. (2006). Multiple functions of Notch signaling in self-renewing organs and cancer. *FEBS Letters*, *580*(12), 2860–8. http://doi.org/10.1016/j.febslet.2006.03.024

Wilson-Rawls, J., Molkentin, J. D., Black, B. L., & Olson, E. N. (1999). Activated notch inhibits myogenic activity of the MADS-Box transcription factor myocyte enhancer factor 2C. *Molecular and Cellular Biology*, *19*(4), 2853–62. Retrieved from http://www.pubmedcentral.nih.gov/articlerender.fcgi?artid=84078&tool=pmcentrez&rendertype=abstract

Windler, S. L., & Bilder, D. (2010). Endocytic internalization routes required for delta/notch signaling. *Current Biology : CB*, *20*(6), 538–43. http://doi.org/10.1016/j.cub.2010.01.049

Winter, V., & Hauser, M.-T. (2006). Exploring the ESCRTing machinery in eukaryotes. *Trends in Plant Science*, *11*(3), 115–23. http://doi.org/10.1016/j.tplants.2006.01.008

Wodarz, A., Ramrath, A., Kuchinke, U., & Knust, E. (1999). Bazooka provides an apical cue for Inscuteable localization in Drosophila neuroblasts. *Nature*, *402*(6761), 544–7. http://doi.org/10.1038/990128

Wu, G., Lyapina, S., Das, I., Li, J., Gurney, M., Pauley, A., … Kitajewski, J. (2001). SEL-10 is an inhibitor of notch signaling that targets notch for ubiquitin-mediated protein degradation. *Molecular and Cellular Biology*, *21*(21), 7403–15. http://doi.org/10.1128/MCB.21.21.7403-7415.2001

Xu, A. (2005). Regions of Drosophila Notch That Contribute to Ligand Binding and the Modulatory Influence of Fringe. *Journal of Biological Chemistry*, *280*(34), 30158–30165. http://doi.org/10.1074/jbc.M505569200

Xu, T. (2001). Microtubules Are Involved in Glucose-dependent Dissociation of the Yeast Vacuolar [H+]-ATPase in Vivo. *Journal of Biological Chemistry*, *276*(27), 24855–24861. http://doi.org/10.1074/jbc.M100637200

Xu, Y., Parmar, A., Roux, E., Balbis, A., Dumas, V., Chevalier, S., & Posner, B. I. (2012). Epidermal growth factor-induced vacuolar (H+)-atpase assembly: a role in signaling via mTORC1 activation. *The Journal of Biological Chemistry*, *287*(31), 26409–22. http://doi.org/10.1074/jbc.M112.352229

Yamada, K., Fuwa, T. J., Ayukawa, T., Tanaka, T., Nakamura, A., Wilkin, M. B., …

Matsuno, K. (2011). Roles of Drosophila Deltex in Notch receptor endocytic trafficking and activation. *Genes to Cells*, *16*(3), 261–272. http://doi.org/10.1111/j.1365-2443.2011.01488.x

Yamashiro, C. T., Kane, P. M., Wolczyk, D. F., Preston, R. A., & Stevens, T. H. (1990). Role of vacuolar acidification in protein sorting and zymogen activation: a genetic analysis of the yeast vacuolar proton-translocating ATPase. *Molecular and Cellular Biology*, *10*(7), 3737–49. Retrieved from http://www.pubmedcentral.nih.gov/articlerender.fcgi?artid=360825&tool=pmcentrez&rendertype=abstract

Yan, Y., Denef, N., & Schüpbach, T. (2009). The vacuolar proton pump, V-ATPase, is required for notch signaling and endosomal trafficking in Drosophila. *Developmental Cell*, *17*(3), 387–402. http://doi.org/10.1016/j.devcel.2009.07.001

Yochem, J., Weston, K., & Greenwald, I. (1988). The Caenorhabditis elegans lin-12 gene encodes a transmembrane protein with overall similarity to Drosophila Notch. *Nature*, *335*(6190), 547–50. http://doi.org/10.1038/335547a0

Zitserman Diana, R. F. (2011). Live-cell Imaging of Sensory Organ Precursor Cells in intact Drosophila Pupae. http://doi.org/10.3791/2706

Zoncu, R., Bar-Peled, L., Efeyan, A., Wang, S., Sancak, Y., & Sabatini, D. M. (2011). mTORC1 senses lysosomal amino acids through an inside-out mechanism that requires the vacuolar H(+)-ATPase. *Science (New York, N.Y.)*, *334*(6056), 678–83. http://doi.org/10.1126/science.1207056